Germline variants in tumor suppressor *FBXW7* lead to impaired ubiquitination and a neurodevelopmental syndrome

Authors

Sarah E.M. Stephenson, Gregory Costain, Laura E.R. Blok, ..., Paul J. Lockhart, John Christodoulou, Tiong Yang Tan

Correspondence

tiong.tan@vcgs.org.au

Stephenson et al., 2022, The American Journal of Human Genetics *109*, 601–617
April 7, 2022
https://doi.org/10.1016/j.ajhg.2022.03.002

CellPress

Germline variants in tumor suppressor *FBXW7* lead to impaired ubiquitination and a neurodevelopmental syndrome

Sarah E.M. Stephenson,[1,2] Gregory Costain,[3,4,5] Laura E.R. Blok,[6] Michael A. Silk,[7,8,9] Thanh Binh Nguyen,[7,8,9] Xiaomin Dong,[1] Dana E. Alhuzaimi,[1] James J. Dowling,[10,11] Susan Walker,[11,12] Kimberly Amburgey,[5,10] Robin Z. Hayeems,[13,14] Lance H. Rodan,[15,16] Marc A. Schwartz,[17,18,19,20] Jonathan Picker,[15,21] Sally A. Lynch,[22] Aditi Gupta,[23,24] Kristen J. Rasmussen,[25] Lisa A. Schimmenti,[26,27,28] Eric W. Klee,[23,24,25,26] Zhiyv Niu,[25,26] Katherine E. Agre,[26] Ilana Chilton,[29] Wendy K. Chung,[29,30] Anya Revah-Politi,[31] P.Y. Billie Au,[32] Christopher Griffith,[33] Melissa Racobaldo,[33] Annick Raas-Rothschild,[34,35] Bruria Ben Zeev,[34,36] Ortal Barel,[37,38]

(Author list continued on next page)

Summary

Neurodevelopmental disorders are highly heterogenous conditions resulting from abnormalities of brain architecture and/or function. *FBXW7* (F-box and WD-repeat-domain-containing 7), a recognized developmental regulator and tumor suppressor, has been shown to regulate cell-cycle progression and cell growth and survival by targeting substrates including CYCLIN E1/2 and NOTCH for degradation via the ubiquitin proteasome system. We used a genotype-first approach and global data-sharing platforms to identify 35 individuals harboring *de novo* and inherited *FBXW7* germline monoallelic chromosomal deletions and nonsense, frameshift, splice-site, and missense variants associated with a neurodevelopmental syndrome. The *FBXW7* neurodevelopmental syndrome is distinguished by global developmental delay, borderline to severe intellectual disability, hypotonia, and gastrointestinal issues. Brain imaging detailed variable underlying structural abnormalities affecting the cerebellum, corpus collosum, and white matter. A crystal-structure model of FBXW7 predicted that missense variants were clustered at the substrate-binding surface of the WD40 domain and that these might reduce FBXW7 substrate binding affinity. Expression of recombinant FBXW7 missense variants in cultured cells demonstrated impaired CYCLIN E1 and CYCLIN E2 turnover. Pan-neuronal knockdown of the *Drosophila* ortholog, *archipelago*, impaired learning and neuronal function. Collectively, the data presented herein provide compelling evidence of an F-Box protein-related, phenotypically variable neurodevelopmental disorder associated with monoallelic variants in *FBXW7*.

Introduction

Neurodevelopment is a complex spatiotemporal process requiring the coordinated action of genetic and environmental cues to regulate a multitude of developmental processes, including cellular proliferation, differentiation, migration, and formation of neural circuits. Neurodevelopmental disorders affect ~2%–5% of children and result in

[1]Murdoch Children's Research Institute, Melbourne, VIC 3052, Australia; [2]Department of Paediatrics, University of Melbourne, Melbourne, VIC 3052, Australia; [3]Division of Clinical and Metabolic Genetics, The Hospital for Sick Children, Toronto, ON M5G 1X8, Canada; [4]Program in Genetics and Genome Biology, The Hospital for Sick Children, Toronto, ON M5G 1X8, Canada; [5]Department of Paediatrics, University of Toronto, Toronto, ON M5G 1X8, Canada; [6]Department of Human Genetics, Donders Institute for Brain, Cognition and Behaviour, Radboud University Medical Center, Nijmegen 6525, the Netherlands; [7]Structural Biology and Bioinformatics, Department of Biochemistry and Molecular Biology, University of Melbourne, Melbourne, VIC 3052, Australia; [8]Australia Cancer Research Funding Facility for Innovative Cancer Drug Discovery, Bio21 Institute, University of Melbourne, Melbourne, VIC 3052, Australia; [9]Computational Biology and Clinical Informatics, Baker Heart and Diabetes Institute, Melbourne, VIC 3004, Australia; [10]Division of Neurology, Hospital for Sick Children, Toronto, ON M5G 1X8, Canada; [11]Program in Genetics and Genome Biology, The Hospital for Sick Children, Toronto, ON M5G 1X8, Canada; [12]The Centre for Applied Genomics, The Hospital for Sick Children, Toronto, ON M5G 1X8, Canada; [13]Child Health Evaluative Sciences, The Hospital for Sick Children, Toronto, ON M5G 1X8, Canada; [14]Centre for Genetic Medicine, The Hospital for Sick Children, Toronto, ON M5G 1X8, Canada; [15]Division of Genetics and Genomics, Boston Children's Hospital, Harvard Medical School, Boston, MA 02115, United States; [16]Department of Neurology, Boston Children's Hospital, Harvard Medical School, Boston, MA 02115, United States; [17]Department of Pediatrics, Harvard Medical School, Boston, MA 02115, United States; [18]Cancer and Blood Disorders Center, Boston Children's Hospital, Boston, MA 02115, United States; [19]Department of Pediatric Oncology, Dana Farber Cancer Institute, Boston, MA 02115, United States; [20]Broad Institute of MIT and Harvard, Cambridge, MA 02115, United States; [21]Department of Child and Adolescent Psychiatry, Boston Children's Hospital, Harvard Medical School, Boston, MA 02115, United States; [22]Department of Clinical Genetics, Children's Health Ireland at Temple Street, Rotunda, Dublin D01 XD99, Ireland; [23]Center for Individualized Medicine, Mayo Clinic, Rochester, MN 55905, United States; [24]Department of Health Sciences Research, Mayo Clinic, Rochester, MN 55905, United States; [25]Department of Laboratory Medicine and Pathology, Mayo Clinic, Rochester, MN 55905, United States; [26]Department of Clinical Genomics, Mayo Clinic, Rochester, MN 55905, United States; [27]Otolaryngology—Head and Neck Surgery (Ear, Nose, and Throat), Mayo Clinic, Rochester, MN 55905, United States; [28]Biochemistry and Molecular Biology, Mayo Clinic, Rochester, MN 55905, United States; [29]Department of Pediatrics, Columbia University Irving Medical Center, New York, NY 10032, United States; [30]Department of Medicine, Columbia University Irving Medical Center, New York, NY 10032, United

(Affiliations continued on next page)

Sebastien Moutton,[39,40,41] Fanny Morice-Picard,[42] Virginie Carmignac,[41] Jenny Cornaton,[40] Nathalie Marle,[43] Orrin Devinsky,[44] Chandler Stimach,[45] Stephanie Burns Wechsler,[46,47] Bryan E. Hainline,[48,49] Katie Sapp,[48,49] Marjolaine Willems,[50] Ange-line Bruel,[51] Kerith-Rae Dias,[52,53] Carey-Anne Evans,[52,53] Tony Roscioli,[52,53,54] Rani Sachdev,[54,55] Suzanna E.L. Temple,[52,53,54] Ying Zhu,[52,56] Joshua J. Baker,[57] Ingrid E. Scheffer,[1,2,58] Fiona J. Gardiner,[58] Amy L. Schneider,[58] Alison M. Muir,[59] Heather C. Mefford,[59] Amy Crunk,[60] Elizabeth M. Heise,[60] Francisca Millan,[60] Kristin G. Monaghan,[60] Richard Person,[60] Lindsay Rhodes,[60] Sarah Richards,[60] Ingrid M. Wentzensen,[60] Benjamin Cogné,[61] Bertrand Isidor,[61] Mathilde Nizon,[61] Marie Vincent,[61] Thomas Besnard,[61] Amelie Piton,[62,63] Carlo Marcelis,[6] Kohji Kato,[64,65] Norihisa Koyama,[66] Tomoo Ogi,[65,67] Elaine Suk-Ying Goh,[68] Christopher Richmond,[69] David J. Amor,[1,2,69] Jessica O. Boyce,[1,2] Angela T. Morgan,[1,2] Michael S. Hildebrand,[1,58] Antony Kaspi,[70,71] Melanie Bahlo,[70,71] Rún Friðriksdóttir,[72] Hildigunnur Katrínardóttir,[72] Patrick Sulem,[72] Kári Stefánsson,[72,73] Hans Tómas Björnsson,[73,74,75] Simone Mandelstam,[2,76] Manuela Morleo,[77,78] Milena Mariani,[79] TUDP Study Group, Marcello Scala,[80,81] Andrea Accogli,[80,81] Annalaura Torella,[77] Valeria Capra,[81] Mathew Wallis,[82] Sandra Jansen,[83] Quinten Waisfisz,[83] Hugoline de Haan,[83] Simon Sadedin,[1,69] Broad Center for Mendelian Genomics, Sze Chern Lim,[1,69] Susan M. White,[1,2,69] David B. Ascher,[7,8,9,84] Annette Schenck,[6] Paul J. Lockhart,[1,2] John Christodoulou,[1,2,69] and Tiong Yang Tan[1,2,69,*]

variable neurocognitive symptoms.[1–3] They are genetically and phenotypically heterogeneous and often require untargeted genomic analysis and a genotype-first approach for the discovery of novel phenotypes.[4] Several neurodevelopmental disorders have been attributed to genes that regulate cell division, underscoring the importance of this process in the development of the central nervous system.[5,6] F-box (FBX) proteins are essential for regulating the

States; [31]Institute for Genomic Medicine and Precision Genomics Laboratory, Columbia University Irving Medical Center, New York, NYk, 10032, United States; [32]Department of Medical Genetics and Alberta Children's Hospital Research Institute, Cumming School of Medicine, University of Calgary, Calgary, AB T2N 4N1, Canada; [33]Division of Pediatrics, University of South Florida, Tampa, FL 33620, United States; [34]Sackler Faculty of Medicine, Tel Aviv University, Tel Aviv-Yafo 6997801, Israel; [35]Institute of Rare Diseases, The Danek Gertner Institute of Human Genetics, Sheba Medical Center, Tel Hashomer, Ramat Gan 52621, Israel; [36]Pediatric Neurology Unit, Safra Children's Hospital, Sheba Medical Center, Tel Hashomer, Ramat Gan 52621, Israel; [37]The Genomic Unit, Sheba Cancer Research Center, Sheba Medical Center, Tel Hashomer, Ramat Gan 52621, Israel; [38]The Wohl Institute for Translational Medicine, Sheba Medical Center, Tel Hashomer, Ramat Gan 52621, Israel; [39]Centre Pluridisciplinaire de Diagnostic PréNatal, Pôle Mère Enfant, Maison de Santé Protestante Bordeaux Bagatelle, Talence, Nouvelle-Aquitaine 33401, France; [40]Reference Center for Developmental Anomalies, Department of Medical Genetics, Dijon University Hospital, Dijon, Bourgogne-Franche-Comté 21000, France; [41]INSERM U1231, Laboratoire de Neurosciences Cognitives, UMR 1231, Genetic of Development Anomalies, University of Burgundy, Dijon, Bourgogne-Franche-Comté 21078 France; [42]Reference Center for Genetic, Complex, and Rare Skin Disorders, Department of Pediatric Dermatology, Bordeaux University Hospital, Bordeaux, Nouvelle-Aquitaine 33000, France; [43]Laboratoire de Génétique Chromosomique et Moléculaire, Pôle de Biologie, Centre Hospitalier Universitaire de Dijon, Dijon, Bourgogne-Franche-Comté 21000 France; [44]Neurology Department, New York University Langone Medical Center, New York, NY 10016, United States; [45]Department of Human Genetics, Emory Healthcare, Atlanta, GA 30322, United States; [46]Department of Human Genetics, Emory University School of Medicine, Atlanta, Georgia, 30322, United States; [47]Department of Pediatrics, Emory University School of Medicine, Atlanta, Georgia, 30322, United States; [48]Indiana University School of Medicine, Indianapolis, Indiana 46202, United States; [49]Indiana University Health Physicians, Indiana University, Indianapolis, Indiana 46202, United States; [50]Reference Center for Developmental Disorders, Department of Medical Genetics, Arnaud de Villeneuve Hospital, Montpellier University Hospital, Montpellier, Occitanie 34295, France; [51]Inserm UMR 1231, Genetics of Developmental Anomalies, University of Bourgogne, University Hospital Federation, Translational Medicine in Development Disorders, Dijon, Bourgogne-Franche-Comté 21078, France; [52]New South Wales Health Pathology East Laboratory, Prince of Wales Private Hospital, Sydney, NSW 2031, Australia; [53]Neuroscience Research Australia, Prince of Wales Clinical School, University of New South Wales, Sydney, New South Wales 2031, Australia; [54]Centre for Medical Genetics, Sydney Children's Hospital, Sydney, New South Wales 2031, Australia; [55]School of Women's and Children's Health, University of New South Wales Medicine, University of New South Wales, Sydney, New South Wales 2052, Australia; [56]Newcastle Genetics of Learning Disability Service, Hunter Genetics, Newcastle, New South Wales 2298, Australia; [57]Department of Pediatrics, Boston Children's Hospital, Harvard Medical School, Boston, MA 02115, United States; [58]Epilepsy Research Centre, Department of Medicine, Austin Health, University of Melbourne, Melbourne, VIC 3084, Australia; [59]Department of Pediatrics, University of Washington, Seattle, WA 98195, United States; [60]GeneDx, Gaithersburg, MD 20877, United States; [61]Medical Genetic Services, The Thorax Institute, INSERM, Centre National de la Recherche Scientifique, University Hospital of Nantes, Nantes, Pays de la Loire 44007, France; [62]Molecular Genetic Unit, Strasbourg University Hospital, Strasbourg, Illkirch-Graffenstaden 67000, France; [63]Institute of Genetics and Molecular and Cellular Biology, INSERM U964, Centre National de la Recherche Scientifique, UMR 7104, University of Strasbourg, Illkirch-Graffenstaden, Grand Est 67400, France; [64]Department of Pediatrics and Neonatology, Nagoya City University Graduate School of Medical Sciences, Nagoya, Chubu 467-8601, Japan; [65]Department of Genetics, Research Institute of Environmental Medicine, Nagoya University, Nagoya, Chubu 464-860, Japan; [66]Department of Pediatrics, Toyohashi Municipal Hospital, Toyohashi, Chubu 441-8570, Japan; [67]Department of Human Genetics and Molecular Biology, Nagoya University Graduate School of Medicine, Nagoya, Chubu 467-8601, Japan; [68]Laboratory Medicine and Genetics, Trillium Health Partners, Mississauga, ON L5B 1B8, Canada; [69]Victorian Clinical Genetics Services, Melbourne, VIC 3052, Australia; [70]Population Health and Immunity Division, The Walter and Eliza Hall Institute for Medical Research, Melbourne, VIC 3052, Australia; [71]Department of Medical Biology, University of Melbourne, Melbourne, VIC 3052, Australia; [72]deCODE Genetics, Amgen, Reykjavik 101, Iceland; [73]Faculty of Medicine, University of Iceland, Reykjavik 101, Iceland; [74]Department of Genetics and Molecular Medicine, Landspitali University Hospital, Reykjavik 101, Iceland; [75]McKusick-Nathans Institute of Genetic Medicine, Johns Hopkins University, Baltimore, MD 21218, United States; [76]Department of Medical Imaging, The Royal Children's Hospital, Melbourne, VIC 3052, Australia; [77]Telethon Institute of Genetics and Medicine, Pozzuoli, Naples 80078, Italy; [78]Department of Precision Medicine, University of Campania "Luigi Vanvitelli," Naples 80138, Italy; [79]Department of Pediatrics, Azienda Socio Sanitaria Territoriale, Lariana Sant'Anna Hospital, San Fermo Della Battaglia, Como 22042, Italy; [80]Department of Neurosciences, Rehabilitation, Opthalmology, Genetics, and Maternal and Child Health, University of Genoa, Genoa, Liguria 16126, Italy; [81]Istituto di Ricovero e Cura a Carattere Scientifico Giannina Gaslini Institute, Genoa, Liguria 16147, Italy; [82]Tasmanian Clinical Genetics Services, Royal Hobart Hospital, Hobart, Tasmania 7000, Australia; [83]Department of Human Genetics, Amsterdam University Medical Centers, Vrije Universiteit Medical Center Amsterdam, Amsterdam, the Netherlands; [84]Department of Biochemistry, University of Cambridge, Cambridge, England CB2 1GA, United Kingdom
*Correspondence: tiong.tan@vcgs.org.au
https://doi.org/10.1016/j.ajhg.2022.03.002.

ubiquitination of proteins involved in the cell cycle. There are 69 human FBX proteins, which are classified into three subcategories on the basis of the structural class of their substrate-binding domains: FBXW proteins contain a tryptophan-aspartic acid 40 (WD40) repeat domain; FBXL proteins contain a leucine-rich repeat; and FBXO proteins contain other protein-interaction domains (reviewed in Nguyen et al. [7] and Zhang et al. [8]). FBX proteins are incorporated as one subunit of a tetrameric SCF (SKP1-CUL1-FBX) ubiquitin ligase complex. First, the FBX protein aggregates the phosphorylated target protein independently of the other complex subunits, then it attaches to the adaptor protein S-phase kinase-associated protein 1 (SKP1), which links it to the major structural scaffold protein cullin 1 (CUL1). CUL1 links SKP1 to the ring-box 1 (RBX1) protein, which facilitates the transfer of a ubiquitin molecule to the protein target, now marked for degradation via the ubiquitin proteasome system (UPS).[8]

To date, germline variants in five genes encoding FBX proteins have been found to underlie neurodevelopmental disorders. *De novo* missense variants in *FBXW11* (MIM: 605651) located in the encoded WD40 domain repeats have been associated with mild to severe neurodevelopmental disability, often accompanied by behavioral abnormalities and mandibular, ocular, and digital features.[9] *De novo* frameshift, nonsense, splicing, and missense variants in *FBXO11* (MIM: 607871) result in mild to severe intellectual disability with dysmorphic facies and behavioral abnormalities.[10,11] *De novo* variants in *FBXO28* (MIM: 609100) have been identified in individuals with severe to profound intellectual disability (ID) and epilepsy with various seizure types,[12,13] confirming the initial suggestions that the gene was the primary phenotypic determinant in chromosome 1q41q42 microdeletion syndrome.[14,15] Autosomal-recessive inheritance has also been observed in FBX-related phenotypes; biallelic variants in *FBXL4* (MIM: 605654) cause mitochondrial DNA depletion syndrome with encephalomyopathy,[16,17] and in *FBXL3* they cause intellectual disability with dysmorphic features and short stature.[18] Additionally, *KDM2B* (MIM: 609078), also known as *FBXL10*, is a candidate neurodevelopmental-disease-associated gene with a homozygous variant identified in two siblings with developmental delay, hypotonia, and infantile spasms;[19] additionally, monoallelic single-nucleotide variants and chromosomal microdeletions involving this gene have also been identified in individuals with syndromic intellectual disability.[20,21]

F-box- and WD-repeat-domain-containing 7 (*FBXW7;* GenBank: NG_029466.2; MIM: 606278) has been extensively studied as a tumor suppressor (reviewed in Yeh et al.[22] and Sailo et al.[23]). However, it has also been implicated in a variety of diverse biological processes, including the immune response,[24,25] liver lipid metabolism,[26] angiogenesis,[27,28] cardiac hypertrophy,[29] haemopoiesis,[30] neurodevelopment[31–36] and excitotoxicity.[37,38] Herein we provide a detailed characterization of 35 individuals from 32 families identified through global matchmaking databases and found to have 28 germline *de novo* and inherited monoallelic *FBXW7* variants associated with neurodevelopmental disability and variable features. Evidence from *in silico* protein modeling, cell-based functional studies, and *Drosophila* neuronal knockdown converge to support the discovery that pathogenic variants in *FBXW7* cause an FBX-related neurodevelopmental syndrome.

Subjects and methods

Subjects and *FBXW7* variant analysis

All procedures were approved by institutional human research ethics committees, and informed consent was obtained for all individuals. Individuals were clinically evaluated in separate centers, and DNA samples were analyzed by chromosomal microarray or genomic sequencing (exome or genome, with singleton or trio analysis) on a clinical or research basis. Contact between researchers was facilitated with web-based tools Matchmaker Exchange[39] and GeneMatcher.[40] High-confidence candidate variants, categorized as either predicted LoF or damaging candidates, absent from gnomAD and classified as pathogenic according to the American College of Medical Genetics (ACMG) guidelines[41] are reported. The functional outcome of splice-site variants was predicted with BDGP NNSPLICE 0.9,[42] NetGene2[43,44] and Splice AI.[45]

In silico modeling of the impact of FBXW7 variant interaction with CYCLIN E1

The structure of CYCLIN E1 (amino acids [aa] 89–395) was built under the default parameters of the i-TASSER website.[46] The complex between FBXW7 and CYCLIN E1 was then modeled with Schrodinger (2020-3). The highest-resolution experimental X-ray structures of FBXW7 (aa 263–706, PDB: 2OVR)[47] and the modeled CYCLIN E1 from i-TASSER were used for building the complex. A restraint docking approach was applied in Schrodinger. There were four restraints (between 4 and 6 Å) that were applied to the residues between FBWX7 and CYCLIN E1, namely Ser384(CYCLIN E1)-Arg479(FBXW7), Thr380(CYCLIN E1)-Arg505(FBXW7), Thr380(CYCLIN E1)-Arg465(FBXW7), and Thr380(CYCLIN E1)-Arg479(FBXW7).[47] We then screened the top solutions to evaluate them by their ability to satisfy the experimental data.

FBXW7 missense variants were first annotated for predicted consequences via the Variant Effect Predictor (release 101) including dbNSFP (4.1a) output.[48,49] MTR scores were included from the MTR-Viewer. We selected a number of these scores to capture conservation, physicochemical properties, and genic intolerance. We examined structural properties by using the mCSM suite to manually map the missense variants to the homology-modeled complex of FBXW7 with CYCLIN E1 bound. We used mCSM to predict changes to thermodynamic stability (ΔΔG) and mCSM-PPI2 to predict changes to binding affinity.[50,51] Additionally, changes to charge, volume, and residue nature were reported for each substitution.

Functional analysis of FBXW7 variants

The open reading frame of *FBXW7* variants (GenBank: NM_001349798.2; c.1267G>A [p.Gly423Arg]; c.1439A>G [p.Asp480Gly]; c.1631T>G [p.Val544Gly]; c.1920C>A [p.Ser640Arg]; c.2020C>T [p.Arg674Trp]; c.2021G>C [p.Arg674Pro]; and c.2066G>A [p.Arg689Gln]); and known substrates E1 CYCLIN

(GenBank: NM_001238.4) and E2 CYCLIN (GenBank: NM_057749.3) were synthesized, their sequences were verified, and they were cloned inframe into C-terminal- epitope-tagged vectors pcDNA3.1/Myc-His (ThermoFisher, V80020) and pcDNA3.1/V5-His (ThermoFisher, V81020), respectively (Integrated DNA Technologies).

HEK293T cells (American Type Culture Collection CRL-3216) were transiently transfected with an *FBXW7* variant alone or in combination with either a known substrate or empty vector through the use of Fugene HD (Promega, E2311) and harvested at 60–72 h after transfection. Where indicated, cells were treated with 5 μM MG-132 (Merck, 1474790) or DMSO (Sigma, D2650) at 48 h after transfection and harvested after 16 h. Protein lysates were obtained by resuspension and sonication (Digital Sonifier Cell Disruptor 250, Branson) in 2% SDS, 10 mM TRIS (pH 7.5) with 1× Complete Protease Inhibitor Cocktail (Roche, 11697498001) followed by protein estimation (ThermoFisher, 23225).

Immunoblots were performed on 50 μg of total protein via the Criterion TGX system (BioRad) and probed sequentially with antibodies to anti-c-Myc (9E10, Abcam, AB32, 1:5000); anti-V5 (ThermoFisher, R960, 1:5000), and GAPDH (1D4, Novus Biologicals, NB300-221, 1:5000). Primary antibodies were detected with goat anti-mouse IgG (H+L, Jackson ImmunoResearch, 115-005-003, 1:10000), and bands were visualized with the Clarity Western ECL Substrate (BioRad, 1705061) and the Amersham Imager 680 (GE Health, 29270772).

Densitometry of detected bands was recorded for semiquantitative analysis between samples. Lanes and bands were identified automatically and then manually modified where appropriate; the rolling-ball method was used for background correction. Individual sample values were first determined by normalization of the intensity of the protein of interest to the housekeeping control protein for each individual sample. To control for individual blot variation, we then normalized each sample to the intensity of the signal of the FBXW7 WT sample before combining samples for statistical significance testing by a two-sample, two-tailed Student's t test; $p < 0.05$ was considered significant.

Drosophila ago knockdown models

Two *Drosophila* UAS-RNAi lines (RNAi-1, BL34802; and RNAi-2, BL31501), both previously validated[52,53] and carrying inducible RNAi constructs against the *FBXW7* homolog *archipelago* (*ago*; CG15010; FBgn0041171), and the matching genetic background control (BL36303) were obtained from the Bloomington *Drosophila* Stock Center. *Drosophila* stocks were maintained at room temperature on standard *Drosophila* diet (sugar, cornmeal, agar, and yeast).

The efficiency and relative strength of *ago* RNAi-1 and *ago* RNAi-2 constructs were determined by quantitative real-time-PCR (qPCR) analysis. The *ago* RNAi-1 and *ago* RNAi-2 lines and their genetic background controls were crossed to the ubiquitous Act-Gal4/TM3 Sb Tb driver, and mRNA was extracted from wandering L3 larva of the appropriate genotype with QIAGEN's Rneasy Lipid Tissue Mini Kit. DNase treatment was performed with QIAGEN's RNase-Free DNase Set, and cDNA was synthesized with the Bio-Rad iScript cDNA synthesis kit according to the manufacturer's protocols. PCRs were performed with primers targeting *ago* (5′-GGCCACGACGATCATGTG-3′ and 5′-GACTTTGAGC GTGCGATCC-3′) and *β′COP* (5′-AACTACAACACCCTGGAGAA GG-3′ and 5′-ACATCTTCTCCCAATTCCAAAG-3′) with the GoTaq qPCR Master Mix (Promega) on an Applied Biosystem Fast 7500 Real-Time machine. The initial denaturation was performed for 10 min at 95°C, followed by 15 s at 95°C and 30 s at 60°C for 40 cycles (qPCR data collection). The products were then denatured at 95°C for 1 min and cooled to 65°C for 1 min (melt curve data collection). For each condition, three biological and three technical replicates were analyzed. Differential gene expression was calculated via the $2^{\Delta\Delta Ct}$ method.[54] The average Ct value for each sample was calculated and subtracted from the Ct value of the reference gene so that the ΔCt value could be calculated.[55] A two-sample t test (equal variance) comparing the $2^{\Delta\Delta Ct}$ values of the RNAi line and genetic background control was performed in Microsoft Excel for calculation of p values).

For inducing neuronal knockdown, the UAS-RNAi lines were crossed to either of two panneuronal promotor lines: (1) elav$^{(III)}$-Gal4 with genotype "w1118; 2xGMR-wIR; elav-Gal4, UAS-Dicer-2" and to (2) elav$^{(I)}$ – Gal4 with genotype "c155-Gal4, GMR-wIR; +; +". The latter is a strong Gal4 insertion into the endogenous elav locus. Crosses were maintained at 25°C, 70% humidity in a 12 h:12 h light:dark cycle. Habituation learning and basal motor function were tested in the light-off jump-reflex habituation and fatigue assays, as previously described.[56] In brief, three- to four-day-old males were individually placed in semi-transparent vials enclosed by two microphones. The filled vials were inserted into two independent 16-unit light-off jump-habituation systems (Aktogen) and left to acclimatize for 5 min before the start of the habituation paradigm assay, in which 32 flies were simultaneously exposed to 100 light-off pulses of 15 ms with a 1 s inter-trial-interval. The noise amplitude produced by wing vibrations was recorded for 500 ms after each light-off pulse. The measured sound amplitudes were filtered with a threshold to remove background noise, leading to the annotation of a jump at amplitude above 0.8. The jumps were collected and analyzed by a custom-made Labview Software (National Instruments). A high initial jump response to the light-off pulse decreased with the increase of the number of repeated pulses. A fly was considered to have habituated when it failed to jump for five consecutive light-off pulses (no jump criterion). The last jump was then stated as the number of trials needed to reach the no-jump criterion (trials to criterion, TTC). If the fraction of flies jumping to at least one of the first five light-off pulses (initial jump response) was <50%, genotypes were classified as non-performers on the basis of reduced motor performance of the tested population. Habituation per genotype was quantified as the mean trials to criterion (mTTC) of all flies of the same genotype.

The fatigue assay was performed after the habituation assay, which was equivalent to the habituation assay but involved two adaptations; (1) increased inter-trial-interval from 1 to 5 s and (2) shortened trial length from 100 to 50 light-off pulses. The increased inter-trial-interval prevented the flies from habituating and thereby elicited a jump response at each light-off trial. As for the habituation assay, the no-jump criterion was five consecutive pulses without a jump. Failing to jump for five consecutive light-off pulses in this assay was identified as a basal failure to execute jumping and was deemed to be due to increased fatigue. The last jump was scored as the number of trials it took to reach the no-jump criterion (TTC). The TTCs of the simultaneously measured flies of the same genotype were averaged (mean TTC (mTTC)).

Statistics

Protein density and qPCR: statistical significance was assessed by a two-sample, two-tailed Student's t test, and $p < 0.05$ was considered significant.

Drosophila behavior: the effect of the genotype on habituation and fatigue was scored by comparison of log-transformed TTC values of the mutant versus the control flies after correction for the experimental day and system via a linear-model regression analysis with R statistical software (v.3.0.0).[56]

Results

Monoallelic *FBXW7* variants are associated with neurodevelopmental disability, brain anomalies, hypotonia, and gastrointestinal issues

Using clinical or research-based chromosomal microarrays, genomic sequencing (trio genome or exome), and the global matchmaking platforms Matchmaker Exchange[39] and GeneMatcher,[40] we have identified 35 individuals (26 male, 74.3%) from 32 families with 28 distinct variants in *FBXW7*. The variants arose *de novo* in 30 individuals, including two individuals displaying mosaicism and two showing familial transmission from an affected parent (Table S1). The clinical phenotype is characterized by neurodevelopmental disability (34/35; 97.1%), including global developmental delay and intellectual disability ranging from borderline to severe, language disorder, and hypotonia (22/35; 62.9%); individual 21 was severely affected and had episodes of developmental regression and progressive spasticity. Seizures of varying types were reported in 8/35 (22.9%) individuals. Feeding difficulties and constipation were each reported in 16/35 (45.7%) individuals. Growth was generally within normal limits, but macrocephaly was noted in 10/35 (28.6%) and microcephaly in 2/35 (5.7%) individuals. Congenital anomalies were diverse and included palatal, uvular, or laryngeal anomalies (11/35, 31.4%); cardiac anomalies (11/35, 31.4%); and cryptorchidism (5/26 males, 19.2%) (Figure 1, Table 1 and Table S2).

There was no recognizable facial gestalt; however, we noted deeply set eyes with upper eyelid fullness in 9/35 (25.7%) individuals. Other craniofacial features in some individuals included cleft (overt and submucous) or high palate (10/35, 28.6%), midface retrusion with class III malocclusion (1/35, 2.9%), and a tall or broad forehead (4/35, 11.4%). In individual 19 with somatic mosaicism of the *FBXW7* variant, we observed cutaneous Blaschkoid dyspigmentation.

Neuroimaging was undertaken in 17 individuals (15 by MRI, one by CT, and one by both modalities); brain anomalies were identified in 13/17 (76.5%) individuals and included an absent, hypoplastic, or dysplastic corpus callosum (7/17; 41.2%); an abnormal cerebellum (5/17; 29.4%); delayed myelination (2/17; 11.7%); a thick brainstem (2/17; 11.7%); and polymicrogyria (2/17; 11.7%) (Table 1 and Table S2). Scattered small subcortical calcifications were noted on a computed tomography brain scan of individual 22. Ten brain MRI scans of seven individuals (3, 18, 19, 21, 25, 28, and 31) were available for systematic review by a pediatric neuroradiologist (S.M.). The most common anomalies were related to the posterior fossa, where the cerebellum was enlarged or at the upper limit of the normal range, except in individual 19, who had severe cerebellar atrophy with large folia and a thick dysmorphic corpus callosum and brainstem. Notably, this individual, previously reported as patient IV.1,[57] also has a familial *CACNA1A* pathogenic variant of variable expressivity, c.835C>T (p.Arg279Cys) (GenBank: NM_023035.2). Although *FBXW7* is a known tumor suppressor, none of the individuals in our cohort has so far developed cancer; the oldest individual is 44 years old. Notably, 13 of the 28 variants observed in this cohort are also reported in somatic form in the COSMIC database, which has collated 1,481 (440 unique) known somatic variants that span the entire coding region of *FBXW7* in various cancer types (Figure S1 and Table S1).

Germline *FBXW7* missense variants identified in this cohort cluster within the substrate-binding surface of the WD40 domain

We identified 28 germline *FBXW7* variants in 35 individuals (Figure 2 and Table S1). Two individuals had large chromosomal deletions encompassing *FBXW7*. One individual had a canonical splice-site variant, c.1236+2T>A, which is predicted to result in donor-site loss. Seven individuals (three *de novo* and four familial) had frameshift variants affecting the longest transcript (GenBank: NM_001349798.2). Two variants, c.1331_1332del (p.Lys444Serfs*27) and c.1332dup (p.Val445Serfs*27), are predicted to undergo nonsense-mediated decay (NMD) with presumed loss of function (LoF). In contrast, c.1331_1332del (p.Asn572Leufs*32) and c.1939A>T (p.Lys647*) are within the 54 bp upstream of the final intron/exon junction and are predicted to escape NMD.[58] These truncated proteins might be targeted for degradation via the UPS. The remaining 25 individuals had 21 unique missense variants clustering at the carboxy-terminal half of the protein, and 16/21 (76.2%) of these variants occurred within the WD40 domain. Three variants, c.1267G>A (p.Gly423Arg); c.2020C>T (p.Arg674Trp); and c.2065C>T (p.Arg689Trp), were recurrent in unrelated individuals.

The crystal structure of the FBXW7 and SKP1 complex has been determined with the substrates CYCLIN E1 and DISC1.[47,59] The F-box domain located in the N-terminal half of FBXW7 mediates interaction with SKP1, whereas the WD40 domain forms a canonical eight-bladed β-propeller structure. Thirteen residues positioned at the top surface of the propeller directly interact with CYCLIN E1 (seven of these also interact with DISC1). The position of the variants identified in this study aligns with the residues required for this interaction: Arg441, Ser462, Arg465, Arg479, Arg505, and Ala599. A further four variants, c.1267G>A ((p.Gly423Arg)); c.1744T>G (p.Ser582Ala); c.2021G>C (p.Arg674Pro); and c.2020C>T (p.Arg674Trp), impact residues adjacent to critical residues Trp425, Leu583, Trp673, respectively.

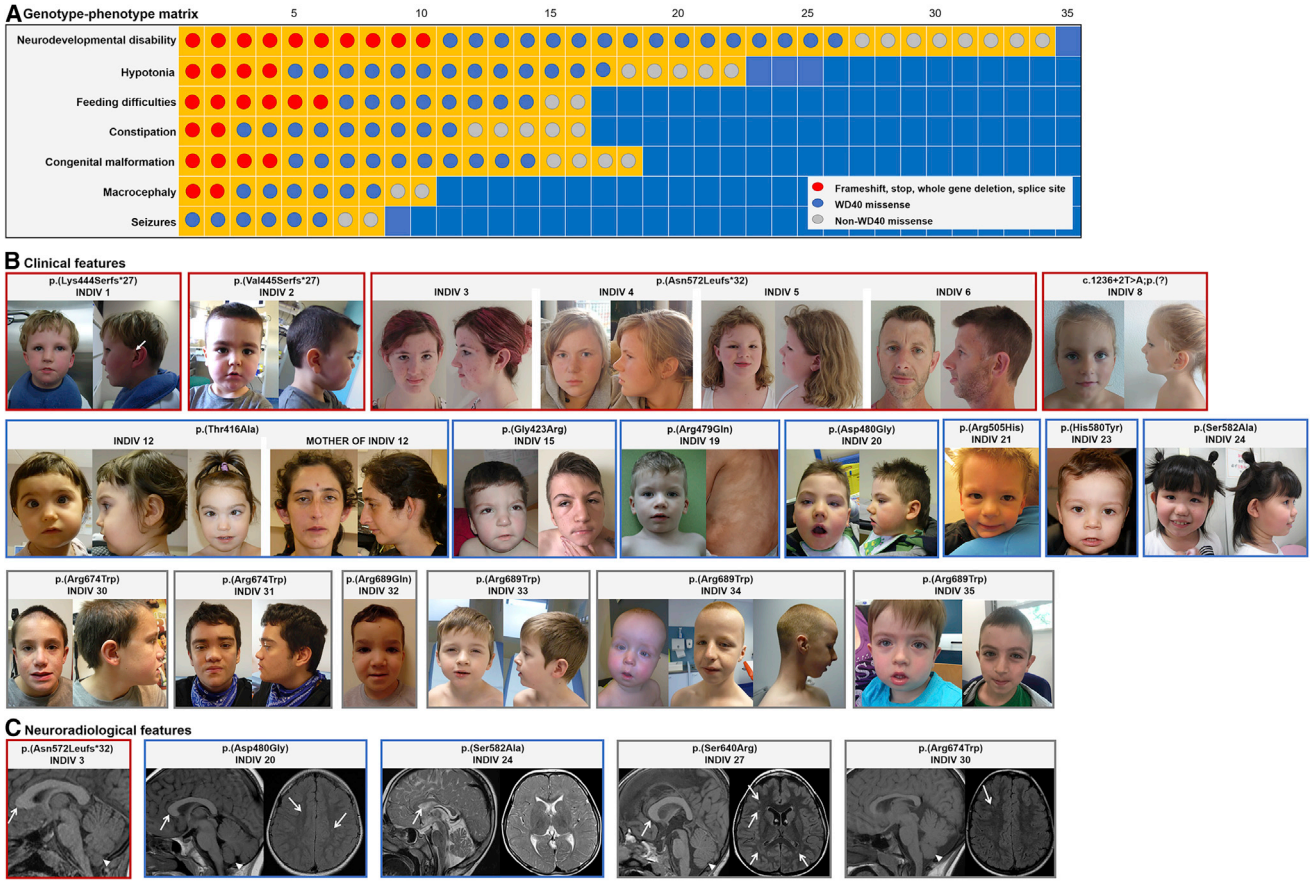

Figure 1. Characteristics of *FBXW7* neurodevelopmental syndrome

(A) Genotype-phenotype matrix of clinical features of key phenotypes associated with *FBXW7* neurodevelopmental variants. Each square represents an individual overlaid with variant class, and each row represents a clinical feature (affected—yellow; unaffected—blue). Variant types are depicted by dots: red (frameshift, stop, whole-gene deletion), blue (missense affecting WD40 domain), and gray (missense not in a WD40 domain).

(B) Clinical features of affected individuals depicting phenotype by variant type: individual 1, aged 3 years, frontal and lateral, with arrow marking preauricular pit; individual 2, aged 3 years 2 months, frontal and lateral; individual 3, aged 14 years 9 months, from family 1, frontal and lateral; individual 4, aged 11 years 9 months, from family 1, frontal and lateral; individual 5, aged 6 years 3 months, from family 1, frontal and lateral; individual 6, aged 44 years, father of individuals 3–5 from family 1, frontal and lateral (note midface retrusion with class III malocclusion); individual 8, aged 5 years, frontal; individual 12 at 12 months, frontal, lateral, and at 26 months, frontal; mother of individual 12, aged 34 years, frontal and lateral; individual 15 at 3 years and 15 years; individual 19 at age 6 years, frontal, and with cutaneous Blaschkoid dyspigmentation suggestive of somatic mosaicism; individual 20 at 5 years, frontal and lateral; individual 21 at 3 years; individual 23 at 3 years; individual 24 at 5 years, frontal and lateral; individual 30 aged 15 years, frontal and lateral; individual 31 aged 15 years, frontal and lateral; individual 32 aged 2 years; individual 33 aged 10 years; individual 34 aged 1 year, frontal, and 12 years, frontal and lateral; individual 35 aged 3 years and 7 years, frontal. Deeply set eyes with upper eyelid fullness are evident in individuals 1, 2, 3, 5, 15, 21, 24, 32 (also in individual 21, not pictured).

(C) Neuroradiological features of selected individuals; sagittal images of T1-weighted brain MRI scans of individuals 3, 20, 27, and 30 and T2-weighted brain scan of individual 24, displaying large cerebellar vermis with tonsillar ectopia (white arrowheads) and thick callosal genu (arrows)—note the generally thinned corpus callosum in individuals 24 and 30; axial T1-weighted brain MRI scans of individuals 20, 27, and 30 and T2-weighted brain scan of individual 24 displaying scattered subcortical white-matter hyperintensities and severely delayed myelination, equivalent to 7–10 months.

To investigate the potential functional impact of the variants observed in this cohort, we mapped the amino acid position to the tertiary structure previously resolved for FBXW7 by crystallography (amino acids 263–706).[47] This demonstrated fthat the amino acids implicated in disease cluster at the surface of the substrate-binding interface (Figure 2 and Figure S2). Using the mutation Cutoff Scanning Matrix (mCSM) suite, we tested the predicted impact of each missense variant on the stability of FBXW7. Our tests demonstrated that 16/21 (76.2%) variants are predicted to decrease FBXW7 stability (average −0.735 ± 1.05 ΔΔG; Table S3). Next, we assessed the distance to the interface and the binding affinity to determine the potential of the variants to impact the interaction with CYCLIN E1. This demonstrated that FBXW7 missense variants identified in this cohort are positioned very close to the interaction interface (average 7.80 ± 5.24 Å) and that 13 (65%) are predicted to decrease the binding affinity of FBXW7 to CYCLIN E1 (average −0.39 ± 0.74 ΔΔG).

Table 1. Demographic and clinical features of affected individuals

Demographic features	
Sex	26 male/9 female
Age range	23 months–44 years, 6 months
Medical history	
Prenatal history	Normal; only one premature birth
Neurologic or CNS features	
Hypotonia (HP: 0001252)	22/35 (62.9%)
Seizures (HP: 0001250)	8/35 (22.9%)
Ataxia (HP: 0001251)	2/35 (5.7%)
Developmental regression (HP: 0002376)	1/35 (2.9%)
Abnormality of brain morphology (HP: 0012443)	13/17 (76.5%)
Macrocephaly (HP: 0000256)	10/35 (28.6%)
Microcephaly (HP: 0000252)	2/35 (5.7%)
Development, cognition, and psychiatric features	
Neurodevelopmental abnormality (HP: 0012759)	34/35 (97.1%)
Mild-moderate developmental delay or intellectual disability (HP: 0011342, HP: 0011343, HP: 0001256, and HP: 0002342)	27/35 (77.1%)
Severe global developmental delay or intellectual disability (HP: 0011344, HP: 0010864)	3/35 (8.6%)
Delayed speech and language development only (HP: 0000750)	1/35 (2.9%)
Specific learning disability (HP: 0001328)	2/35 (5.7%)
No neurodevelopmental abnormality	1/35 (2.9%)
Ophthalmologic features	
Strabismus (HP: 0000486)	5/35 (14.3%)
Abnormality of refraction (HP: 0000539)	6/35 (17.1%)
Astigmatism (HP: 0000483)	1/35 (2.9%)
Cerebral visual impairment (HP: 0100704)	1/35 (2.9%)
Audiology and hearing	
Mixed hearing impairment (HP: 0000410)	2/35 (5.7%)
Oral, dentition, and other ENT features	
Abnormal palate or uvula morphology (HP: 0000174), (HP: 0000172)	10/35 (28.6%)
Laryngeal cleft (HP: 0008751)	1/35 (2.9%)
Cardiac features	
Abnormal heart morphology (HP: 0001627)	11/35 (31.4%)
Respiratory features	
Recurrent pneumonia (HP: 0006532)	3/35 (8.6%)
Gastrointestinal and feeding features	
Feeding difficulties, including difficulties with nasogastric tube feeding (HP: 0011968, HP: 0040288)	16/35 (45.7%); 5/16 (31.3%)
Constipation (HP: 0002019)	16/35 (45.7%)
Gastresophageal reflux (HP: 0002020)	7/35 (20.0%)
Renal and genitourinary features	
Cryptorchidism (HP: 0000028)	5/26 (19.2%)
Hematologic features	
Neutropenia (HP: 0001875)	2/35 (5.7%)

n = 35; the frequency of clinical features is expressed as a fraction (and percentage) of the number assessed for that feature.

None of the variants detected in this cohort were observed in the population database, gnomAD v2.1 (140k exomes and genomes); however, for each of three variants—c.1394G>A (p.Arg465His), c.1436G>A (p.Arg479Gln), and c.1796C>T (p.Ala599Val) —an ultra-rare (allele frequency < 0.000005) alternative amino acid substitution, c.1393C>T (p.Arg465Cys), c.1435C>G (p.Arg479Gly), and c.1796C>G (p.Ala599Gly), respectively, has been observed. Nevertheless, these gnomAD substitutions were detected with allele balance rates of $\leq$ 45% where mosaicism could not be excluded (Table S1). To further assess how the variants observed in our cohort differed from variants reported in gnomAD, we investigated the impact of the 78 gnomAD missense variants on the resolved FBXW7 crystal structure. Although the majority of gnomAD variants (69; 89%) are predicted to have a destabilizing effect on the protein (average -0.723 ± 0.616 $\Delta\Delta G$), these variants are dispersed throughout the structure and positioned much farther from the interface with CYCLIN E1 (average 29.24 ± 17.24 Å) than the variants identified in this study (Figure S1 and Table S4). Furthermore, the gnomAD variants are predicted to have a very small effect on the binding affinity to CYCLIN E1 (average -0.064 ± 0.25 $\Delta\Delta G$).

Disease-associated variants impair the ability of FBXW7 to degrade substrates CYCLIN E1 and CYCLIN E2

To experimentally determine the functional consequences of *FBXW7* variants observed in this cohort, we cloned a subset into a mammalian expression vector with a C-terminal Myc tag and exogenously expressed in HEK293T cells. We selected variants within the WD40 domain (p.Gly423Arg, p.Asp480Gly, p.Val544Gly, and p.Ser640Arg) and outside the WD40 domain (p.Arg674Trp, p.Arg674Pro, and p.Arg689Gln) for cloning. The steady-state amount of FBXW7 protein was assessed by immunoblot, and all mutant proteins were detected (Figure 3A). Relative to $FBXW7^{wild\ type}$, $FBXW7^{Arg674Trp}$ and $FBXW7^{Arg689Gln}$ demonstrated a decrease in steady-state

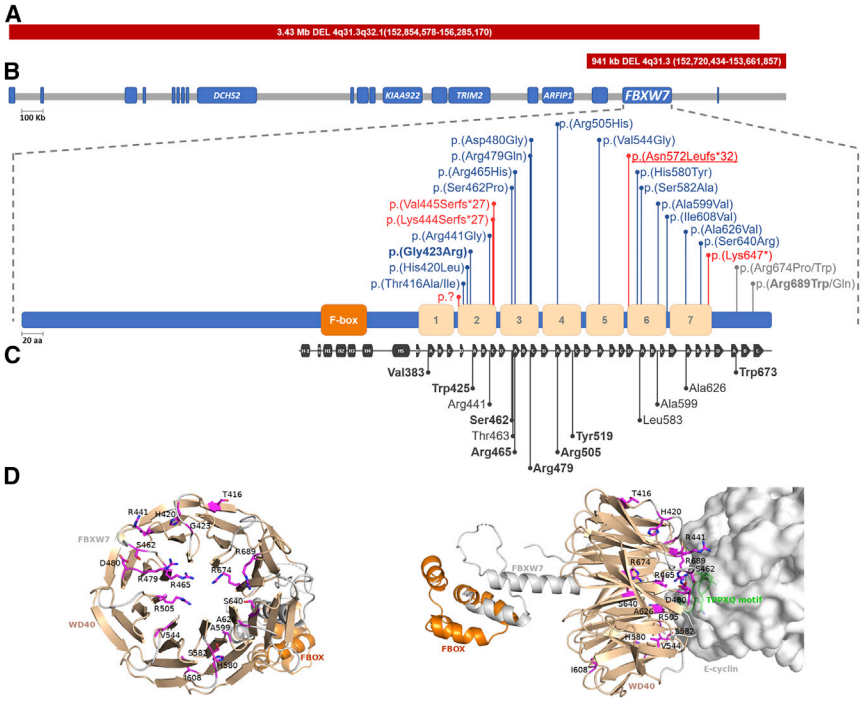

Figure 2. *FBXW7* variants detected in this cohort cluster within the substrate-binding surface of the WD40 domain

(A) The gene structure surrounding *FBXW7* on chromosome 4 (GRCh37: 4q31–3q32.1) demonstrates the genomic position of two large genomic deletions identified in individuals 8 and 9 (thick red bars above chromosome).

(B) Missense *FBXW7* variants identified in this study cluster within the WD40-repeat domain. Frameshift, stop-gain, or splice-site (red) and missense (blue—within the WD40 domain; and gray—outside the WD40 domain) variants are shown above the protein. Recurrent non-familial (bold); recurrent familial (underlined); F-box domain (orange); and a WD40-repeat domain (beige) derived from DECIPHER.

(C) Representation of the resolved structure of FBXW7 when in complex with a CYCLIN E1 degron (residues 360–390) demonstrating that the residues of FBXW7 that directly interact with CYCLIN E1 span similar residues as disease variants identified in this cohort. The positions of FBXW7 residues that directly interact with CYCLIN E1 are shown below the schematic depiction. F-box helices (rectangles H-1, H0, and H1–H3), linker α-helical domain (rectangles H4–H5), and the canonical eight-bladed β-propeller structure of the WD40 domain with each blade consisting of four antiparallel β strands (arrows [A–D] are shown,[47] Amino acids in bold have also been shown to directly interact with DISC1.[59]

(D) *FBXW7* variants associated with neurodevelopmental disorder are predominantly located at the substrate-binding surface of the WD40 repeat domain. The location of residues (in sticks with carbon atoms in purple, nitrogen atoms in blue, and oxygen atoms in red) impacted by mutations is shown on the tertiary structure of FBXW7 (cartoon) in configuration with CYCLIN E1 (surface in gray). The docking location of the conserved FBXW7 substrate-binding TPPXQ motif (cartoon in green) of CYCLIN E1 is demonstrated in close proximity to many of the impacted residues. Figure S1 provides an overlay of the variant residue with the wild-type residue for each individual variant, allowing identification of the change predicted in interaction for each missense variant.

protein amount, 0.42-fold and 0.16-fold, respectively, but only FBXW7^{Arg689Gln} reached statistical significance ($p = 0.007$) (Figure 3B). After treatment with UPS inhibitor MG-132, only FBXW7^{Arg689Gln} was found to have a steady-state protein amount that was increased relative to those of FBXW7$^{wild\ type}$ (3.4-fold, $p = 0.003$; Figure 3C). This suggests that most missense variants tested (six of seven) are unlikely to cause protein instability or consequent degradation by the UPS *in vivo*.

Next, we assessed the functional impact of these missense variants by co-expressing them with C-terminal V5-tagged substrates CYCLIN E1 and CYCLIN E2 in HEK293T cells. As expected, steady-state protein amounts of CYCLIN E1 and CYCLIN E2 were reduced when co-expressed with FBXW7$^{wild\ type}$ ($p = 0.002$ and $p = 0.0003$, respectively). This confirmed that exogenously expressed wild-type FBXW7 retains its ability to ubiquitinate and degrade CYCLIN E1 and CYCLIN E2 *in vitro* and is provides a suitable way to assess variant effects. Collectively, variants within the WD40 domain appear to have a greater impact on the ability of FBXW7 to degrade CYCLIN E1 and CYCLIN E2 than the variants outside the WD40 domain (Figures 3D and 3E and Figures 3G/and 3H, respectively). FBXW7^{Gly423Arg}, FBXW7^{Val544Gly}, and FBXW7^{Ser640Arg} were less efficient at degrading substrate; CYCLIN E1 steady-state protein amounts were elevated by 1.7-fold ($p = 0.002$), 1.4-fold ($p = 0.007$), and 1.3-fold ($p = 0.06$), respectively, in comparison to amounts seen with FBXW7^{wildtype} (Figure 3E). Similarly, CYCLIN E2 steady-state protein amounts were elevated by 2.5-fold ($p = 5 \times 10^{-5}$), 2.6-fold ($p = 4.6 \times 10^{-6}$), and 2.8-fold ($p = 7.5 \times 10^{-6}$), respectively. By contrast, FBXW7^{Asp480Gly} did not have a consistent effect on steady-state protein amounts of the two substrates. Although it was more efficient at degrading CYCLIN E1 than FBXW7^{wildtype} (0.6-fold, $p = 0.002$) it was less efficient at degrading CYCLIN E2 (1.8-fold, $p = 0.02$).

The variants outside the WD domain have a more subtle impact on CYCLIN E1 and CYCLIN E2 steady-state protein amounts. Although CYCLIN E1 steady-state protein amounts were slightly increased when co-expressed with FBXW7^{Arg674Trp} and FBXW7^{Arg674Pro}, this did not achieve statistical significance. However, the steady-state protein amounts of CYCLIN E2 was found to be elevated 1.6-fold ($p = 0.005$) and 1.6-fold ($p = 0.02$), respectively compared to FBXW7^{wildtype}. Notably, FBXW7^{Arg689Gln}, which was found to be turned over by the UPS, had CYCLIN E1 and CYCLIN E2 steady-state protein amounts comparable to FBXW7^{wildtype}, suggesting that the variant protein is able to efficiently degrade CYCLIN E1 and CYCLIN E2.

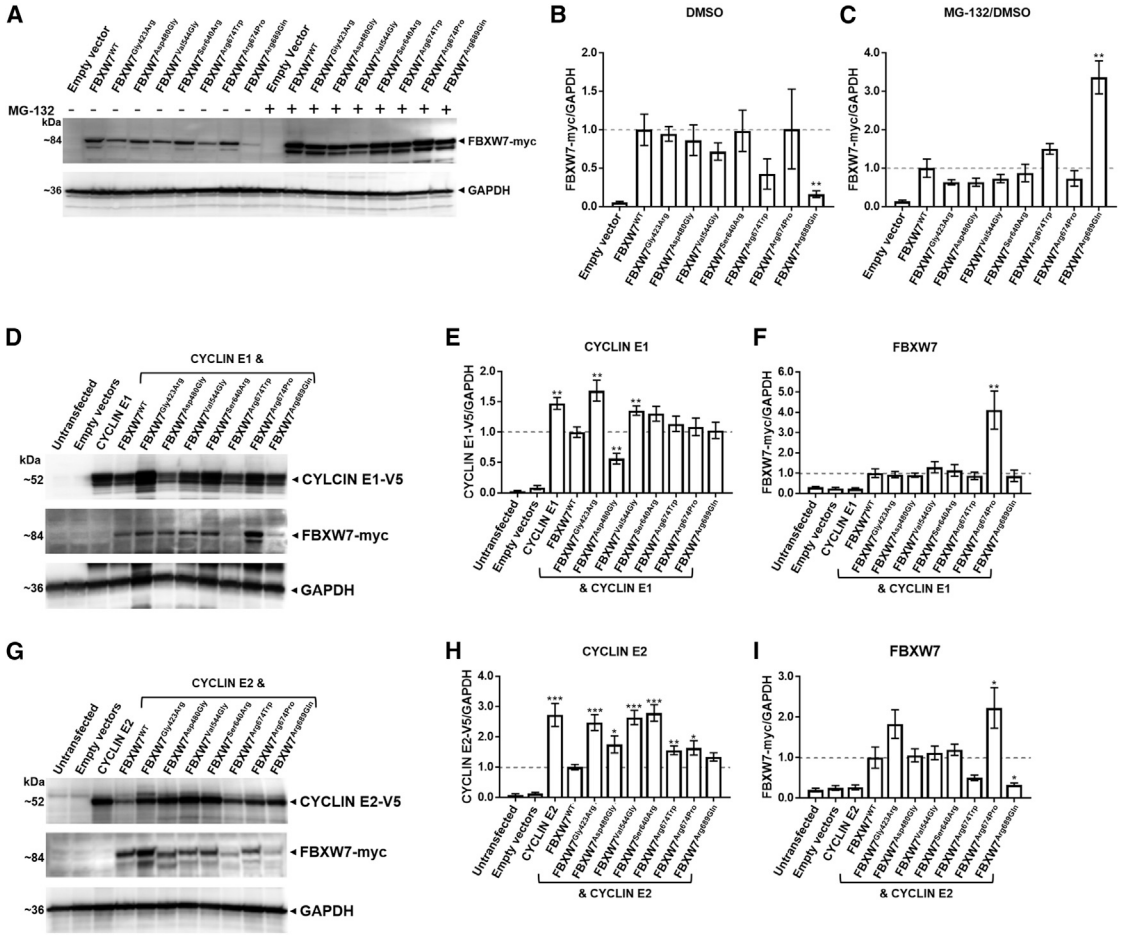

Figure 3. Disease-associated variants impair the ability of FBXW7 to degrade substrates CYCLIN E1 and CYCLIN E2

(A) The majority of disease-associated FBXW7 variants do not impact steady-state protein amounts. Representative immunoblots of wild-type or mutant FBXW7 with and without inhibition of the ubiquitin proteasome system are shown. HEK293T cells exogenously expressing wild-type FBXW7 or mutant FBXW7 with a C-terminal Myc tag for 32 h were treated with 5 μM MG-132 for 16 h (four independent replicates).

(B) Quantification of FBXW7:GAPDH from DMSO-treated samples of mutant FBXW7 protein in (A) relative to $FBXW7^{wild\ type}$; statistical support for altered steady-state amounts of the mutant FBXW7 protein was only evident for $FBXW7^{Arg689Gln}$ ($p = 0.007$).

(C) Quantification of FBXW7:GAPDH in MG-132-treated cells and versus their DMSO-treated counterpart in (A), demonstrating the change in steady-state mutant FBXW7 protein relative to $FBXW7^{wild\ type}$ protein after UPS inhibition; statistical support for altered steady-state protein amount was only evident for $FBXW7^{Arg689Gln}$ ($p = 0.003$).

(D) Certain FBXW7 mutant proteins demonstrate impaired CYCLIN E1 substrate degradation. Representative immunoblots of wild-type or mutant FBXW7 co-expressed with the substrate CYCLIN E1 are shown. Whole-cell lysates extracted from HEK293T cells that exogenously expressed wild-type FBXW7 or mutant FBXW7 with a C-terminal Myc tag and CYCLIN E1 with a C-terminal V5 tag for 48 h are shown (nine independent replicates).

(E) Quantification of CYCLIN E1:GAPDH in (D) for samples expressing mutant FBXW7 versus $FBXW7^{wild\ type}$ protein; statistical support for altered steady-state protein amount of CYCLIN E1 was evident for $FBXW7^{Gly423Arg}$ ($p = 0.002$), $FBXW7^{Asp480Gly}$ ($p = 0.002$), and $FBXW7^{Val544Gly}$ ($p = 0.007$).

(F) Quantification of FBXW7:GAPDH in (D) for FBXW7 mutant proteins versus $FBXW7^{wild\ type}$ protein when cells were co-transfected with CYCLIN E1. Statistical support for altered steady-state protein amount was evident only for $FBXW7^{Arg674Pro}$ ($p = 0.005$).

(G) The majority of FBXW7 mutant proteins demonstrate impaired CYCLIN E2 substrate degradation. Representative immunoblots of wild-type or mutant FBXW7 co-expressed with the substrate CYCLIN E2 are shown. Whole-cell lysates extracted from HEK293T cells that exogenously expressed wild-type FBXW7 or mutant FBXW7 with a C-terminal Myc tag and CYCLIN E2 with a C-terminal V5 tag for 48 h are shown (ten independent replicates).

(H) Quantification of CYCLIN E2:GAPDH in (G) for samples expressing FBXW7 mutant protein versus $FBXW7^{wild\ type}$ protein; statistical support for altered steady-state protein amount of CYCLIN E2 was evident for $FBXW7^{Gly423Arg}$ ($p = 0.00005$), $FBXW7^{Asp480Gly}$ ($p = 0.02$), $FBXW7^{Val544Gly}$ ($p = 0.000005$), $FBXW7^{Ser640Arg}$ ($p = 0.000007$), $FBXW7^{Arg674Trp}$ ($p = 0.005$), and $FBXW7^{Arg674Pro}$ ($p = 0.02$).

(I) Quantification of FBXW7:GAPDH in (G) for FBXW7 mutant proteins versus $FBXW7^{wild\ type}$ protein when cells were co-transfected with CYCLIN E2; statistical support for altered steady-state protein amount was evident for $FBXW7^{Arg674Pro}$ ($p = 0.04$) and $FBXW7^{Arg674Pro}$ ($p = 0.02$). All graphs present mean ± SEM. Student's t test: *$p < 0.05$; **$p < 0.01$; and ***$p < 0.001$.

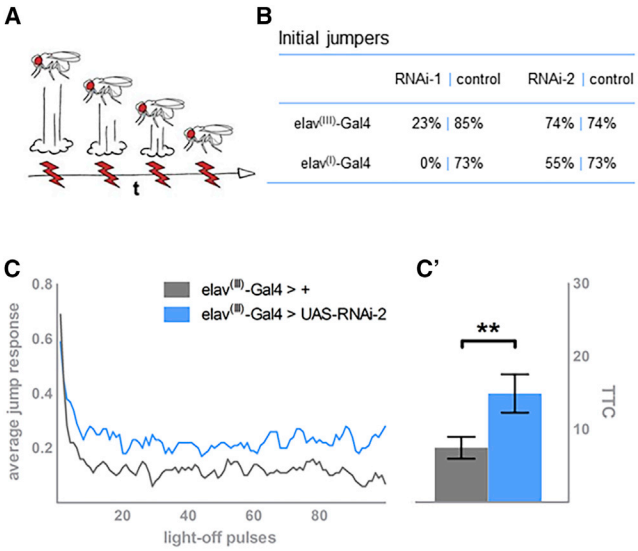

Figure 4. Knockdown of the *FBXW7 Drosophila* ortholog *ago*, specifically in neurons, can lead to deficits in habituation learning deficits and more severe neuronal dysfunction

(A) Simplified scheme of the habituation assay, used for assessing the stimulus-induced escape response of individual flies upon repeated exposure. In controls, as depicted, the initial high jump response gradually wanes. Of note, in reality, the amplitude of jumps does not wane, but the frequency decreases in the tested population.

B) Knockdown of *ago* with RNAi-1 and either elav$^{(I)}$-Gal4 or elav$^{(III)}$-Gal4 severely impairs jumping. Knockdown of *ago* with RNAi-2 driven by either driver is less detrimental, allowing assessment of habituation learning.

(C) Neuronal knockdown of *ago* by elav$^{(III)}$-Gal4 and RNAi-2 reduces the ability of flies to habituate to the stimulus (in blue); in ccontrast to their genetic-background controls (in gray), they keep jumping with increased frequency throughout the course of the experiment.

(D) Quantification of habituation according to *m*ean *t*rials *t*o no-jump *c*riterion (mTTC). Precise genotypes tested in (C) and (D): w/Y; 2xGMR-wIR/+; elav-Gal4$^{(III)}$, UAS-Dicer-2/ UAS-RNAi-2 (in blue; n = 71, mTTC = 14.91, p = 0.0015). Genetic background control w/Y; 2xGMR-wIR/+; elav-Gal4$^{(III)}$, UAS-Dicer-2/+ (in gray; n = 71, mTTC = 7.46). Statistical significance was assessed by a linear-model regression analysis on the log-transformed mTTC values; *p = 0.05, **p = 0.01, and ***p < 0.001.

FBXW7 mutant protein steady state protein amounts when co-expression with CYCLIN E1 or CYCLIN E2 were also assessed and it was found that FBXW7^{Arg674Pro} steady-state protein amounts were increased by 4.1-fold (p = 0.2) and 2.2-fold (p = 0.02) relative to FBXW7^{wildtype,} respectively (Figure 3F and 3I). These studies provide evidence in an *in vivo* cell culture model that FBXW7 missense variants identified in this cohort may destabilize the mutant protein and impact the ability of FBXW7 to degrade target substrates.

Neuronal knockdown of the *FBXW7 Drosophila* ortholog *archipelago* causes cognitive and severe neurological deficits

To address the consequences of partial loss of *FBXW7* function (as seen for most of the investigated variants) *in vivo*, we turned to *Drosophila melanogaster* as a model. The *Drosophila* genome encodes a one-to-one *FBXW7* ortholog termed archipelago (*ago*). The two proteins share 61% amino acid similarity, and the F-box domain and the seven WD40 repeats are highly conserved (Figure S3).[60] The E3 ubiquitin ligase function of FBXW7, its role in cell-cycle progression and growth, and its substrate cyclin e (ortholog of CYCLIN E1/2) have been confirmed in flies.[60,61] Partial loss of *ago* function was attempted with the UAS-Gal4 system,[62] and two previously validated lines carrying *ago*-specific UAS-RNA interference constructs (RNAi-1 and RNAi-2).[52,53] We first determined efficiency and relative strength of *ago* RNAi-1 and *ago* RNAi-2 constructs by quantitative RT-PCR upon ubiquitous knockdown by using the Act-GAL4 driver. The driver crossed to the genetic background of both RNAi lines served as a control in all experiments. Both lines led to lower levels of *ago*, albeit to different degrees. The expression level of *ago* relative to control levels was 19% in *ago* RNAi-1 (p = 0.005) and 67% (p = 0.11) in *ago* RNAi-2 (Figure S5). Because the latter was also previously shown to be effective in downregulating *ago*,[52] we crossed both lines and the control to the pan-neuronal promotor line elav-Gal4$^{(III)}$ to generate neuron-specific *ago* knockdown and control animals. Progeny of the appropriate genotypes were selected and subjected to characterization of basal motor function and habituation, a simple form of learning frequently defective in *Drosophila* models of intellectual disability,[56,63] in the light-off jump reflex habituation paradigm (Figure 4A). In this assay, individual flies are exposed to 100 light-off pulses (trials) with a 1 s inter-trial interval. Wild-type flies will initially startle in response the light-off stimulus, but they learn to suppress their escape response upon repeated, non-harmful stimuli.

Elav-Gal4$^{(III)}$-mediated neuronal knockdown of *ago* with the strong RNAi-1 line severely affected the flies' ability to jump and participate in the assay (23% of initial jumpers, Figure 4B), revealing moderate neurological defects, which precluded an assessment of habituation learning. Knockdown of *ago* with the mild RNAi-2 line was less detrimental and did not impair the jump response (74% of initial jumpers, Figure 4B), yet caused a deficit in habituation learning (Figure 4C): *ago* knockdown flies (in blue) adapted incompletely and more slowly to the light-off stimuli in comparison to their genetic background controls (gray). Quantification of habituation via the mean trials to no-jump criterion (mTTC, see "subjects and methods") demonstrated this defect to be significant; *ago* knockdown flies need on average twice as many trials as their controls to succeed in suppressing their jump response (n = 71, p = 0.002, Figure 4D). These results are in agreement with the qPCR results. Using an independent, stronger pan-neuronal promotor line (elav c155$^{(I)}$-GAL4)[64] further confirmed this finding. Elav c155$^{(I)}$-GAL4-induced RNAi-1 knockdown completely abolished jumping (0%, Figure 4B), whereas the combination with RNAi-2 affected initial jumping (55%, Figure 4B) but still resulted in

sufficient performance for habituation testing. This combination resulted in a faster decline of the jump response with decreased mTTC in comparison to the control ($p = 1.6 \times 10^{-3}$; Figure S4). Further experiments using a fatigue regime (see "subjects and methods") revealed that this premature decay in the jump response was due to impaired neuronal function, not to faster adaptation ($p = 1.4 \times 10^{-5}$; Figure S4). Together, our results showed that loss of the *FBXW7* fly ortholog *ago* affected learning or compromised neuronal function more severely the higher its level of knockdown.

Discussion

FBXW7 variants are associated with a variable neurodevelopmental syndrome

Here we provide detailed clinical and functional characterization of the neurodevelopmental syndrome associated with germline monoallelic variants in *FBXW7*. In support of our finding, *FBXW7* was recently identified as one of 28 developmental-disorder-associated genes in a large multicenter cohort by bioinformatic analysis for gene-specific enrichment of *de novo* mutations, but without deep phenotyping.[65] The neurodevelopmental phenotype involves mild to severe global developmental delay and intellectual disability. At the mildest end of the spectrum, isolated speech delay (n = 1) and learning difficulties or borderline intellect (n = 2) were observed; only one individual was reported to have no neurodevelopmental issues (but had hypotonia). In contrast, the majority of the cohort had mild to moderate intellectual disability (n = 27), and severe neurodevelopmental disability was observed in three individuals, including one with an additional diagnosis of familial *CACNA1A*-related disorder[57] and another with episodic developmental regression. However, in the latter proband, no other candidate genomic variants were identified as an alternative cause, and the reason for the regressive episodes remains unclear in this individual. After neurodevelopmental disability, the next most frequently observed neurologic feature was hypotonia, common also to the other F-box-related neurodevelopmental syndromes associated with germline pathogenic variants in *FBXL4*. *FBXO11*, *FBXW11*, and *FBXO28*,[9–11,13,16,17], but not in *FBXL3*.[18]

The neurodevelopmental phenotype associated with *FBXW7* has substantial clinical overlap with that of *FBXW11*; areas of overlap include mild to severe neurodevelopmental disability, speech and language delay, micro- or macrocephaly, and brain anomalies, including corpus callosum hypoplasia, dilated ventricles, and white matter atrophy. However, in contrast to individuals with *FBXW11* variants,[9] those in the *FBXW7* cohort did not commonly display autistic and/or stereotypical behaviors, psychiatric features, or ocular abnormalities.

It is notable that the *FBXO11*-related neurodevelopmental phenotype is just as variable; its severity ranges from normal cognition to profound disability.[10,11,66] Individuals with *FBXO11* variants were also found to have variability in head size, a similar observation made of the *FBXW7* cohort, although we found that macrocephaly was more common than microcephaly. Macrocephaly has been observed in an individual with focal segmental glomerulosclerosis, Wilms tumor, invasive ductal breast carcinoma, and a 157 kb partial chromosomal deletion of *FBXW7*, but her neurodevelopmental phenotype was not reported.[67] The DECIPHER database lists five individuals with copy-number losses that are various sizes and involve *FBXW7*. Three of these individuals have neurodevelopmental disability, and one experiences constipation. Another individual was reported with a 120.84 kb deletion including *FBXW7*, as well as two deletions in homozygous form on chromosomes 9 and 14, but the only listed phenotype was T cell acute lymphoblastic leukemia.

FBXW7 is a critical tumor suppressor and one of the most commonly mutated genes in human cancer (it is identified in 3.5% of all cancers).[68] More recently, truncating variants in *FBXW7* have been suggested to predispose the carrier to Wilms tumor in four individuals, and a missense variant was identified in an individual with a rhabdoid tumor; however, the individual's neurodevelopmental phenotype was not well described.[69] The oldest individual in this cohort is 44 years old, and although no cancer has so far been observed, longer-term follow-up will be necessary if we are to determine whether there is any cancer predisposition risk.

When we compared the frequency of key clinical features between variant types, no genotype-phenotype correlation was apparent, similar to findings for the comparison undertaken in a *FBXO11* cohort.[10] We observed three variants (p.Gly423Arg, p.Arg674Trp, and p.Arg689Trp) recurring in unrelated individuals. The degree of neurodevelopmental disability and hypotonia appeared to be consistent between individuals with the same variant. However, there was some variability in head size, and macrocephaly was inconsistently observed in each genotype. The familial cases demonstrated intra-familial variability. For instance, the family carrying the p.Asn572Leufs*32 variant (individuals 3–6) were ascertained from a speech-and-language-disorders cohort. The proband (individual 3) had cleft palate and neurodevelopmental disability, but her sisters were less severely affected. Their father (individual 6) only had borderline-low verbal IQ. Neuroimaging was only undertaken in the proband, but it would be interesting to investigate whether her sisters and father also had similar brain anomalies. Furthermore, the p.Asn572Leufs*32 variant is likely to escape NMD, as is the p.Lys647* variant identified in individual 7, whose phenotype is relatively mild compared to those of the individuals with missense variants. This observation suggests that a truncated FBXW7 might lead to a milder phenotype. We did not identify any individuals with variants affecting FBXW7's N-terminal region, including the F-box. It is possible that the phenotypic consequences of variants in this region are either lethal or sub-clinical, although the latter appears to be more

likely given the lack of regional missense constraint relative to the WD40 domain in gnomAD. Addressing this possibility, along with the possibility that milder phenotypes might emerge over time, will require the study of additional affected individuals.

Another explanation for variable expressivity among individuals carrying pathogenic variants in the same gene is the possibility of multiple diagnoses.[70] This is well illustrated in individuals 19 and 31. Individual 19, in addition to carrying the mosaic *FBXW7* variant, is heterozygous for a maternally inherited *CACNA1A* pathogenic variant.[57] This combination is responsible for his more severe phenotype compared to that of his relatives carrying the *CACNA1A* variant alone and that of the other individuals in the *FBXW7* cohort, and is likely to also explain the difference in his cerebellar abnormalities. Individual 31 also has a *de novo* likely pathogenic variant in *KMT2D*, and this is reflected in his facial features, including long palpebral features characteristic of Kabuki syndrome and the deeply set eyes and upper eyelid fullness observed in other individuals in the *FBXW7* cohort. We also considered whether mosaicism for the *FBXW7* variant might account for phenotypic attenuation or variable expressivity. We found that individuals 19 and 25 had clinical and genomic features suggestive of mosaicism, yet their phenotype was typical and no less severe than the rest of the cohort, which probably reflects the variable consequences of mosaicism. The emerging phenotype associated with variants in FBX genes appears to be characterized by neurodevelopmental disability with variable involvement of other systems. We speculate that these FBX proteins might function in convergent molecular and/or developmental pathways and that other FBX-related genes might subsequently be identified as playing a role in neurodevelopmental disorders.

FBXW7 missense variants identified in this cohort impair substrate turnover

Individuals harboring germline *FBXW7* variants in this study demonstrate considerable phenotypic heterogeneity. *FBXW7* encodes three isoforms; FBXW7α, FBXW7β, and FBXW7γ. All three contain the F-box and WD40 domain, but they differ at the N-terminal sequences that dictate their subcellular location; nucleus, cytoplasm, and nucleolus, respectively.[71] Studies in mice indicate that the isoforms also demonstrate different tissue specificity.[72] All variants identified in this study, whole-gene deletions as well as LoF, truncating, and missense variants, are predicted to affect the function of all three FBXW7 isoforms. In addition, FBXW7 has been shown to undergo multiple post-translational modifications, including auto-ubiquitination, de-ubiquitination, and dimerization (reviewed in[8]). There are numerous reported FBXW7 substrates, including CYCLIN E1/E2,[61,73,74] PSEN1,[75] NOTCH1/2/4,[76,77] MYC,[78] JUN,[79,80] REV-ERBα,[81,82] KLF5,[79] DISC1,[59] MCL-1,[81] CCDC6,[83] and mTOR.[84] FBXW7 recognizes substrates upon phosphorylation at a conserved Cdc4 phosphodegron, a short linear motif that is inert until phosphorylated.[8] Substrate binding occurs when the degron phosphorylations interact with two FBXW7 β-propeller pockets and upstream phosphodegron residues fit into a hydrophobic groove.[85] Our *in silico* protein modeling suggests the amino acids implicated in this neurodevelopmental syndrome mainly cluster at the surface of the substrate-binding interface and are likely to impair substrate binding (Figure 2). We have demonstrated that some *FBXW7* missense variants can affect steady-state FBXW7 protein amounts, suggesting that in some cases protein instability might lead to degradation of the mutant protein via the UPS. However, the majority of mutant proteins investigated were not turned over by the UPS more than the wild-type protein but demonstrated reduced capacity to turn over known substrates CYCLIN E1 and CYCLIN E2 (Figure 3). Fascinatingly, one mutant, $FBXW7^{Asp480Gly}$, demonstrated divergent effects: it was less efficient at degrading CYCLIN E2 but more efficient at degrading CYCLIN E1 in comparison to $FBXW7^{wild\ type}$ and thus acted in a substrate-dependent manner. Collectively, our data suggest that the neurodevelopmental-disability-associated variants observed in this cohort are likely to alter binding affinity to substrates, and we hypothesize that other known substrates are likely to also be impacted.

Within a cell of an individual harboring a neurodevelopmental-disease-associated *FBXW7* missense variant, FBXW7 can exist as a monomer (wild type or mutant) or as dimers (either as wild type only and mutant only or as both wild type and mutant) that can function at the cytosol, nucleus, or nucleolus. The impact on protein stability, binding affinity, and ubiquitin-ligase activity is likely to be variant specific, and although we propose that the phenotype is largely reflective of haploinsufficiency or loss of function (evident in those individuals with whole-gene deletions and NMD-predicted variants), we cannot rule out the possibility that some variants might have alternative mechanisms. Interrogation of gnomAD demonstrates that *FBXW7* is intolerant of loss-of-function variation (pLI = 1.00), further supporting the notion that haploinsufficiency or loss of function is the predominant mechanism of disease. Some of the phenotypic variability of *FBXW7* neurodevelopmental disability might, at least in part, be reflective of the functional consequence of the genotype or other, yet-unidentified modifiers. Identification of additional individuals with a broader spectrum of *FBXW7* variants (including predicted LoF variants) associated with neurodevelopmental disability and further molecular characterization will most likely lead to a deeper understanding of genotype-phenotype correlation.

Animal models support a role for FBXW7 in development broadly and specifically in the nervous system

FBXW7 is a critical tumor suppressor and one of the most commonly deregulated ubiquitin-proteasome-system proteins in human cancer. However, this clinical cohort clearly demonstrates that *FBXW7* also functions in human neurological development. Animal *Fbxw7* models—knockout,

haploinsufficient, and knock-in—also support a fundamental role for FBXW7 in development broadly, and in the brain specifically. *Fbxw7*-knockout mice die *in utero* at embryonic day 10.5, and they manifest hematopoietic abnormalities as well as abnormalities of vascular development and heart-chamber maturation.[86,87] Heterozygous knock-in *FBXW7* human-cancer mutations p.Arg465Cys and p.Arg482Gln (in mice, affecting residues Arg468 and Arg482) lead to perinatal lethality as a result of abnormal lung development, open eyes at birth (43%), and/or cleft palate (30%).[87] Notably, heterozygous null animals show no lung abnormality, demonstrating that these missense variants are distinct from null alleles.[88] Furthermore, heterozygous conditional gut-specific deletion of *Fbxw7* (*villin-Cre*) result in an impaired differentiation of intestinal goblet cells,[88] providing support for a role for FBXW7 in the development and function of the gut, which is significant because nearly half of individuals in our cohort manifested constipation (16/35, 45.7%).

Fbxw7$^{\text{nestin-Cre}}$-knockout mice that lack expression exclusively in the central and peripheral nervous system (including in precursors of neuronal and glial cells) die in the perinatal period as a result of defective suckling and present with several morphological brain abnormalities, including third-ventricle dilation and distortion, hypoplastic pons, an abnormal cerebellum, and markedly reduced cellularity of the cortex. Notch, a key regulator of glial and neuronal cell fate in the brain, accumulates in cells and skews radial glia differentiation toward the astrocytic lineage by increasing apoptosis of neuronal precursors.[33,36] *Fbxw7* haploinsufficiency in the mouse nervous system has also been investigated with a nestin-Cre system and has been shown to be associated with impaired differentiation of neural stem cells; such an impairment has also been shown to occur via a Notch-dependent mechanism. During development, it is proposed that *Fbxw7* haploinsufficiency leads to alterations of Notch-mediated lateral inhibition, an interaction between adjacent cells that drives them toward different final states.[88] Collectively, these studies provide evidence that *Fbxw7* is a key regulator of neural-stem-cell differentiation and maintenance in the brain, and we speculate that dysregulation of Notch lateral inhibition during brain development might underpin the broad spectrum of brain abnormalities identified in *FBXW7* neurodevelopmental syndrome.

Several studies have also investigated the role of *FBXW7* orthologs in myelination. *Fbxw7*$^{\text{Cre-dhh}}$-knockout mice that lack expression in Schwann cells of the peripheral nervous system demonstrated enhanced myelination —these mice made thicker myelin sheaths and in some cases, unexpectedly, myelinated multiple axons in a manner similar to the way in which oligodendrocytes of the central nervous system myelinate axons. In addition, *Fbxw7*$^{\text{Cre-dhh}}$ knockout led to an early increase in Schwann cells, smaller Remak bundles, and hypermyelination. These effects could be ameliorated by knockout of the substrate mTOR, but had no effect on the myelination of multiple axons.[32] In the zebrafish central nervous system, *fbxw7*^{vu56} homozygous-mutant larvae and morpholino knockdown of *fbxw7* demonstrate excessive oligodendrocyte cells and hypermyelination as a result of elevated Notch and mTOR signaling.[31,34]

In this study, in light of the fact that neurodevelopmental disability was the major hallmark of this cohort, we specifically aimed to support the notion of the role of *FBXW7* in an intellectual-disability- and cognition-relevant assay. Specifically, we asked whether *FBXW7*, in addition to its functions in neural stem cells and glia, could also be required more directly, in postmitotic neurons, for basal neuronal and cognitive function. To address this, and also because, as in mice, *ago* null animals are embryonic lethal,[60,89] we targeted the gene in a tissue-specific manner. We used two pan-neuronal promotor lines and two independent RNAi lines to generate an allelic series. Our results revealed that the *FBXW7* ortholog *ago* is indispensable in postmitotic neurons; animals with the stronger promotor and UAS-RNAi line were severely impaired, whereas less-stringent conditions kept locomotor function intact and revealed deficits in habituation learning. The gene therefore joins a steeply increasing number of intellectual-disability- and autism-spectrum-disorder-associated genes[56,63,90] that are implicated in this fundamental form of learning that is crucial for information processing, sensory filtering, and cognition. These also include mTOR-pathway genes such as *PTEN* & TSC1,[56] to which *FBXW7* has already been connected.[31] Further studies should aim to dissect *FBXW7* targets that are mediating the defects in cognitive functioning and study their reversibility; the established *Drosophila* model is suitable for this purpose. Collectively, the multiple lines of evidence presented herein converge to support the identification of *FBXW7* variants as causal for a human neurodevelopmental disorder.

Data and code availability

The datasets supporting the current study have not been deposited in a public repository because of restrictions related to patient consent, but they are available from the corresponding author on request.

Supplemental information

Supplemental information can be found online at https://doi.org/10.1016/j.ajhg.2022.03.002.

Acknowledgments

The authors thank the affected individuals and all family members for participating in this research. Please see the supplemental information for a complete list of Acknowledgments and funding.

Declaration of interests

I.E.S. has served on scientific advisory boards for UCB, Eisai, GlaxoSmithKline, BioMarin, Nutricia, Rogcon, Chiesi, Encoded

Therapeutics, Xenon Pharmaceuticals, and Knopp Biosciences; has received speaker honoraria from GlaxoSmithKline, UCB, BioMarin, Biocodex, and Eisai; has received funding for travel from UCB, Biocodex, GlaxoSmithKline, Biomarin and Eisai; has served as an investigator for Zogenix, Zynerba, Ultragenyx, GW Pharma, UCB, Eisai, Anavex Life Sciences, Ovid Therapeutics, Epygenyx, Encoded Therapeutics and Marinus; and has consulted for Zynerba Pharmaceuticals, Atheneum Partners, Ovid Therapeutics, Care Beyond Diagnosis, Epilepsy Consortium and UCB. She may accrue future revenue on pending patent WO2009/086591; her patent for *SCN1A* testing is held by Bionomics and is licensed to various diagnostic companies; and she has a patent for a molecular diagnostic/therapeutic target for benign familial infantile epilepsy (BFIE) (PRRT2), WO/2013/059884. She receives and/or has received research support from the National Health and Medical Research Council of Australia, Medical Research Future Fund, Health Research Council of New Zealand, CURE, Australian Epilepsy Research Fund, and the National Institute of Neurological Disorders and Stroke of the National Institutes of Health. J.P. is co-chief scientific officer for Global Gene Corp. All other authors declare no competing interests.

Received: October 28, 2021
Accepted: February 28, 2022
Published: April 7, 2022

Web resources

DECIPHER, https://www.deciphergenomics.org/
ESP, http://evs.gs.washington.edu/EVS/
ExAC, http://exac.broadinstitute.org
GeneMatcher, https://genematcher.org/
Github, https://github.com
gnomAD, http://gnomad.broadinstitute.org/
Human Phenotype Ontology, https://hpo.jax.org/app/
Online Mendelian Inheritance in Man, http://www.omim.org
UCSC Genome Browser, https://genome.ucsc.edu
1000 Genomes, http://www.internationalgenome.org

References

1. Deciphering Developmental Disorders, S.; and Deciphering Developmental Disorders Study (2017). Prevalence and architecture of de novo mutations in developmental disorders. Nature *542*, 433–438. https://doi.org/10.1038/nature21062.
2. Lemke, J.R. (2020). Predicting incidences of neurodevelopmental disorders. Brain *143*, 1046–1048. https://doi.org/10.1093/brain/awaa079.
3. Wilfert, A.B., Sulovari, A., Turner, T.N., Coe, B.P., and Eichler, E.E. (2017). Recurrent de novo mutations in neurodevelopmental disorders: properties and clinical implications. Genome Med. *9*, 101. https://doi.org/10.1186/s13073-017-0498-x.
4. Bruel, A.L., Vitobello, A., Tran Mau-Them, F., Nambot, S., Sorlin, A., Denommé-Pichon, A.S., Delanne, J., Moutton, S., Callier, P., Duffourd, Y., et al. (2020). Next-generation sequencing approaches and challenges in the diagnosis of developmental anomalies and intellectual disability. Clin. Genet. *98*, 433–444. https://doi.org/10.1111/cge.13764.
5. Colas, P. (2020). Cyclin-dependent kinases and rare developmental disorders. Orphanet J. Rare Dis. *15*, 203. https://doi.org/10.1186/s13023-020-01472-y.
6. LiCausi, F., and Hartman, N.W. (2018). Role of mTOR Complexes in Neurogenesis. Int. J. Mol. Sci. *19*, E1544. https://doi.org/10.3390/ijms19051544.
7. Nguyen, K.M., and Busino, L. (2020). The Biology of F-box Proteins: The SCF Family of E3 Ubiquitin Ligases. Adv. Exp. Med. Biol. *1217*, 111–122. https://doi.org/10.1007/978-981-15-1025-0_8.
8. Zhang, Z., Hu, Q., Xu, W., Liu, W., Liu, M., Sun, Q., Ye, Z., Fan, G., Qin, Y., Xu, X., et al. (2020). Function and regulation of F-box/WD repeat-containing protein 7. Oncol. Lett. *20*, 1526–1534. https://doi.org/10.3892/ol.2020.11728.
9. Holt, R.J., Young, R.M., Crespo, B., Ceroni, F., Curry, C.J., Bellacchio, E., Bax, D.A., Ciolfi, A., Simon, M., Fagerberg, C.R., et al. (2019). De Novo Missense Variants in FBXW11 Cause Diverse Developmental Phenotypes Including Brain, Eye, and Digit Anomalies. Am. J. Hum. Genet. *105*, 640–657. https://doi.org/10.1016/j.ajhg.2019.07.005.
10. Gregor, A., Sadleir, L.G., Asadollahi, R., Azzarello-Burri, S., Battaglia, A., Ousager, L.B., Boonsawat, P., Bruel, A.L., Buchert, R., Calpena, E., et al.; University of Washington Center for Mendelian Genomics; and DDD Study (2018). De Novo Variants in the F-Box Protein FBXO11 in 20 Individuals with a Variable Neurodevelopmental Disorder. Am. J. Hum. Genet. *103*, 305–316. https://doi.org/10.1016/j.ajhg.2018.07.003.
11. Jansen, S., van der Werf, I.M., Innes, A.M., Afenjar, A., Agrawal, P.B., Anderson, I.J., Atwal, P.S., van Binsbergen, E., van den Boogaard, M.J., Castiglia, L., et al. (2019). De novo variants in FBXO11 cause a syndromic form of intellectual disability with behavioral problems and dysmorphisms. Eur. J. Hum. Genet. *27*, 738–746. https://doi.org/10.1038/s41431-018-0292-2.
12. Balak, C., Belnap, N., Ramsey, K., Joss, S., Devriendt, K., Naymik, M., Jepsen, W., Siniard, A.L., Szelinger, S., Parker, M.E., et al. (2018). A novel FBXO28 frameshift mutation in a child with developmental delay, dysmorphic features, and intractable epilepsy: A second gene that may contribute to the 1q41-q42 deletion phenotype. Am. J. Med. Genet. A. *176*, 1549–1558. https://doi.org/10.1002/ajmg.a.38712.
13. Schneider, A.L., Myers, C.T., Muir, A.M., Calvert, S., Basinger, A., Perry, M.S., Rodan, L., Helbig, K.L., Chambers, C., Gorman, K.M., et al. (2021). FBXO28 causes developmental and epileptic encephalopathy with profound intellectual disability. Epilepsia *62*, e13–e21. https://doi.org/10.1111/epi.16784.
14. Au, P.Y., Argiropoulos, B., Parboosingh, J.S., and Micheil Innes, A. (2014). Refinement of the critical region of 1q41q42 microdeletion syndrome identifies FBXO28 as a candidate causative gene for intellectual disability and seizures. Am. J. Med. Genet. A. *164A*, 441–448. https://doi.org/10.1002/ajmg.a.36320.
15. Cassina, M., Rigon, C., Casarin, A., Vicenzi, V., Salviati, L., and Clementi, M. (2015). FBXO28 is a critical gene of the 1q41q42 microdeletion syndrome. Am. J. Med. Genet. A. *167*, 1418–1420. https://doi.org/10.1002/ajmg.a.37033.
16. Bonnen, P.E., Yarham, J.W., Besse, A., Wu, P., Faqeih, E.A., Al-Asmari, A.M., Saleh, M.A., Eyaid, W., Hadeel, A., He, L., et al. (2013). Mutations in FBXL4 cause mitochondrial encephalopathy and a disorder of mitochondrial DNA maintenance. Am. J. Hum. Genet. *93*, 471–481. https://doi.org/10.1016/j.ajhg.2013.07.017.

17. Gai, X., Ghezzi, D., Johnson, M.A., Biagosch, C.A., Shamseldin, H.E., Haack, T.B., Reyes, A., Tsukikawa, M., Sheldon, C.A., Srinivasan, S., et al. (2013). Mutations in FBXL4, encoding a mitochondrial protein, cause early-onset mitochondrial encephalomyopathy. Am. J. Hum. Genet. *93*, 482–495. https://doi.org/10.1016/j.ajhg.2013.07.016.
18. Ansar, M., Paracha, S.A., Serretti, A., Sarwar, M.T., Khan, J., Ranza, E., Falconnet, E., Iwaszkiewicz, J., Shah, S.F., Qaisar, A.A., et al. (2019). Biallelic variants in FBXL3 cause intellectual disability, delayed motor development and short stature. Hum. Mol. Genet. *28*, 972–979. https://doi.org/10.1093/hmg/ddy406.
19. Charng, W.L., Karaca, E., Coban Akdemir, Z., Gambin, T., Atik, M.M., Gu, S., Posey, J.E., Jhangiani, S.N., Muzny, D.M., Doddapaneni, H., et al. (2016). Exome sequencing in mostly consanguineous Arab families with neurologic disease provides a high potential molecular diagnosis rate. BMC Med. Genomics *9*, 42. https://doi.org/10.1186/s12920-016-0208-3.
20. Labonne, J.D., Lee, K.H., Iwase, S., Kong, I.K., Diamond, M.P., Layman, L.C., Kim, C.H., and Kim, H.G. (2016). An atypical 12q24.31 microdeletion implicates six genes including a histone demethylase KDM2B and a histone methyltransferase SETD1B in syndromic intellectual disability. Hum. Genet. *135*, 757–771. https://doi.org/10.1007/s00439-016-1668-4.
21. Yokotsuka-Ishida, S., Nakamura, M., Tomiyasu, Y., Nagai, M., Kato, Y., Tomiyasu, A., Umehara, H., Hayashi, T., Sasaki, N., Ueno, S.I., and Sano, A. (2021). Positional cloning and comprehensive mutation analysis identified a novel KDM2B mutation in a Japanese family with minor malformations, intellectual disability, and schizophrenia. J. Hum. Genet. *66*, 597–606. https://doi.org/10.1038/s10038-020-00889-4.
22. Yeh, C.H., Bellon, M., and Nicot, C. (2018). FBXW7: a critical tumor suppressor of human cancers. Mol. Cancer *17*, 115. https://doi.org/10.1186/s12943-018-0857-2.
23. Sailo, B.L., Banik, K., Girisa, S., Bordoloi, D., Fan, L., Halim, C.E., Wang, H., Kumar, A.P., Zheng, D., Mao, X., et al. (2019). FBXW7 in Cancer: What Has Been Unraveled Thus Far? Cancers (Basel) *11*, E246. https://doi.org/10.3390/cancers11020246.
24. Song, Y., Lai, L., Chong, Z., He, J., Zhang, Y., Xue, Y., Xie, Y., Chen, S., Dong, P., Chen, L., et al. (2017). E3 ligase FBXW7 is critical for RIG-I stabilization during antiviral responses. Nat. Commun. *8*, 14654. https://doi.org/10.1038/ncomms14654.
25. Zhang, C., Chen, F., Feng, L., Shan, Q., Zheng, G.H., Wang, Y.J., Lu, J., Fan, S.H., Sun, C.H., Wu, D.M., et al. (2019). FBXW7 suppresses HMGB1-mediated innate immune signaling to attenuate hepatic inflammation and insulin resistance in a mouse model of nonalcoholic fatty liver disease. Mol. Med. *25*, 29. https://doi.org/10.1186/s10020-019-0099-9.
26. Onoyama, I., Suzuki, A., Matsumoto, A., Tomita, K., Katagiri, H., Oike, Y., Nakayama, K., and Nakayama, K.I. (2011). Fbxw7 regulates lipid metabolism and cell fate decisions in the mouse liver. J. Clin. Invest. *121*, 342–354. https://doi.org/10.1172/JCI40725.
27. Izumi, N., Helker, C., Ehling, M., Behrens, A., Herzog, W., and Adams, R.H. (2012). Fbxw7 controls angiogenesis by regulating endothelial Notch activity. PLoS ONE *7*, e41116. https://doi.org/10.1371/journal.pone.0041116.
28. Pronk, M.C.A., Majolée, J., Loregger, A., van Bezu, J.S.M., Zelcer, N., Hordijk, P.L., and Kovačević, I. (2019). FBXW7 regulates endothelial barrier function by suppression of the cholesterol synthesis pathway and prenylation of RhoB. Mol. Biol. Cell *30*, 607–621. https://doi.org/10.1091/mbc.E18-04-0259.
29. Gao, W., Guo, N., Zhao, S., Chen, Z., Zhang, W., Yan, F., Liao, H., and Chi, K. (2020). FBXW7 promotes pathological cardiac hypertrophy by targeting EZH2-SIX1 signaling. Exp. Cell Res. *393*, 112059. https://doi.org/10.1016/j.yexcr.2020.112059.
30. Thompson, B.J., Jankovic, V., Gao, J., Buonamici, S., Vest, A., Lee, J.M., Zavadil, J., Nimer, S.D., and Aifantis, I. (2008). Control of hematopoietic stem cell quiescence by the E3 ubiquitin ligase Fbw7. J. Exp. Med. *205*, 1395–1408. https://doi.org/10.1084/jem.20080277.
31. Kearns, C.A., Ravanelli, A.M., Cooper, K., and Appel, B. (2015). Fbxw7 Limits Myelination by Inhibiting mTOR Signaling. J. Neurosci. *35*, 14861–14871. https://doi.org/10.1523/JNEUROSCI.4968-14.2015.
32. Harty, B.L., Coelho, F., Pease-Raissi, S.E., Mogha, A., Ackerman, S.D., Herbert, A.L., Gereau, R.W., 4th, Golden, J.P., Lyons, D.A., Chan, J.R., and Monk, K.R. (2019). Myelinating Schwann cells ensheath multiple axons in the absence of E3 ligase component Fbxw7. Nat. Commun. *10*, 2976. https://doi.org/10.1038/s41467-019-10881-y.
33. Matsumoto, A., Onoyama, I., Sunabori, T., Kageyama, R., Okano, H., and Nakayama, K.I. (2011). Fbxw7-dependent degradation of Notch is required for control of "stemness" and neuronal-glial differentiation in neural stem cells. J. Biol. Chem. *286*, 13754–13764. https://doi.org/10.1074/jbc.M110.194936.
34. Snyder, J.L., Kearns, C.A., and Appel, B. (2012). Fbxw7 regulates Notch to control specification of neural precursors for oligodendrocyte fate. Neural Dev. *7*, 15. https://doi.org/10.1186/1749-8104-7-15.
35. Jandke, A., Da Costa, C., Sancho, R., Nye, E., Spencer-Dene, B., and Behrens, A. (2011). The F-box protein Fbw7 is required for cerebellar development. Dev. Biol. *358*, 201–212. https://doi.org/10.1016/j.ydbio.2011.07.030.
36. Hoeck, J.D., Jandke, A., Blake, S.M., Nye, E., Spencer-Dene, B., Brandner, S., and Behrens, A. (2010). Fbw7 controls neural stem cell differentiation and progenitor apoptosis via Notch and c-Jun. Nat. Neurosci. *13*, 1365–1372. https://doi.org/10.1038/nn.2644.
37. Ko, Y.U., Kim, C., Lee, J., Kim, D., Kim, Y., Yun, N., and Oh, Y.J. (2019). Site-specific phosphorylation of Fbxw7 by Cdk5/p25 and its resulting decreased stability are linked to glutamate-induced excitotoxicity. Cell Death Dis. *10*, 579. https://doi.org/10.1038/s41419-019-1818-4.
38. Ko, Y.U., Song, H.Y., Kim, W.K., Yune, T.Y., Yun, N., and Oh, Y.J. (2020). Calpain-mediated cleavage of Fbxw7 during excitotoxicity. Neurosci. Lett. *736*, 135265. https://doi.org/10.1016/j.neulet.2020.135265.
39. Philippakis, A.A., Azzariti, D.R., Beltran, S., Brookes, A.J., Brownstein, C.A., Brudno, M., Brunner, H.G., Buske, O.J., Carey, K., Doll, C., et al. (2015). The Matchmaker Exchange: a platform for rare disease gene discovery. Hum. Mutat. *36*, 915–921. https://doi.org/10.1002/humu.22858.
40. Sobreira, N., Schiettecatte, F., Valle, D., and Hamosh, A. (2015). GeneMatcher: a matching tool for connecting investigators with an interest in the same gene. Hum. Mutat. *36*, 928–930. https://doi.org/10.1002/humu.22844.

41. Richards, S., Aziz, N., Bale, S., Bick, D., Das, S., Gastier-Foster, J., Grody, W.W., Hegde, M., Lyon, E., Spector, E., et al.; ACMG Laboratory Quality Assurance Committee (2015). Standards and guidelines for the interpretation of sequence variants: a joint consensus recommendation of the American College of Medical Genetics and Genomics and the Association for Molecular Pathology. Genet. Med. *17*, 405–424. https://doi.org/10.1038/gim.2015.30.
42. Reese, M.G., Eeckman, F.H., Kulp, D., and Haussler, D. (1997). Improved splice site detection in Genie. J. Comput. Biol. *4*, 311–323. https://doi.org/10.1089/cmb.1997.4.311.
43. Hebsgaard, S.M., Korning, P.G., Tolstrup, N., Engelbrecht, J., Rouzé, P., and Brunak, S. (1996). Splice site prediction in Arabidopsis thaliana pre-mRNA by combining local and global sequence information. Nucleic Acids Res. *24*, 3439–3452. https://doi.org/10.1093/nar/24.17.3439.
44. Brunak, S., Engelbrecht, J., and Knudsen, S. (1991). Prediction of human mRNA donor and acceptor sites from the DNA sequence. J. Mol. Biol. *220*, 49–65. https://doi.org/10.1016/0022-2836(91)90380-o.
45. Jaganathan, K., Kyriazopoulou Panagiotopoulou, S., McRae, J.F., Darbandi, S.F., Knowles, D., Li, Y.I., Kosmicki, J.A., Arbelaez, J., Cui, W., Schwartz, G.B., et al. (2019). Predicting Splicing from Primary Sequence with Deep Learning. Cell *176*, 535–548.e24. https://doi.org/10.1016/j.cell.2018.12.015.
46. Yang, J., and Zhang, Y. (2015). I-TASSER server: new development for protein structure and function predictions. Nucleic Acids Res. *43* (W1), W174–W181. https://doi.org/10.1093/nar/gkv342.
47. Hao, B., Oehlmann, S., Sowa, M.E., Harper, J.W., and Pavletich, N.P. (2007). Structure of a Fbw7-Skp1-cyclin E complex: multisite-phosphorylated substrate recognition by SCF ubiquitin ligases. Mol. Cell *26*, 131–143. https://doi.org/10.1016/j.molcel.2007.02.022.
48. McLaren, W., Gil, L., Hunt, S.E., Riat, H.S., Ritchie, G.R., Thormann, A., Flicek, P., and Cunningham, F. (2016). The Ensembl Variant Effect Predictor. Genome Biol. *17*, 122. https://doi.org/10.1186/s13059-016-0974-4.
49. Liu, X., Jian, X., and Boerwinkle, E. (2011). dbNSFP: a lightweight database of human nonsynonymous SNPs and their functional predictions. Hum. Mutat. *32*, 894–899. https://doi.org/10.1002/humu.21517.
50. Pires, D.E., Ascher, D.B., and Blundell, T.L. (2014). mCSM: predicting the effects of mutations in proteins using graph-based signatures. Bioinformatics *30*, 335–342. https://doi.org/10.1093/bioinformatics/btt691.
51. Rodrigues, C.H.M., Myung, Y., Pires, D.E.V., and Ascher, D.B. (2019). mCSM-PPI2: predicting the effects of mutations on protein-protein interactions. Nucleic Acids Res. *47* (W1), W338–W344. https://doi.org/10.1093/nar/gkz383.
52. Li, L., Anderson, S., Secombe, J., and Eisenman, R.N. (2013). The Drosophila ubiquitin-specific protease Puffyeye regulates dMyc-mediated growth. Development *140*, 4776–4787. https://doi.org/10.1242/dev.096941.
53. Nam, S., and Cho, K.O. (2020). Wingless and Archipelago, a fly E3 ubiquitin ligase and a homolog of human tumor suppressor FBW7, show an antagonistic relationship in wing development. BMC Dev. Biol. *20*, 14. https://doi.org/10.1186/s12861-020-00217-1.
54. Livak, K.J., and Schmittgen, T.D. (2001). Analysis of relative gene expression data using real-time quantitative PCR and the 2(-Delta Delta C(T)) Method. Methods *25*, 402–408. https://doi.org/10.1006/meth.2001.1262.
55. Qureshi, R., and Sacan, A. (2013). A novel method for the normalization of microRNA RT-PCR data. BMC Med. Genomics *6* (*Suppl 1*), S14. https://doi.org/10.1186/1755-8794-6-S1-S14.
56. Fenckova, M., Blok, L.E.R., Asztalos, L., Goodman, D.P., Cizek, P., Singgih, E.L., Glennon, J.C., IntHout, J., Zweier, C., Eichler, E.E., et al. (2019). Habituation Learning Is a Widely Affected Mechanism in Drosophila Models of Intellectual Disability and Autism Spectrum Disorders. Biol. Psychiatry *86*, 294–305. https://doi.org/10.1016/j.biopsych.2019.04.029.
57. Angelini, C., Van Gils, J., Bigourdan, A., Jouk, P.S., Lacombe, D., Menegon, P., Moutton, S., Riant, F., Sole, G., Tournier-Lasserve, E., et al. (2019). Major intra-familial phenotypic heterogeneity and incomplete penetrance due to a CACNA1A pathogenic variant. Eur. J. Med. Genet. *62*, 103530. https://doi.org/10.1016/j.ejmg.2018.08.011.
58. Pawlicka, K., Kalathiya, U., and Alfaro, J. (2020). Nonsense-Mediated mRNA Decay: Pathologies and the Potential for Novel Therapeutics. Cancers (Basel) *12*, E765. https://doi.org/10.3390/cancers12030765.
59. Yalla, K., Elliott, C., Day, J.P., Findlay, J., Barratt, S., Hughes, Z.A., Wilson, L., Whiteley, E., Popiolek, M., Li, Y., et al. (2018). FBXW7 regulates DISC1 stability via the ubiquitin-proteosome system. Mol. Psychiatry *23*, 1278–1286. https://doi.org/10.1038/mp.2017.138.
60. Moberg, K.H., Bell, D.W., Wahrer, D.C., Haber, D.A., and Hariharan, I.K. (2001). Archipelago regulates Cyclin E levels in Drosophila and is mutated in human cancer cell lines. Nature *413*, 311–316. https://doi.org/10.1038/35095068.
61. Koepp, D.M., Schaefer, L.K., Ye, X., Keyomarsi, K., Chu, C., Harper, J.W., and Elledge, S.J. (2001). Phosphorylation-dependent ubiquitination of cyclin E by the SCFFbw7 ubiquitin ligase. Science *294*, 173–177. https://doi.org/10.1126/science.1065203.
62. Brand, A.H., and Perrimon, N. (1993). Targeted gene expression as a means of altering cell fates and generating dominant phenotypes. Development *118*, 401–415.
63. Stessman, H.A., Xiong, B., Coe, B.P., Wang, T., Hoekzema, K., Fenckova, M., Kvarnung, M., Gerdts, J., Trinh, S., Cosemans, N., et al. (2017). Targeted sequencing identifies 91 neurodevelopmental-disorder risk genes with autism and developmental-disability biases. Nat. Genet. *49*, 515–526. https://doi.org/10.1038/ng.3792.
64. Gonzales, E.D., Tanenhaus, A.K., Zhang, J., Chaffee, R.P., and Yin, J.C. (2016). Early-onset sleep defects in Drosophila models of Huntington's disease reflect alterations of PKA/CREB signaling. Hum. Mol. Genet. *25*, 837–852. https://doi.org/10.1093/hmg/ddv482.
65. Kaplanis, J., Samocha, K.E., Wiel, L., Zhang, Z., Arvai, K.J., Eberhardt, R.Y., Gallone, G., Lelieveld, S.H., Martin, H.C., McRae, J.F., et al.; Deciphering Developmental Disorders Study (2020). Evidence for 28 genetic disorders discovered by combining healthcare and research data. Nature *586*, 757–762. https://doi.org/10.1038/s41586-020-2832-5.
66. Fritzen, D., Kuechler, A., Grimmel, M., Becker, J., Peters, S., Sturm, M., Hundertmark, H., Schmidt, A., Kreiß, M., Strom, T.M., et al. (2018). De novo FBXO11 mutations are associated with intellectual disability and behavioural anomalies. Hum. Genet. *137*, 401–411. https://doi.org/10.1007/s00439-018-1892-1.

67. Roversi, G., Picinelli, C., Bestetti, I., Crippa, M., Perotti, D., Ciceri, S., Saccheri, F., Collini, P., Poliani, P.L., Catania, S., et al. (2015). Constitutional de novo deletion of the FBXW7 gene in a patient with focal segmental glomerulosclerosis and multiple primitive tumors. Sci. Rep. *5*, 15454. https://doi.org/10.1038/srep15454.
68. Consortium, A.P.G.; and AACR Project GENIE Consortium (2017). AACR Project GENIE: Powering Precision Medicine through an International Consortium. Cancer Discov. *7*, 818–831. https://doi.org/10.1158/2159-8290.CD-17-0151.
69. Mahamdallie, S., Yost, S., Poyastro-Pearson, E., Holt, E., Zachariou, A., Seal, S., Elliott, A., Clarke, M., Warren-Perry, M., Hanks, S., et al. (2019). Identification of new Wilms tumour predisposition genes: an exome sequencing study. Lancet Child Adolesc. Health *3*, 322–331. https://doi.org/10.1016/S2352-4642(19)30018-5.
70. Posey, J.E., Harel, T., Liu, P., Rosenfeld, J.A., James, R.A., Coban Akdemir, Z.H., Walkiewicz, M., Bi, W., Xiao, R., Ding, Y., et al. (2017). Resolution of Disease Phenotypes Resulting from Multilocus Genomic Variation. N. Engl. J. Med. *376*, 21–31. https://doi.org/10.1056/NEJMoa1516767.
71. Welcker, M., Orian, A., Grim, J.E., Eisenman, R.N., and Clurman, B.E. (2004). A nucleolar isoform of the Fbw7 ubiquitin ligase regulates c-Myc and cell size. Curr. Biol. *14*, 1852–1857. https://doi.org/10.1016/j.cub.2004.09.083.
72. Matsumoto, A., Onoyama, I., and Nakayama, K.I. (2006). Expression of mouse Fbxw7 isoforms is regulated in a cell cycle- or p53-dependent manner. Biochem. Biophys. Res. Commun. *350*, 114–119. https://doi.org/10.1016/j.bbrc.2006.09.003.
73. Strohmaier, H., Spruck, C.H., Kaiser, P., Won, K.A., Sangfelt, O., and Reed, S.I. (2001). Human F-box protein hCdc4 targets cyclin E for proteolysis and is mutated in a breast cancer cell line. Nature *413*, 316–322. https://doi.org/10.1038/35095076.
74. Klotz, K., Cepeda, D., Tan, Y., Sun, D., Sangfelt, O., and Spruck, C. (2009). SCF(Fbxw7/hCdc4) targets cyclin E2 for ubiquitin-dependent proteolysis. Exp. Cell Res. *315*, 1832–1839. https://doi.org/10.1016/j.yexcr.2008.11.017.
75. Li, J., Pauley, A.M., Myers, R.L., Shuang, R., Brashler, J.R., Yan, R., Buhl, A.E., Ruble, C., and Gurney, M.E. (2002). SEL-10 interacts with presenilin 1, facilitates its ubiquitination, and alters A-beta peptide production. J. Neurochem. *82*, 1540–1548. https://doi.org/10.1046/j.1471-4159.2002.01105.x.
76. Wu, G., Lyapina, S., Das, I., Li, J., Gurney, M., Pauley, A., Chui, I., Deshaies, R.J., and Kitajewski, J. (2001). SEL-10 is an inhibitor of notch signaling that targets notch for ubiquitin-mediated protein degradation. Mol. Cell. Biol. *21*, 7403–7415. https://doi.org/10.1128/mcb.21.21.7403-7415.2001.
77. Fukushima, H., Shimizu, K., Watahiki, A., Hoshikawa, S., Kosho, T., Oba, D., Sakano, S., Arakaki, M., Yamada, A., Nagashima, K., et al. (2017). NOTCH2 Hajdu-Cheney Mutations Escape SCF^{FBW7}-Dependent Proteolysis to Promote Osteoporosis. Mol. Cell *68*, 645–658.e5. https://doi.org/10.1016/j.molcel.2017.10.018.
78. Popov, N., Herold, S., Llamazares, M., Schülein, C., and Eilers, M. (2007). Fbw7 and Usp28 regulate myc protein stability in response to DNA damage. Cell Cycle *6*, 2327–2331. https://doi.org/10.4161/cc.6.19.4804.
79. Zhao, D., Zheng, H.Q., Zhou, Z., and Chen, C. (2010). The Fbw7 tumor suppressor targets KLF5 for ubiquitin-mediated degradation and suppresses breast cell proliferation. Cancer Res. *70*, 4728–4738. https://doi.org/10.1158/0008-5472.Can-10-0040.
80. Nateri, A.S., Riera-Sans, L., Da Costa, C., and Behrens, A. (2004). The ubiquitin ligase SCFFbw7 antagonizes apoptotic JNK signaling. Science *303*, 1374–1378. https://doi.org/10.1126/science.1092880.
81. Tong, J., Tan, S., Nikolovska-Coleska, Z., Yu, J., Zou, F., and Zhang, L. (2017). *FBW7*-Dependent Mcl-1 Degradation Mediates the Anticancer Effect of Hsp90 Inhibitors. Mol. Cancer Ther. *16*, 1979–1988. https://doi.org/10.1158/1535-7163.Mct-17-0032.
82. Zhao, X., Hirota, T., Han, X., Cho, H., Chong, L.W., Lamia, K., Liu, S., Atkins, A.R., Banayo, E., Liddle, C., et al. (2016). Circadian Amplitude Regulation via FBXW7-Targeted REV-ERBα Degradation. Cell *165*, 1644–1657. https://doi.org/10.1016/j.cell.2016.05.012.
83. Morra, F., Luise, C., Merolla, F., Poser, I., Visconti, R., Ilardi, G., Paladino, S., Inuzuka, H., Guggino, G., Monaco, R., et al. (2015). FBXW7 and USP7 regulate CCDC6 turnover during the cell cycle and affect cancer drugs susceptibility in NSCLC. Oncotarget *6*, 12697–12709. https://doi.org/10.18632/oncotarget.3708.
84. Okazaki, H., Matsunaga, N., Fujioka, T., Okazaki, F., Akagawa, Y., Tsurudome, Y., Ono, M., Kuwano, M., Koyanagi, S., and Ohdo, S. (2014). Circadian regulation of mTOR by the ubiquitin pathway in renal cell carcinoma. Cancer Res. *74*, 543–551. https://doi.org/10.1158/0008-5472.CAN-12-3241.
85. Welcker, M., Larimore, E.A., Swanger, J., Bengoechea-Alonso, M.T., Grim, J.E., Ericsson, J., Zheng, N., and Clurman, B.E. (2013). Fbw7 dimerization determines the specificity and robustness of substrate degradation. Genes Dev. *27*, 2531–2536. https://doi.org/10.1101/gad.229195.113.
86. Ikenoue, T., Terakado, Y., Zhu, C., Liu, X., Ohsugi, T., Matsubara, D., Fujii, T., Kakuta, S., Kubo, S., Shibata, T., et al. (2018). Establishment and analysis of a novel mouse line carrying a conditional knockin allele of a cancer-specific FBXW7 mutation. Sci. Rep. *8*, 2021. https://doi.org/10.1038/s41598-018-19769-1.
87. Davis, H., Lewis, A., Spencer-Dene, B., Tateossian, H., Stamp, G., Behrens, A., and Tomlinson, I. (2011). FBXW7 mutations typically found in human cancers are distinct from null alleles and disrupt lung development. J. Pathol. *224*, 180–189. https://doi.org/10.1002/path.2874.
88. Sancho, R., Blake, S.M., Tendeng, C., Clurman, B.E., Lewis, J., and Behrens, A. (2013). Fbw7 repression by hes5 creates a feedback loop that modulates Notch-mediated intestinal and neural stem cell fate decisions. PLoS Biol. *11*, e1001586. https://doi.org/10.1371/journal.pbio.1001586.
89. Mortimer, N.T., and Moberg, K.H. (2013). The archipelago ubiquitin ligase subunit acts in target tissue to restrict tracheal terminal cell branching and hypoxic-induced gene expression. PLoS Genet. *9*, e1003314. https://doi.org/10.1371/journal.pgen.1003314.
90. McDiarmid, T.A., Belmadani, M., Liang, J., Meili, F., Mathews, E.A., Mullen, G.P., Hendi, A., Wong, W.R., Rand, J.B., Mizumoto, K., et al. (2020). Systematic phenomics analysis of autism-associated genes reveals parallel networks underlying reversible impairments in habituation. Proc. Natl. Acad. Sci. USA *117*, 656–667. https://doi.org/10.1073/pnas.1912049116.

The American Journal of Human Genetics, Volume *109*

Supplemental information

Germline variants in tumor suppressor *FBXW7* lead to impaired ubiquitination and a neurodevelopmental syndrome

Sarah E.M. Stephenson, Gregory Costain, Laura E.R. Blok, Michael A. Silk, Thanh Binh Nguyen, Xiaomin Dong, Dana E. Alhuzaimi, James J. Dowling, Susan Walker, Kimberly Amburgey, Robin Z. Hayeems, Lance H. Rodan, Marc A. Schwartz, Jonathan Picker, Sally A. Lynch, Aditi Gupta, Kristen J. Rasmussen, Lisa A. Schimmenti, Eric W. Klee, Zhiyv Niu, Katherine E. Agre, Ilana Chilton, Wendy K. Chung, Anya Revah-Politi, P.Y. Billie Au, Christopher Griffith, Melissa Racobaldo, Annick Raas-Rothschild, Bruria Ben Zeev, Ortal Barel, Sebastien Moutton, Fanny Morice-Picard, Virginie Carmignac, Jenny Cornaton, Nathalie Marle, Orrin Devinsky, Chandler Stimach, Stephanie Burns Wechsler, Bryan E. Hainline, Katie Sapp, Marjolaine Willems, Ange-line Bruel, Kerith-Rae Dias, Carey-Anne Evans, Tony Roscioli, Rani Sachdev, Suzanna E.L. Temple, Ying Zhu, Joshua J. Baker, Ingrid E. Scheffer, Fiona J. Gardiner, Amy L. Schneider, Alison M. Muir, Heather C. Mefford, Amy Crunk, Elizabeth M. Heise, Francisca Millan, Kristin G. Monaghan, Richard Person, Lindsay Rhodes, Sarah Richards, Ingrid M. Wentzensen, Benjamin Cogné, Bertrand Isidor, Mathilde Nizon, Marie Vincent, Thomas Besnard, Amelie Piton, Carlo Marcelis, Kohji Kato, Norihisa Koyama, Tomoo Ogi, Elaine Suk-Ying Goh, Christopher Richmond, David J. Amor, Jessica O. Boyce, Angela T. Morgan, Michael S. Hildebrand, Antony Kaspi, Melanie Bahlo, Rún Friðriksdóttir, Hildigunnur Katrínardóttir, Patrick Sulem, Kári Stefánsson, Hans Tómas Björnsson, Simone Mandelstam, Manuela Morleo, Milena Mariani, TUDP Study Group, Marcello Scala, Andrea Accogli, Annalaura Torella, Valeria Capra, Mathew Wallis, Sandra Jansen, Quinten Waisfisz, Hugoline de Haan, Simon Sadedin, Broad Center for Mendelian Genomics, Sze Chern Lim, Susan M. White, David B. Ascher, Annette Schenck, Paul J. Lockhart, John Christodoulou, and Tiong Yang Tan

Acknowledgements

UDP-Vic acknowledges financial support from the Murdoch Children's Research Institute and the Harbig Foundation. The Rare Disease Flagship acknowledges financial support from the Royal Children's Hospital Foundation, the Murdoch Children's Research Institute, and the Harbig Foundation. The research conducted at the Murdoch Children's Research Institute and Baker Heart and Diabetes Institute was supported by the Victorian Government's Operational Infrastructure Support Program. Sequencing and analysis of Individual 1 were provided by the Broad Institute of MIT and Harvard Center for Mendelian Genomics (Broad CMG) and was funded by the National Human Genome Research Institute, the National Eye Institute, and the National Heart, Lung and Blood Institute grant UM1 HG008900 to Daniel MacArthur and Heidi Rehm.

The research pertaining to Individual 18 was supported by Telethon Undiagnosed Diseases Program (TUDP, GSP15001).

Sequencing of Individual 31 was funded by CREGEMES and Sanger validated by Claire Feger.

The research conducted at The Hospital for Sick Children (Canada) was supported in part by the Norm Saunders Complex Care Initiative, SickKids Centre for Genetic Medicine, and University of Toronto McLaughlin Centre.

The Chair in Genomic Medicine awarded to J.C. is generously supported by The Royal Children's Hospital Foundation.

This work was in part supported by a grant awarded under the Australian National Health & Medical Research Council (NHMRC) Centre for Research Excellence Scheme

(APP1117394) to L.E.R.B., A.S., T.R., K-R.D., C-A.E. and by a personal Vici grant (09150181910022) from The Netherlands Organization for Scientific Research (NWO) to A.S.

Research reported in this publication was supported by the National Cancer Institute of the National Institutes of Health under Award Number T32CA136432. The content is solely the responsibility of the authors and does not necessarily represent the official views of the National Institutes of Health.

D.B.A, T.B.N. and M.S. were supported by an Investigator Grant from the National Health and Medical Research Council (NHMRC) of Australia (GNT1174405).

This publication was supported by the National Center for Advancing Translational Sciences, National Institutes of Health, through Grant Number UL1TR001873. The content is solely the responsibility of the authors and does not necessarily represent the official views of the NIH.

M.S.H., M.B. and A.T.M. are funded by a National Health and Medical Research Council (NHMRC) Centre of Research Excellence Grant (1116976). M.B. was funded by an NHMRC Senior Research Fellowship (ID:1102971).

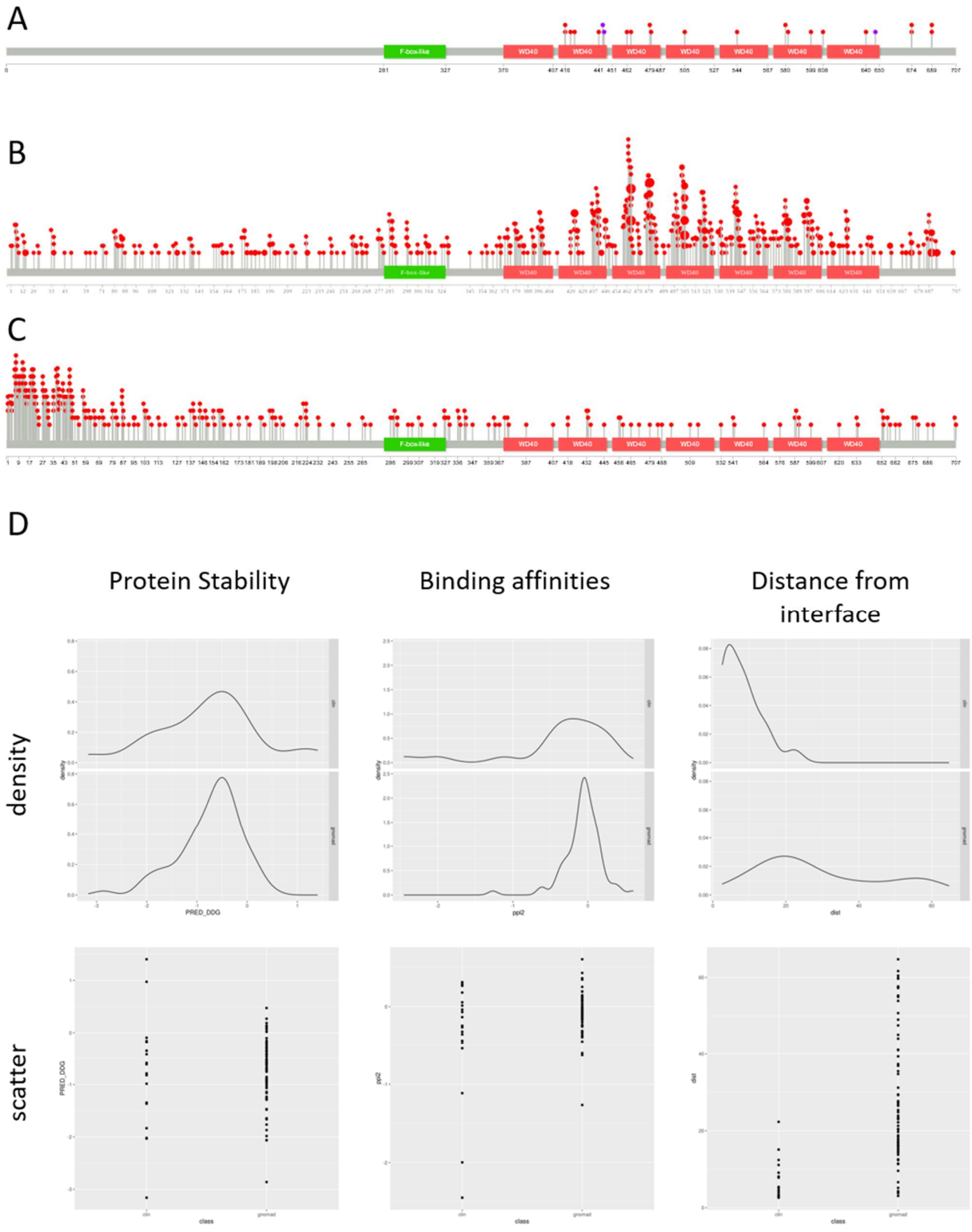

Figure S1: Distribution of neurodevelopment variants within FBXW7 relative to known COSMIC and gnomAD variants. (**A**) Location of patient-ascertained missense variants (red) and stop-gained and frameshift variants (purple). (**B**) Distribution of 1481 (440 unique) Catalogue Of Somatic Mutations In Cancer (COSMIC) somatic mutations (red) in FBXW7, where bubble size corresponds to the number of observations.

(**C**) Distribution of 280 missense variants (277 unique) in FBXW7 gnomAD v2.1 (140k exomes and genomes) variants with bubble size corresponding to the number of observations. (**D**) Comparison of structural predictors of neurodevelopmental disease variants to gnomAD variants. The gnomAD dataset was filtered to only those within the FBXW7 experimental structure, which includes residues 263 - 706, giving 78 variants only. Of these, the majority are very rare in the population (Allele Count: No. observations – 1:55, 2:14, 3:5, 6:2, 7:1, 12:1). Protein stability, determined using mutation Cutoff Scanning Matrix (mCSM), predicted the majority of gnomAD variants to also have a destabilizing effect, and to be similarly distributed to the patient cohort variants. Binding affinity, determined using mCSM-Protein–protein interactions (PPI) 1&2 (ΔΔG), suggests that gnomAD variants have a much smaller effect on binding affinity compared to the patient variants. Additionally, the gnomAD variants are dispersed throughout the structure and are, on average, further from the predicted interface with CYCLIN E1. See Table S3 for individual variant data.

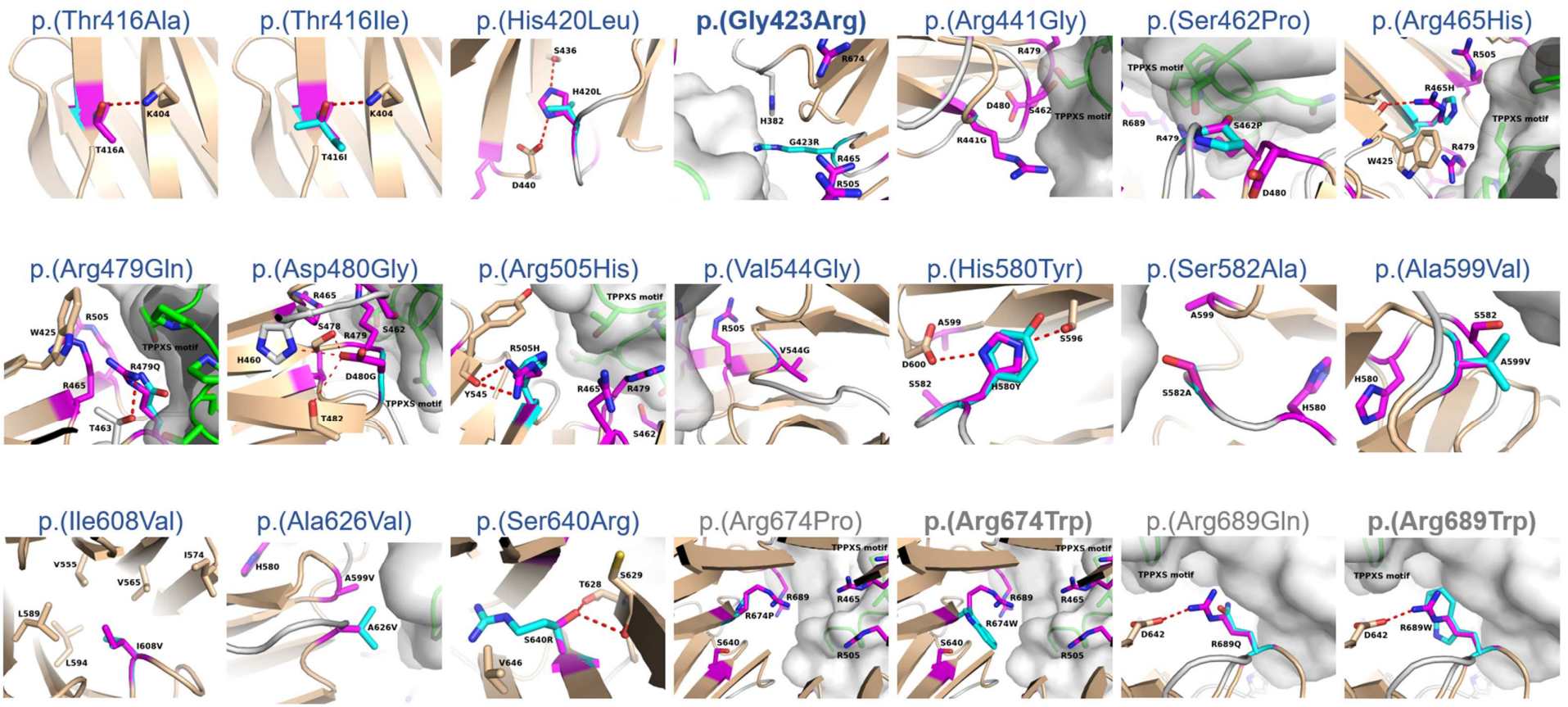

Figure S2: Change in interaction with CYCLIN E1 predicted by each variant

Zoom-in of the interaction of wild-type/variant residues of FBXW7 and its surrounding residues. The variant residues are overlaid on wild-type residues to identify the changes in interaction when variant occurs. FBXW7 is shown in brown ribbon, while CYCLIN E1 is shown in a light gray surface. All wild-type, and variant residues are shown in magenta and cyan sticks, respectively, while surrounding residues of FBXW7 and TPPXS motif of CYCLIN E1 are shown in brown and green sticks. The Oxygen and Nitrogen atoms are in red, and blue, respectively. Hydrogen bond interactions are shown in the red dash lines. Variants that reoccur are indicated by the bold title.

Figure S3: Amino acid alignment of human FBXW7 and Drosophila Ago sequences

Uniprot (www.uniprot.org) sequence alignment of Homo sapiens (ENSP00000474725/1-707) and Drosophila melanogaster (FBpp0073101/1-1326) FBXW7 (ago) proteins. Highlighted in yellow the F-Box, in gray the seven D40 repeats of the WD40 domain.

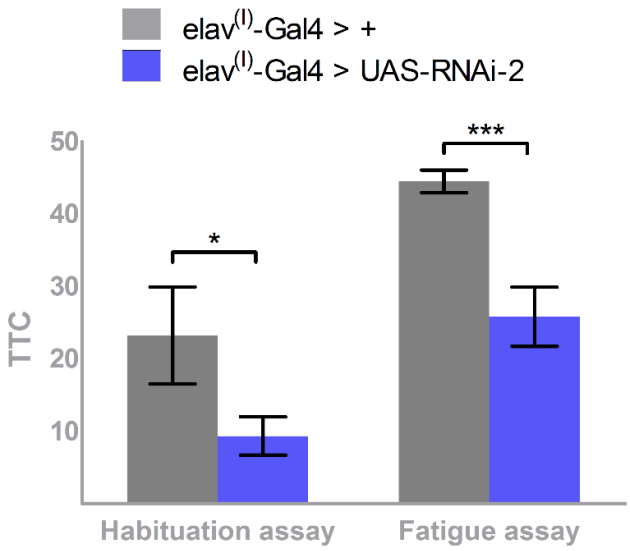

Figure S4: Knockdown of ago in Drosophila neurons induced by the elav$^{(l)}$-Gal4 driver causes faster decline of jump response due to fatigue

The knockdown of ago leads to a lower mTTC compared to the controls. Increasing the inter-trial interval in the fatigue assay, preventing habituation from being formed, demonstrates that this lower TTC is not due to improved habituation but due to motor fatigue. Precise genotypes tested in the fatigue assay: elav$^{(l)}$ C155-Gal4, GMR-wIR /Y; +/+; +/+ of genetic background control in gray and elav$^{(l)}$ C155-Gal4, GMR-wIR /Y; +/+; UAS-RNAi-2/+ of RNAi-2 knockdown in blue. $N_{control}$ = 42, N_{RNAi-2} = 48, $mTTC_{control}$ = 44.53, $mTTC_{RNAi-2}$= 25.85, p = 1.35E-5 . Statistical significance was assessed by a linear model regression analysis on the log transformed mTTC values, * P < 0.05, ** P < 0.01, *** P < 0.001.

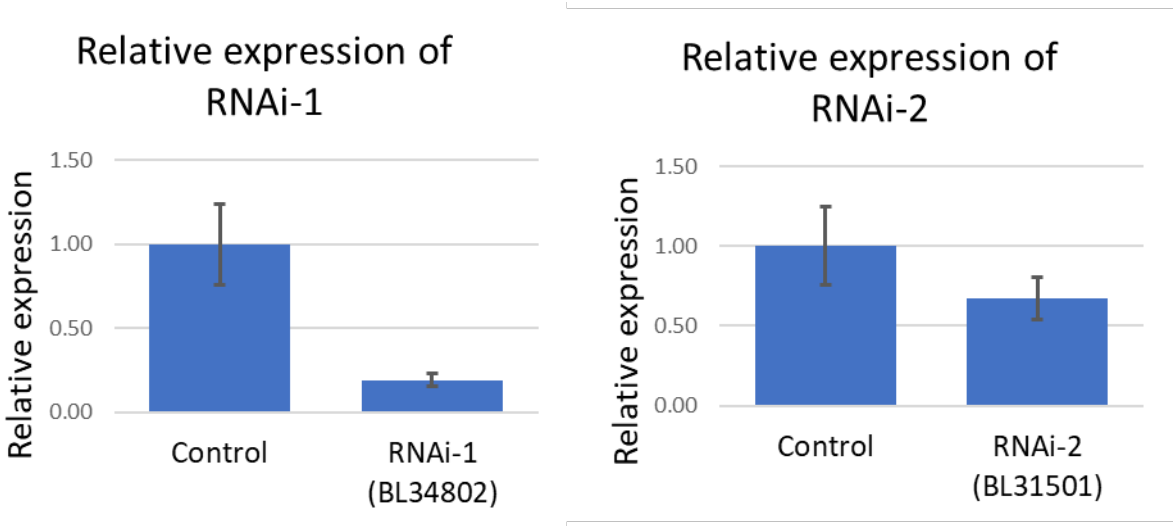

Figure S5: Relative expression of ago in Drosophila knockdown lines

Quantitative RT-PCR was performed on wandering L3 larva from RNAi-1 and RNAi-2 lines crossed to the ubiquitous Act-Gal4/TM3 Sb Tb driver to determine the level of *ago* expression using exon spanning primers to *ago* and *β'COP*. Error bars represent standard deviation.

Table S1: Analysis of FBXW7 neurodevelopmental syndrome variants

Individual	Inheritance	gDNA (Chr4; GRCh37)	Exon	cDNA	Protein	Occurs within WD40 domain	gnomAD - germline variants		COSMIC - somatic variants		CADD		FATHMM			GERP++ RS		MPC		MTR		MutationAssessor			PROVEAN			Polyphen2			SIFT			VEST4	
							Same variant	Alternative change at same amino acid residue	Same variant	Alternative change at same amino acid residue	score	rank score	score	rank score	predicted conseq-uence	score	rank score	score	rank score	score	rank score	score	rank score	predicted conseq-uence	score	rank score	predicted conseq-uence	score	rank score	predicted conseq-uence	score	rank score	predicted conseq-uence	score	rank score
1	de novo	g.153249446_153249447del	11	c.1331_1332del	p.(Lys444Serfs*27)	NMD predicted	Absent	3 LoF variants upstream	Absent	p.(Lys444Glyfs*55), p.(Lys444Argfs*32), p.(Lys444fs*2), more than 10 NMD predicted variants	-	-	-	-	-	-	-	-	-	-	-	-	-	-	-	-	-	-	-	-	-	-	-	-
2	de novo	g.153249446dup	11	c.1332dup	p.(Val445Serfs*27)	NMD predicted	Absent	3 LoF variants upstream	Absent	p.(Val445Cysfs*53), p.(Val445Aspfs*27), more than 10 NMD predicted variants	-	-	-	-	-	-	-	-	-	-	-	-	-	-	-	-	-	-	-	-	-	-	-	-
3	familial	g.153245477_153245478del	13	c.1713_1714del	p.(Asn572Leufs*32)	Truncation predicted	Absent	3 LoF variants upstream	Absent	More than 10 NMD predicted variants	-	-	-	-	-	-	-	-	-	-	-	-	-	-	-	-	-	-	-	-	-	-	-	-
4																																				
5																																				
6																																				
7	de novo	g.153244218T>A	14	c.1939A>T	p.(Lys647*)	Truncation predicted	Absent	3 LoF variants upstream	Absent	p.(Lys647Asnfs*5) in stomach carcinoma, more than 10 NMD predicted variants	-	-	-	-	-	-	-	-	-	-	-	-	-	-	-	-	-	-	-	-	-	-	-	-
8	de novo	g.153250822A>T	intron 10	c.1236+2T>A	p.?	N/A	Absent	Alternative change at same nucleotide: Absent	Present (stomach carcinoma)	Alternative change at same nucleotide: c.1236+2T>C (large intestine adenocarcinoma)																										
9	de novo	arr[GRCh37] 4q31.3(152720434_153661857)x1 dn	N/A	N/A	Entire gene deleted	N/A	N/A	N/A	N/A	N/A	-	-	-	-	-	-	-	-	-	-	-	-	-	-	-	-	-	-	-	-	-	-	-	-
10	de novo	arr[GRCH37] 4q31.3q32.1(152854578_156285170)x1 dn,4q32.1q34.1(161464002_175617314)x3 dn,4q34.1q34.3(175858796_179802170)x3 dn	N/A	N/A	Entire gene deleted	N/A	N/A	N/A	N/A	N/A	-	-	-	-	-	-	-	-	-	-	-	-	-	-	-	-	-	-	-	-	-	-	-	-
11	de novo	g.153249531G>A	11	c.1247C>T	p.(Thr416Ile)	Yes	Absent	Absent	Absent	Absent	4.22	0.86	0.13	0.61	T	5.90	0.95	2.78	0.99	0.56	0.97	1.37	0.34	L	-5.66	0.87	D	1.00	0.92	D	0.05	0.56	D	0.78	0.80
12	familial	g.153249532T>C	11	c.1246A>G	p.(Thr416Ala)	Yes	Absent	Absent	Absent	Absent	4.08	0.81	0.04	0.62	T	5.90	0.95	2.40	0.97	0.56	0.97	1.71	0.44	L	-4.80	0.81	D	0.98	0.81	D	0.02	0.59	D	0.80	0.81
13	de novo	g.153249519T>A	11	c.1259A>T	p.(His420Leu)	Yes	Absent	Absent	Absent	Multiple	4.13	0.83	-1.50	0.81	D	5.90	0.95	3.08	0.99	0.87	0.59	4.72	1.00	H	-10.92	0.99	D	1.00	0.97	D	0.00	0.91	D	0.94	0.95
14	de novo	g.153249511C>T	11	c.1267G>A	p.(Gly423Arg)	Yes	Absent	Absent	Present (multiple tissue types)	Multiple	4.35	0.89	0.16	0.61	T	5.90	0.95	3.01	0.99	0.67	0.92	1.21	0.30	L	-7.94	0.96	D	1.00	0.97	D	0.00	0.91	D	0.94	0.96
15																																				
16	de novo	g.153249457G>C	11	c.1321C>G	p.(Arg441Gly)	Yes	Absent	Absent	Present (lung carcinoma, rhabdomyosarcoma)	Multiple	3.72	0.70	2.02	0.21	T	4.08	0.47	3.14	0.99	0.55	0.97	0.42	0.13	N	-6.83	0.93	D	0.99	0.80	D	0.03	0.91	D	0.84	0.86
17	de novo	g.153249394A>G	11	c.1384T>C	p.(Ser462Pro)	Yes	Absent	Absent	Absent	p.(Ser462Tyr), p.(Ser462Phe)	4.33	0.89	0.86	0.74	T	6.05	0.98	2.78	0.99	0.54	0.97	2.65	0.77	M	-4.96	0.82	D	0.93	0.92	D	0.00	0.78	D	0.87	0.89
18	de novo	g.153249384C>T	11	c.1394G>A	p.(Arg465His)	Yes	Absent	p.(Arg465Cys) (allele balance 45% or lower)	Present (more than 5 tissue types)	Multiple	4.17	0.84	0.97	0.43	T	6.05	0.98	3.08	0.99	0.61	0.95	1.26	0.32	L	-4.96	0.82	D	1.00	0.97	D	0.02	0.91	D	0.78	0.79
19	de novo (mosaic 14%)	g.153247366C>T	12	c.1436G>A	p.(Arg479Gln)	Yes	Absent	p.(Arg479Gly) (allele balance 25-30%)	Present (more than 5 tissue types)	Multiple	4.17	0.84	1.02	0.41	T	5.72	0.89	2.93	0.99	0.80	0.75	0.84	0.21	L	-3.97	0.74	D	1.00	0.97	D	0.02	0.51	D	0.64	0.65
20	de novo	g.153247363T>C	12	c.1439A>G	p.(Asp480Gly)	Yes	Absent	Absent	Present (colon adenocarcinoma)	Multiple	4.46	0.91	-2.49	0.89	D	5.72	0.89	3.19	0.99	0.86	0.60	3.93	0.96	H	-6.95	0.93	D	1.00	0.97	D	0.00	0.91	D	0.99	0.99
21	de novo	g.153247288C>T	12	c.1514G>A	p.(Arg505His)	Yes	Absent	Absent	Present (more than 5 tissue types)	Multiple	4.17	0.85	0.05	0.62	T	4.87	0.63	3.08	0.99	0.55	0.97	1.50	0.38	L	-4.96	0.82	D	1.00	0.97	D	0.01	0.78	D	0.75	0.75
22	de novo	g.153247171A>C	12	c.1631T>G	p.(Val544Gly)	Yes	Absent	Absent	Present (large intestine adenocarcinoma)	p.(Val544Asp) (mouth squamous cell carcinoma)	4.29	0.88	-0.79	0.74	T	5.72	0.89	3.18	0.99	0.55	0.97	4.32	0.98	H	-6.95	0.93	D	1.00	0.92	D	0.00	0.91	D	0.64	0.66
23	de novo	g.153245453G>A	13	c.1738C>T	p.(His580Tyr)	Yes	Absent	Absent	Present (large intestine adenocarcinoma)	Multiple	4.09	0.82	-1.49	0.81	T	5.70	0.89	2.95	0.99	0.75	0.84	4.04	0.97	H	-5.96	0.89	D	1.00	0.97	D	0.01	0.56	D	0.89	0.89
24	de novo	g.153245447A>C	13	c.1744T>G	p.(Ser582Ala)	Yes	Absent	Absent	Absent	Multiple	4.02	0.79	1.00	0.41	T	5.70	0.89	0.97	0.97	0.76	0.83	1.46	0.37	L	-2.70	0.61	D	0.98	0.75	D	0.10	0.59	T	0.66	0.67
25	de novo (mosaic 23%)	g.153245395G>A	13	c.1796C>T	p.(Ala599Val)	Yes	Absent	p.(Ala599Gly) (allele balance 35-40%)	Absent	Absent	4.29	0.88	0.94	0.44	T	5.45	0.80	2.69	0.99	0.86	0.62	0.86	0.21	L	-3.96	0.74	D	1.00	0.84	D	0.02	0.78	D	0.63	0.64
26	de novo	g.153244280G>A	14	c.1877C>T	p.(Ala626Val)	Yes	Absent	Absent	Present (large intestine adenocarcinoma)	p.(Ala626Thr), p.(Ala626Pro), p.(Ala626Asp)	4.13	0.83	0.96	0.43	T	5.67	0.88	2.73	0.99	0.63	0.94	1.71	0.44	L	-3.91	0.74	D	1.00	0.91	D	0.00	0.78	D	0.74	0.76
27	de novo	g.153244237G>T	14	c.1920C>A	p.(Ser640Arg)	Yes	Absent	Absent	Absent	Absent	3.40	0.62	0.97	0.43	T	3.03	0.34	2.87	0.99	0.81	0.72	2.58	0.75	M	-4.91	0.82	D	1.00	0.92	D	0.06	0.60	T	0.87	0.92
28	de novo	g.153245369T>C	13	c.1822A>G	p.(Ile608Val)	No	Absent	Absent	Absent	Absent	2.43	0.40	0.90	0.45	T	5.45	0.80	1.39	0.85	0.37	0.99	0.18	0.09	N	-0.86	0.23	N	0.05	0.30	B	0.22	0.19	T	0.36	0.41
29	de novo	g.153244136C>G	14	c.2021G>C	p.(Arg674Pro)	No	Absent	Absent	Absent	p.(Arg674Trp), p.(Arg674Gln)	4.13	0.83	2.21	0.18	T	4.82	0.62	3.35	1.00	0.52	0.98	2.67	0.78	M	-6.83	0.93	D	1.00	0.89	D	0.00	0.78	D	0.81	0.85
30	de novo	g.153244137G>A	14	c.2020C>T	p.(Arg674Trp)	No	Absent	Absent	Present (glioma, cervix squamous cell carcinoma, atypical meningioma, prostate adenocarcinoma)	p.(Arg674Gln) (colon adenocarcinoma, stomach adenocarcinoma)	3.77	0.71	2.20	0.19	T	1.62	0.23	2.77	0.99	0.52	0.98	2.67	0.78	M	-7.80	0.96	D	1.00	0.92	D	0.00	0.91	D	0.80	0.88
31																																				
32	de novo	g.153244091C>T	14	c.2066G>A	p.(Arg689Gln)	No	Absent	Absent	Present (more than 5 tissue types)	p.(Arg689Glu), p.(Arg689Trp)	4.14	0.83	2.25	0.18	T	4.82	0.62	2.62	0.98	0.40	0.99	2.70	0.79	M	-3.92	0.73	D	1.00	0.89	D	0.03	0.68	D	0.82	0.87
33	de novo	g.153244092G>A	14	c.2065C>T	p.(Arg689Trp)	No	Absent	Absent	Present (more than 5 tissue types)	p.(Arg689Glu), p.(Arg689Gln)	4.22	0.86	2.20	0.19	T	5.67	0.88	2.77	0.99	0.40	0.99	2.70	0.79	M	-7.88	0.96	D	1.00	0.97	D	0.03	0.91	D	0.86	0.91
34																																				
35																																				

Tolerated (T); Deleterious (D); Low (L); Medium (M); High (H); Combined Annotation Dependent Depletion (CADD); Functional Analysis through Hidden Markov Models (FATHMM); Genomic Evolutionary Rate Profiling (GERP) ++ rejected substitutions" (RS) score; missense badness, PolyPhen-2, and constraint (MPC); Missense Tolerance Ratio (MTR); Protein Variation Effect Analyzer (PROVEAN); Polymorphism Phenotyping v2 (PolyPhen-2); Sorting Intolerant From Tolerant (SIFT); Variant Effect Scoring Tool (VEST).

Table S2: Clinical details of Individuals with FBXW7 neurodevelopmental syndrome

INDIVIDUAL	1	2	3	4	5	6	7	8	9	10	11	12
VARIANT TYPE	Predicted Loss of Function								GENE DELETION		MISSENSE, AFFECTING WD40 DOMAIN	
Variant Details												
Mode of discovery	Trio WES (Broad)	Exome sequencing with parental variant segregation	Family-based WGS	Family-based WGS	Family-based WGS	Family-based WGS	Solo WES	Trio WES	Array CGH Agilent 180K	SNP array (Illumina Infinium CoreExome-24 v1.1, hg19) [VCGS]	Gene Dx Trio WES	Solo WES
cDNA (NM_001349798.2)	c.1331_1332del	c.1332dup	c.1713_1714del	c.1713_1714del	c.1713_1714del	c.1713_1714del	c.1939A>T	c.1236+2T>A	N/A	N/A	c.1247C>T	c.1246A>G
gDNA (Chr4; GRCh37)	g.153249446_153249447del	g.153249446dup	g.153245477_153245478del	g.153245477_153245478del	g.153245477_153245478del	g.153245477_153245478del	g.153244218T>A	g.153250822A>T	arr [GRCh37] 4q31.3(152720434_153661857)x1 dn	arr[GRCH37] 4q31.3q32.1(152854578_156285170)x1 dn,4q32.1q34.1(161464002_175617314)x3 dn,4q34.1q34.3(175858796_179802170)x3 dn	g.153249531G>A	g.153249532T>C
Protein level	p.(Lys444Serfs*27)	p.(Val445Serfs*27)	p.(Asn572Leufs*32)	p.(Asn572Leufs*32)	p.(Asn572Leufs*32)	p.(Asn572Leufs*32)	p.(Lys647*)	p.?	DEL	DEL	p.(Thr416Ile)	p.(Thr416Ala)
Same variant in gnomAD	Absent	Absent	Absent	Absent	Absent	Absent	Absent	Absent	N/A	N/A	Absent	Absent
Alternative change at same amino acid residue in gnomAD	3 LoF variants upstream	3 LoF variants upstream	3 LoF variants upstream	3 LoF variants upstream	3 LoF variants upstream	3 LoF variants upstream	3 LoF variants upstream	Alternative change at same nucleotide: Absent	N/A	N/A	Absent	Absent
Same variant in COSMIC	Absent	Absent	Absent	Absent	Absent	Absent	Absent	Present (stomach carcinoma)	N/A	N/A	Absent	Absent
Alternative change at same amino acid residue in COSMIC	p.(Lys444Glyfs*55), p.(Lys444Argfs*32), p.(Lys444fs*2), more than 10 NMD predicted variants	p.(Val445Cysfs*53), p.(Val445Aspfs*27), more than 10 NMD predicted variants	More than 10 NMD predicted variants	More than 10 NMD predicted variants	More than 10 NMD predicted variants	More than 10 NMD predicted variants	p.(Lys647Asnfs*5) in stomach carcinoma, more than 10 NMD predicted variants	Alternative change at same nucleotide: c.1236+2T>C (large intestine adenocarcinoma)	N/A	N/A	Absent	Absent
Exon (NM_001349798.2)	11	11	13	13	13	13	14	intron 10	N/A	N/A	11	11
Occurs within WD40 domain	NMD predicted	NMD predicted	Truncation predicted	Truncation predicted	Truncation predicted	Truncation predicted	Truncation predicted	N/A	N/A	N/A	Yes	Yes
Inheritance	De novo	De novo	Paternal	Paternal	Paternal	Unknown	De novo	De novo	De novo	De novo	De novo	Inherited from mother with ID
Other candidate variants	*PDP2*: de novo LoF variant	No	No	No	No	No	No	No	Other inherited CNV (see below)	No	arr[GRCh37] 22q11.22q11.23(22997609_24961234)x3 pat	Yes NCOR1:NM_001190440:exon27:c.3734G>A:p.Arg1245Gln (mat) + NCOR1:NM_001190440:exon3:c.244C>A:p.(Pro82Thr) [no known disease association]
Demographic Features												
Sex	Male	Male	Female	Female	Female	Male	Male	Female	Male	Male	Male	Female
Age at last assessment	11 years	3 years 2 months	14 years 9 months	11 years 9 months	6 years 3 months	44 years 6 months	9y	5 years	7 years 2 months	2 years 2 months	18 yo	3y
Other												
Medical History												
Prenatal history	Increased nuchal fold at 12/40; normal chromosomes on amniocentesis	suspicion of preeclampsia	NAD	NAD	NAD	NAD	NAD	Born at 36+5 weeks, birth weight 3390 gr, Apgar scores 7 and 8. Neonatal jaundice treated with phototherapy.	Feet malposition during pregnancy. Mother had positive syphilis serology. Born at 40 weeks: (weight 4,080g; height 51 cm; OFC 35.5 cm). Neonatal jaundice. Negative syphilis serology at age 4 years	40+2/40 Emergency LUSCS for non-reassuring CTG. Nil antenatal concerns. Growth scans normal.	Unremarkable	no
Neurological problems	Hypotonia, tactile issues	Hypotonia	Hypotonia	NAD	NAD	NAD	NAD	No hypotonia	No neurological signs at testing.	Early hypotonia. No seizures. No regression.	After onset of seizures at age 7 years, his academic and intellectual functions deteriorated. Now in special ed.	Unsteady gait, Broad-based gait
Brain imaging	CT brain only - no structural abnormalities reported	N/A	Large cerebellar vermis with low-lying tonsils 3.6 mm below foramen magnum (Arnold-Chiari malformation)	N/A	N/A	N/A	N/A	N/A	N/A	N/A	N/A	thin corpus callosum
Developmental / cognitive / psychiatric problems	Global developmental delay ; now borderline IQ, attends mainstream school with some assistance; some anxiety	neonatal sucking difficulties delayed motor milestones : crawled on four legs at 18 months, walked independently at 21 months hypotonia and hyperlaxity. first words at 2,5 years. But at 3y 2 months : can solve puzzles easily, recognizes some letters, can count to five, recognizes colours. Can stay focused on an activity, nice. Speech iompediment but can produce more than 50 significant words	Global developmental delay; learning difficulty, ID, speech/language problems; delayed fine motor skills; sensory processing; ?ASD, no dx - paed says not enough for diagnosis, but all have mild symptoms	Delayed language; late walker; delayed socially; attention, mood; learning disorder; psychiatrist involved; ?ASD, no dx - paed says not enough for diagnosis, but all have mild symptoms	Delayed language; poor gross motor skills; attention/mood. ?ASD, WL for ASD ax through Austin health	Borderline non-verbal IQ	walk at 14m/speech delay/learning difficulties	Walking 18 months, first words 18 months. Speech development disorder. At the age of 4 years sentences of 3-4 words. Problems with pronounciation. Non-verbal development at low average level. Problems with loud noises, lives in her own world. No formal diagnosis of ASD. Mild sleeping problems.	Head control before 4 months, sit alone between 9 and 11 months, walk at age 16 months, mild delayed speech, learning difficulties and global reeducation since age 4 years (speech therapy, psychomotor therapy, psychological therapy). Anxiety, low self-confidence, impulsivity, low treatment speed index (74) and normal indices (between 88 and 97) of WPPSI-IV testing at age 5 years 3 months	Moderate global developmental delay. Early gross motor delays with minimal weight-bearing and lower limb use prior to age 2 years. First independent steps 22 months. No reported fine motor concerns. Severe speech delay: grunts / vocalises. Only "mum" and "dad" at 2 years.	Very mild delays in gross motor skills, mild cognitive delays (eg, color naming) until onset of seizures at age 7 yo, then more learning, attentional and cogntiive delays. Still with impaired coordination	Global moderate developmental delay, walking at 20m, firts words at 2y
Ophthalmologic problems	No	Astigmatism	No	No	No	No	No	Hypermetropia, amblyopia	Hypermetropia, strabismus (orthoptic therapy)	No	No	strabismus
Audiology / hearing	Normal	Normal	Acute OME, x2 sets of grommets, no concerns with hearing	Normal	Acute OM as baby, no gommets, no concerns with hearing	Normal	Normal	Normal	Normal	Normal	Normal	Normal
Oral / dentition / other ENT problems	Submucous cleft palate	High palate, widely spaced teeth	tonsillectomy; cleft soft palate; Class III malocclusion; orthodontics; on WL for rhinoplasty	Submucous cleft palate; tonsillectomy; orthodontics	tonsillectomy and superior adenoidectomy after speech assessment; orthodontics; speech did not improve after T&As; on waiting list for pharyngoplasty	Class III malocclusion due to midface retrusion	Normal	Normal	no	Ankyloglossia. Poor suck/swallow coordination. Obstructive/noisy upper airway breathing.	No	hypoplastic uvula
Cardiac problems	Bicuspid aortic valve, PDA requiring surgical closure	Atrial septal defect	No	No	Heart mumur when born, innocent, no follow up needed, ECG and echo normal	No	No	No	No	No(referred for echocardiogram, pending)	No	spontaneously resolving VSD
Respiratory problems	No	No	Moderate OSA; no asthma	OSA and snoring; hospitalised for pneumonia at 3, no asthma	OSA, now resolved	Mild asthma as child, flares up every once in a while	No	No	No	No	No	No
Gastrointestinal problems/ feeding difficulties	Poor feeding in newborn period requiring NGT feeds; Chronic constipation	neonatal sucking difficulties. Nocturnal saliva swallowing difficulties responsible for coughing and nocturnal wakings	Cleft-related feeding difficulties; fussy eater; mainly carbs	Hyperphagia; eats good variety of foods and textures; constipation	fussy eater	No	No	No	No	Early difficulties with latching and ongoing poor coordination of suck and swallow. Early difficulty initiating solids.	No	No
Renal / genitourinary problems	Bilateral cryptorchidism; non-functioning right multicystic dysplastic kidney	initial inguinal testis but now normal. Normal abdominal and kidneys US	No	No	No	No	No	No	No	No	No	No
Hematologic problems	No	No	No	No	No	No	No	No	No	No	No	No
Endocrine problems	No	No	No	Seem by Endo at RCH; above % charts for both height and weight; lost 20kg in a year, high BMI; involved in study related to diabetes, does not have diabetes; no longer linked in with Endo at RCH	High end of %ile charts on height and weight, no official measurements yet because of COVID, but Mum said heading in same direction as Marcelle	No	No	No	No	No	No	testosterone assay and pelvis ultrasound normal
Musculoskeletal problems	Sprengel deformity scapulae, webbed neck	Joint laxity	No	No	No	No	No	No	No	Small fingers, broad thumbs.	No	Joint laxity
Immunological problems	No	No	No	No	No	No	No	No	No	No	No	No
Skin	Normal	Normal	Acne, on roaccutane	Acne, on roaccutane	Normal	Normal	Normal	Normal	Skin telangiectasia (cheeks, upper part of the back), regression of a congenital blue nevi of the back	Normal	Normal	hypertrichosis
Malignancy	No	No	No	No	No	No	No	No	No	No	No	No
Other			Sensory processing difficulties; on medication for anxiety and depression	On medication for anxiety and depression	WL for pharyngoplasty, post pharyngeal wall flap, 'non-cleft VPI'; anxiety, but not medicated	On medication for anxiety and depression			fragile X syndrome			
Family History												
Similarly affected family members	No	no	3	3	3	3 (daughters)	no	No	Difficult to assess, child growing in a foster family, mother has possibly similar difficulties but no evaluation data during her scholing, she did her first year of primary school twice and specialized education at age 10 years; father had mild learning difficulties with attention deficiency, difficulties in writting, and general clumsiness without ataxia or neurological deficit	No	Father had absence epilepsy in childhood, shares the same duplication listed above	mother with ID and hypertrichosis, father with ID and microcephaly (-3.5SD),
Consanguinity	No	No	No	No	No	No	No	No	No	No		no
Full siblings	1		2	2	2	NA	NA	0, two half sisters	2	No	Older brother - healthy, 5	fetus with ventriculomegaly, hypoplastic thumbs, IUGR, anal imperforation, pelvic kidney, right aortic arch.
Other	Paternal SLE		Father	Father	Father	Daughters		Brother of mother with ADHD and dev delay. Other brother of mother with ADHD only.	3 paternal half brother from 2 women, mother pregnant from another partner	Mother learning difficulties (16p13.11 duplication)		
Physical Examination												at 2y 3m
Height	50th centile	105.1cm (+3SD)	Age 17 y: 160 cm (32nd centile)	Age 15 y: 175 cm (98th centile)	Age 10 y: 156 cm (>98th centile)	Age 47 y: 187 cm (92nd centile)	152 cm (+4SD)	At age 3 years 6 months 110.2 cm (2.02 SD)	127 cm (+1.4 SD)	72nd centile (3y)	159.4 cm (1st-3rd centile)	88 (+0,5SD)
Weight	10th centile	21.5 kg (+5 SD)	Age 17 y: 53 kg (36th centile)	Age 15 y: 82kg (98th centile)	Age 10 y: 64 kg (>98th centile)	Age 47 y: 86 kg (87th centile)	42 kg (+4SD)	20.1 kg (0.97 SD)	27.4 kg (+1.8 SD)	99th centile (3y)	53.1 kg (3rd-10th centile)	10,5 (-1,5SD)
Head circumference	50th centile	54.5 cm (+3.2 SD)	Age 13 y: 2nd centile	Age 5y3m: 53 cm (98th centile)	Age 4y9m: 52.5 cm (95th centile)	N/A	54.5 cm (+1SD)	53.5 cm (2.28 SD)	52.4 cm (median)	80th centile (2y)	50.6 cm (<2nd centile)	44 (-3SD)
Facial features	Broad forehead, high nasal root, deeply set eyes, periorbital fullness, malar flattening, short philtrum, thin upper and lower lips vermilion, webbed neck, underdeveloped superior crus of ears with left-sided preauricular pit	"de novo postnatal macrosomia", epicanthus, thick eyebrows, synophris, large lobules of ears, deeply set eyes, periorbital fullness, downturned mouth,	Deeply set eyes, periorbital fullness	Not dysmorphic	Deeply set eyes, periorbital fullness	Midface retrusion	Not dysmorphic	Prominent forehead, no frontal bossing. Upslant, hypertelorism/telecanthus, almond shaped eyes. Nose normal. Thin upper lip. Ears low set and posteriorly rotated, normal shape.	Mild facial asymmetry with low set right ear, thick eyebrows, thin upper lip	Prominent metopic suture. Flat occiput. Broad nasal bridge / hypertelorism. Lateral eversion of eyelids. Small ears with thickened helices. Mild micrognathia. Thin upper lip with flat philtrum.	Mildly dysmorphic	Downturned corner of the mouth, synophrys, highly arched eyebrows
Hands / feet	Tapering fingers, single palmar crease on R, small feet with pes planus and overlapping toes	Single palmar crease, clinodactyly	Normal	Normal	Normal	Normal	Normal	Toes 2-5 clinodactyly.	Metatarsus varus (surgery at age 2.5 years, intermittent physiotherapy and orthopaedic sole)	Small, fleshy hands & fingers with broad thumbs. Small toes. Single palmar creases.	Normal	flat feet, right single transverse palmar fold
Other findings	No	unaffected Mother 170 cm (+1,2SD) OFC 54,8 (-0,5SD) ; father 174 cm (-0,2SD) OFC 58 cm (+1,5SD)		Obesity	No	No	other people in the maternal family with over weight/height	No Analyses peformed: FMR1, SNP-array, WES and metabolic screening. With metabolic screening low activity of very long chain acyl-CoA dehydrogenase (VLCAD). She turned out te be a carrier of VLCADD.	arr [GRCh37] 4q31.3(152720434_153661857)x1dn, 6q21(114465667_114548253)x3 mat, 7q36,2(154223820_154390398)x3pat	No	No	No
		at birth : 38+2WG : 3240g/51cm/OFC35cm							intragenic *DPP6* duplication inherited from the father			
									HS3ST5 exon 3 duplication (UTR) inherited from the mother			

INDIVIDUAL	13	14	15	16	17	18	19	20	21	22	23	24
VARIANT TYPE	MISSENSE, AFFECTING WD40 DOMAIN											
Variant Details												
Mode of discovery	Trio WES (GeneDx)	Trio WES	Trio WES	Trio WES	Trio WGS	Trio WES	Pair WES (Research) Deep WES on skin biopsy; normal depth for patient blood	Trio WES (DDD)	Trio WES (Mayo)	Trio WES	Trio WES (GeneDx)	Trio WES
cDNA (NM_001349798.2)	c.1259A>T	c.1267G>A	c.1267G>A	c.1321C>G	c.1384T>C	c.1394G>A	c.1436G>A	c.1439A>G	c.1514G>A	c.1631T>G	c.1738C>T	c.1744T>G
gDNA (Chr4; GRCh37)	g.153249519T>A	g.153249511C>T	g.153249511C>T	g.153249457G>C	g.153249394A>G	g.153249384C>T	g.153247366C>T	g.153247363T>C	g.153247288C>T	g.153247171A>C	g.153245453G>A	g.153245447A>C
Protein level	p.(His420Leu)	p.(Gly423Arg)	p.(Gly423Arg)	p.(Arg441Gly)	p.(Ser462Pro)	p.(Arg465His)	p.(Arg479Gln)	p.(Asp480Gly)	p.(Arg505His)	p.(Val544Gly)	p.(His580Tyr)	p.(Ser582Ala)
Same variant in gnomAD	Absent	Absent	Absent	Absent	Absent	Absent	Absent	Absent	Absent	Absent	Absent	Absent
Alternative change at same amino acid residue in gnomAD	Absent	Absent	Absent	Absent	Absent	p.(Arg465Cys) (allele balance 45% or lower)	p.(Arg479Gly) (allele balance 25-30%)	Absent	Absent	Absent	Absent	Absent
Same variant in COSMIC	Absent	Present (multiple tissue types)	Present (multiple tissue types)	Present (lung carcinoma, rhabdomyosarcoma)	Absent	Present (more than 5 tissue types)	Present (more than 5 tissue types)	Present (colon adenocarcinoma)	Present (more than 5 tissue types)	Present (large intestine adenocarcinoma)	Present (large intestine adenocarcinoma)	Absent
Alternative change at same amino acid residue in COSMIC	Multiple	Multiple	Multiple	Multiple	p.(Ser462Tyr), p.(Ser462Phe)	Multiple	Multiple	Multiple	Multiple	p.(Val544Asp) (mouth squamous cell carcinoma)	Multiple	Multiple
Exon (NM_001349798.2)	11	11	11	11	11	11	12	12	12	12	13	13
Occurs within WD40 domain	Yes	Yes	Yes	Yes	Yes	Yes	Yes	Yes	Yes	Yes	Yes	Yes
Inheritance	De novo	De novo	De novo	De novo	De novo	De novo	De novo, post-zygotic (mosaic: 14%)	De novo	De novo	De novo	De novo	De novo
Other candidate variants	No	No	No	No	No	No	Yes CACNA1A:NM_023035.2:c.835C>T p.(Arg279Cys)	No	No	No	No	No
Demographic Features												
Sex	Male	Male	Male	Male	Male	Female	Male	Male	Male	Female	Male	Female
Age at last assessment	10 years, 2 months	14 yo	15	5 years	Information gathered from clinical record and obtained from parents	9.5 years	(currently 6 years)	16 years	3 years	23 months	3 years	6 years
Other			Macedonian					DDD4K.02106 in DDD paper				
Medical History												
Prenatal history	non-contributory, born at 38 weeks 1 day	uneventful	Unremarkable	Uncomplicated pregnancy and term delivery	Planned Caesarean after 42 weeks of gestation, because of size and drop in fetal movement, weight at birth: 5230 g (<99 percentile, +3.4 SD), length: 57 cm (<99 percentile, +2.6 SD), head circumference: 40 cm (99 percentile, +2.5 SD)	normal	Born at 40 weeks. Uneventful pregnancy. Weight at birth : 3520g.	Normal (well bar ear infection in mum and she took ear drops)	Delivered at 36 weeks, induced for maternal cholestasis. BW 8lbs. 15oz., hospitalized for 6 days.	Normal	Unremarkable. Term delivery, Cesarean section for breech presentation	Normal
Neurological problems	hypotonia diagnosed shortly after birth	history of seizures; hypotonia	Hypotonia; macrocephaly	Generalized hypotonia	hypotonia	neonatal hypotonia and failure to thrive	Generalized severe hypotonia;	apgars 8 @1 min, 10 at 5 min. home day 4 fine, ducky episode day 12, floppy, generalised hypotonia; on CBZ for his seizures which has stabilised;	Hypotonia	Severe progressive spasticity;	Hypotonia. Broad-based gait but not frankly ataxic. No seizures. Normal EMG/NCS.	no hypotonia, no seizures
Brain imaging	N/A	N/A	agenesis of corpus callosum	Brain MRI (2 years of age) shows dysmorphic corpus callosum, scattered foci of T2 prolongation in periventricular white matter	N/A	N/A	Brain MRI: cerebellar hypoplasia but large folia and big cisterna magna	Crowded posterior fossa with enlarged cerebellum and thick vermis with low-lying tonsils just above foramen magnum; thick brainstem, normal corpus callosum	Brain: abnormal sulcal pattern suggestive of polymicrogyria, thin corpus callosum, delayed myelination	Brain Atrophy per MRI Scattered small subcortical calcifications (Brain CT)	Normal brain MRI/spine with MRS.	Delayed myelination; generally thin corpus callosum
Developmental / cognitive / psychiatric problems	normal	Developmental delay waled at age 3; intellectual disability. Very few words. Dx of Autism spectrum disorder	Global dev delay all milestones/moderate intellectual disability	Moderate global developmental delay (language limited and has speech apraxia, ambulatory)	motor developmental delay, normal language development, normal fine motor development	Global developmental delay	Global developmental delay with marked generalized hypotonia, only syllabes for speech; (walking independently after 4 years)	Severe global developmental delay (babbling, mama dada but not consistent, non ambulatory); Sleep disturbance	Motor and speech delay	Severe progressive developmental delay with episodes of regression	Global developmental delay: gross motor (walking independently after 2 years) and expressive speech	Moderate global developmental delay (4 months head control 9 months sitting 31 months walking)
Ophthalmologic problems	No	No	Bilateral esotropia/hypermetropia	Mild hypermetropia, nasolacrimal duct obstruction	No	No	No	Esophoria	No	No	No reported concerns	No
Audiology / hearing	bilateral mixed hearing loss requiring hearing aids	Normal	Normal	Chronic OM s/p TM tubes, normal audiometry	Normal	Normal	moderate conductive hearing loss	Normal	Normal	Normal	Normal	Normal
Oral / dentition / other ENT problems	normal	High palate	High palate	Normal dentition, no caries	No	Anterior open-bite malocclusion	No	Carious teeth	Laryngeal cleft	High palate	No reported concerns	No
Cardiac problems	No	interrupted aortic arch; multiple ASD and VSDs; subaortic stenosis. Severe LV dysfunction.	No	Normal ECHO	delay in ductus arteriosus closure after birth, but normal echocardiogram at 3 weeks of age	Surgical correction for patent ductus arteriosus, now she has minimal shunts for perimembranous interventricular defect and ostium secundum interatrial defect.	No	No	No	Persistent left superior vena cava to coronary sinus	No	Atrial Septal Defect
Respiratory problems	respiratory distress at birth, no current issues	No	No	No	No	Recurrent pneumonia, low ciliar functioning	No	No	No	recurrent pneumonia	No	No
Gastrointestinal problems/ feeding difficulties	feeding dysfunction in infancy requiring Gtube, Nissen fundoplication (GERD), currently eats by mouth with no vomiting, diarrhea or constipation	Gtube fed; Constipation	Severe persistent constipation	Severe feeding difficulties with velopharyngeal insufficiency, GERD, constipation	poor feeding, constipation	Episodic constipation	Constipation	Chronic constipation, gastro-oesophageal reflux	Constipation (negative testing for Hirschprung); G-tube dependence; GERD	failure to gain weight	Severe constipation. Negative rectal biopsy for Hirschprung.	No
Renal / genitourinary problems	No	Cryptorchidism	Nephromegaly/Normal function	Nocturia	normal renal ultrasound at 14 mo	No	No	Cryptorchidism	No	No	No	No
Hematologic problems	No	Neutropenia; Thrombocytopenia	No	Neutropenia (resolved) and intermittent normocytic anemia	iron deficiency (4 µmol/L at 5 mo)	neonatal anemia	No	No	No	No	No	No
Endocrine problems	No	No	No	No	No	No	No	Vitamin D deficiency	No	No	No	No
Musculoskeletal problems	muscle fatigue	Tall	Normal birth centiles;subsequent overgrowth with all centile being >>> 97th ; review at age 15 growth now normalizing with centiles ; as adolescent more Marfan like habitus with long torsi and US:LS ratio 0.79 & arm span >length by 3.7 cm; small chest with mild pectus excavatum;	Left sided hemihyperplasia	No	Beighton score 6/9 + pectus carinatum + mild scoliosis	discrete limb length asymetry (Left>Right)	Dislocated hip	No	increased muscle tone	No	No
Immunological problems	No	No	No	Hypogammaglobulinemia	No	IgG1 deficit	No	No	Recurrent infections/pneumonia, Possible IgA deficiency	No	No	No
Skin	Normal	Normal	Pigmented naevus on lower right buttock	Normal	white patches on skin and a rash	Hypopigmented skin across Blaschko lines	Pigmentary mosaicism including cafe-au-lait spots in a patchy pattern without midline separation and hyperpigmentation in a blaschkolinear pattern Naevus flammeus	Normal	Normal	Normal	Normal	Normal
Malignancy	No	No	No	No	No	No	No	No	No	No	No	No
Other	normal microarray in 2013, mildly low carnitine responding to supplementation	Admission to ICU for hyperammonemia		Severe fatigue, drop attacks (unclear etiology)	narrow shoulders						CMA, MS-MLPA for Angelman, and FMR1 testing negative	
Family History												
Similarly affected family members	no	None	Nil	7 year old brother with hemihyperplasia, but developmentally normal. Does not carry FBXW7 variant.	No	no	No	No	NO	none	No	No, She is an only child, from healthy unrelated Japanese parents.
Consanguinity	no	No	Nil	No	No	no	No	No	NO	no	No	No
Full siblings	yes	Full Sister - 16 yo - Healthy	2- well and developmentally age appropriate	1	1	1 male, 1 female	No	0	5		2	
Other				Non-contributory	Parents unaffected		No	One half sibling	NO			
Physical Examination												
Height	142.3 cm (72nd centile)	167 cm (53rd centile)	All consistently above 97th centile till about age 13 then has started normalizing and at last exam (age 15) head circumference remains above 97th centile but other centiles on 50th.	89th centile	At 10 mo: 75 cm (64th percentile)	141 (75-90°%)	120 cm (+1,5 SD) at 6 years	Age 5 m: 66 cm (52nd centile)	107.0 cm (95th percentile)	142.3 cm	102 cm (65th centile)	103 cm, -1.9 SD
Weight	30.9 kg (44th centile)	58.8 kg (69th centile)	50th centile	92nd centile	At 10 mo: 11 kg (81st percentile)	32,9 (50°%)	23,6 Kg (+1 SD) at 6 years	Age 5 y: 21.7 kg (87th centile)	18.1 kg (90-95th percentile)	30.9 kg	16kg (60th centile)	16.4kg, -1.1SD
Head circumference	57 cm (99th centile)	N/A	head circumference remains above 97th centile	>99th %ile, z= +3	At 10 mo: 49 cm (99th percentile, +2.4 SD)	57 (>97°%)	54.2 cm (+2 SD) at 6 years	Age 5 y: 52 cm (66th centile)	Macrocephaly - 54.6 cm (>95th centile)	46 at 2y	52cm (83rd centile)	48.5cm, -1.5SD
Facial features	Not dysmorphic	Myopathic facies; Hypoteloric, thin upper and lower lips vermilion, highly arched eyebrows with synophrys; thick eyelashes, left preauricular pit.	Long palpebral fissures which were down slanting with long thick curly eyelashes upltilted nose with a flat tip; low set posterior rotated ears with overfolded helices and prominent inferior and superior crus ; jowl-like cheeks and his mouth was small with down turned corners; high palate	somewhat flat face, short nose, downturned corners of mouth	small chin, deep set eyes	long face, bulbous nose, posteriorly rotated ears, high narrow palate, nasal voice	Mild dysmorphic facial -metopic ridge, overfolded helices, epicanthal folds, bulbous nose, uptented upper lip,	Long palpebral fissures, dimple lower lip, philtral pillars prominent	Mild dysmorphic facial features- Overfolded helices, Bilateral epicanthal folds, down slanted palpebral fissures, deep-set eyes, periorbital fullness, High arched palate, Wide nasal bridge, Scaphocephalic with a prominent occiput, Metopic but not sagittal ridging.	Puffy eyelids and cheeks ,small mouth slightly broad nose	mild frontal bossing, raised philtrum, thin upper lip,	Deep-set eyes, periorbital fullness, anteverted ears, depressed nasal bridge and broad nasal tip.
Hands / feet	Normal	Normal	Although his hands were large consistent with the rest of his habitus, his fingers were actually short (10th centile); broad thumbs. splayed forefeet with 2-3 syndactyly.	hemihyperplasia of left leg	fat pad on top of foot	Normal	finger hyperlaxity and mild proximal rigidity	Tapered digits, hypermobile joints, single palmar crease bilaterally, persistent fetal finger pads, broad small feet	Thickening of palms	Finger swelling	Normal	Normal
Other findings	No	No	small chest with mild pectus excavatum; small umbilical hernia;	No	long eyelashes	No	No	BW 3.48kg, HC 35.5cm at birth	Thymus bulge with valsalva. T&A removed	No	No	No
										153247171A>C		

INDIVIDUAL	25	26	27	28	29	30	31	32	33	34	35
VARIANT TYPE	MISSENSE, AFFECTING WD40 DOMAIN			MISSENSE, NOT AFFECTING WD40 DOMAIN							
Variant Details											
Mode of discovery	Trio Exome	Trio WES	Trio WGS (research)	Trio WES	Trio WES (GeneDx)	Trio WES	Trio WES	Trio WES	Solo WES	trio WES	Trio WES
cDNA (NM_001349798.2)	c.1796C>T	c.1877C>T	c.1920C>A	c.1822A>G	c.2021G>C	c.2020C>T	c.2020C>T	c.2066G>A	c.2065C>T	c.2065C>T	c.2065C>T
gDNA (Chr4; GRCh37)	g.153245395G>A	g.153244280G>A	g.153244237G>T	g.153245369T>C	g.153244136C>G	g.153244137G>A	g.153244137G>A	g.153244091C>T	g.153244092G>A	g.153244092G>A	g.153244092G>A
Protein level	p.(Ala599Val)	p.(Ala626Val)	p.(Ser640Arg)	p.(Ile608Val)	p.(Arg674Pro)	p.(Arg674Trp)	p.(Arg674Trp)	p.(Arg689Gln)	p.(Arg689Trp)	p.(Arg689Trp)	p.(Arg689Trp)
Same variant in gnomAD	Absent	Absent	Absent	Absent	Absent	Absent	Absent	Absent	Absent	Absent	Absent
Alternative change at same amino acid residue in gnomAD	p.(Ala599Gly) (allele balance 35-40%)	Absent	Absent	Absent	Absent	Absent	Absent	Absent	Absent	Absent	Absent
Same variant in COSMIC	Absent	Present (large intestine adenocarcinoma)	Absent	Absent	Absent	Present (glioma, cervix squamous cell carcinoma, atypical meningioma, prostate adenocarcinoma)	Present (glioma, cervix squamous cell carcinoma, atypical meningioma, prostate adenocarcinoma)	Present (more than 5 tissue types)	Present (more than 5 tissue types)	Present (more than 5 tissue types)	Present (more than 5 tissue types)
Alternative change at same amino acid residue in COSMIC	Absent	p.(Ala626Thr), p.(Ala626Pro), p.(Ala626Asp)	Yes (one in NCI's GDC)	Absent	p.(Arg674Trp), p.(Arg674Gln)	p.(Arg674Gln) (colon adenocarcinoma, stomach adenocarcinoma)	p.(Arg674Gln) (colon adenocarcinoma, stomach adenocarcinoma)	p.(Arg689Glu), p.(Arg689Trp)	p.(Arg689Glu), p.(Arg689Gln)	p.(Arg689Glu), p.(Arg689Gln)	p.(Arg689Glu), p.(Arg689Gln)
Exon (NM_001349798.2)	13	14	14	13	14	14	14	14	14	14	14
Occurs within WD40 domain	Yes	Yes	Yes	No	No	No	No	No	No	No	No
Inheritance	De novo (mosaic: 23.3% of 103 reads)	De novo	De novo	De novo	De novo	De novo	De novo	De novo	De novo	De novo	De novo
Other candidate variants	No	No	No	No	No	No	No	KMT2D: de novo NM_003482.4:c.16012T>C p.(Cys5338Arg)	No	No	No
Demographic Features											
Sex	Male	Male	Female	Male	Male	Male	Male	Male	Male	Male	Male
Age at last assessment	22 months	3 yrs	7 years	11 years	2 years (currently 4 years)	15 years	14 years	2 years	10 years	12 years	7 y
Other		Caucasian		Caucasian							
Medical History											
Prenatal history	1565g, 33 weeks premature, SGA, tracked small on US but no dx of IUGR. Vaginal. Mother G1P0, 30years old. NICU for 19 days for jaundice, hypoglycemia and feeding difficulties. Abnormal newborn hearing screen.	Born at 41+4 wks. Uncomplicated pregnancy and delivery. BW 3872g.	Low maternal serum PAPP-A; Velamentous cord insertion; Term birth and Apgars 9/9; Birth weight, length, and head circumference within normal range	Normal	Born at 42wks to a G9P6 41yo mother, BW = 7lbs, Length = 48.5cm, HC = 34.5cm. NICU for 2 days due to mild respiratory distress and poor feeding. Parents report a history of increased nuchal fold and extra skin fold in the back of the neck at birth, which resolved. Mother took Prilosec for GERD during pregnancy. Newborn screen was normal. NHS was completed 3 times.	Unremarkable pregnancy. Born at term. BW 3450g. Apgars 8,9. Mom recalls concerns re being "blue" at delivery but no resuscitation needed.	Normal	Normal	Normal	Normal	Hyperechogenic kidneys; hypotonia and respiratory distress at birth (Apgar 4-7-9)
Neurological problems	motor developmental delay, mild hypotonia. Focal seizures (left anterior temporal area) confirmed by EEG and is now on antiepileptic medication	Hypotonia. Tonic upgaze eye movements in infancy. Myoclonic and myoclonic-tonic seizures from 4-5 months of age. EEG findings suggestive of developmental epileptic encephalopathy with multifocal and generalised discharges.	Generalized hypotonia; Treatment-refractory seizures;	Early Onset Absence Epilepsy (EOAE); rare isolated myoclonic seizures	Generalized hypotonia	Normal tone on exam (from 8 years). Achilles tendon contracture (tight heel cords). Abnormality of coordination. Possible ataxia. Has history of migraines with photophobia.	epilepsy started at 4y6m; hypotonia; ataxia; upper hand dyskinetic involuntary movements and stereotypies	Normal	hypotonia, language trouble	hypotonia	Global DD, hypotonia, drooling
Brain imaging	Brain MRI 3/2018: prominent extraaxial fluid but otherwise normal for age.	MRI brain abnormal sulcal pattern suggestive of polymicrogyria.	Brain MRI x3 - Large cerebellum with crowded posterior fossa at 9 months, the vermis continues to grow from 42mm to 46mm at 3.5 years, thereafter it mildly shrinks to 41mm at 9 years – this could be related to antiepilepsy medications. The dysmorphic corpus callosum is not thickened at 9 months but is thick at 3.5 and 9 years. On the last scan there is generalised mild ventriculomegaly and increased size of the extra-axial CSF spaces	N/A	N/A	MRI brain shows big cerebellum 46mm with crowded posterior fossa and tonsils low lying at foramen magnum; thick brainstem, scattered bilateral fl/T2 hyperintensities in subcortical white matter,frontal, parietal and temporal similar to Individual 25. Volume and myelination ok; thin corpus callosum	normal brain MRI	N/A	Brain MRI (2 yo) : non specific white matter hypersignals, widening of Virchow–Robin spaces, vermis upper limits 41mm, low right tonsil, mega cisterna magna; thick brainstem; normal myelination and corpus callosum	N/A	Brain MRI: normal
Developmental / cognitive / psychiatric problems	Developmental concerns at 2 months when he was not lifting his head or tracking. Rolled over at 9 months, sat on own at 10 months, pulled to stand at 14 months, crawled at 14 months, cruising at 16 months, walking at 22 months is very wobbly and still needs support. Speech - at 22 months has 2-3 spontaneous words, but usually only repeats or echos. Developmental delay, global, mild and making progress. Cruising age 16 mos; not walking yet 22 mos. Few words, mostly repeats words at 22 mos. Social and affectionate.	Motor and speech delay. Walked at 19/20 months of age. Minimal speech at 3yrs of age.	Global developmental delay (non-verbal, non-ambulatory)	Learning difficulties/Borderline IQ FSIQ=70	Mild-moderate global developmental delay (Sitting at 8mo, talking at 13mo and walking at 24mo). EI evaluation showed average cognition with delayed expression language and motor skills. At 22mo his pediatrician reported that he was able to point and vocalize to show his wants, as well as use two word combinations, but he could not run without falling. By 26mo months he could use pronouns and verbalize immediate experiences, but he could not walk up and down stairs one step at a time.	Moderate ID. GDD - walked at 29 months. Speech delay with first words at 4 years and sentence at 6 years, still not fully understandable at age 9. In grade 9 was operating at grad 4-5 level for academics, and is in life skills program at school. Has compulsive behaviours, paricularly trichotillomania. NO autism.	severe delay; no words; understands simple orders; walked at 32 m;	Speech delay	moderate global developmental delay, walking at 23 mo, global motor delay, global and facial hypotonia, fine motor trouble, 1st words at 4yo, can say words, language trouble, good non-verbal communication, good level of understanding of simple orders, not toilet-trained	moderate developmental delay	Global moderate psychomotor delay, delayed and limited speech, dyslalia
Ophthalmologic problems	Intermittent strabismus/esotropia. Hypermetropia but no rx for glasses. Amblyopia and treated with patching.	No	Visual impairment; Bilateral ptosis; Cortical visual impairment	Myopia	No	Hypermetropia	No	No	No	No	No
Audiology / hearing	5db bilateral SNHL. Hx 2 ear infections. Tubes placed at 17 months. Mixed hearing loss with mild sensorineural hearing loss, conductive hearing loss with chronic middle ear effusion s/p ear tubes. *Note: pt is also compound heterozygote for 2 different pathogenic variants in GJB2*	Normal newborn hearing assessment. Normal assessment at 1 year of age.	Unclear	Normal	Failed NHS, but eventually had a normal ABR in both ears	Normal	Normal	Normal	Normal	Normal	Normal
Oral / dentition / other ENT problems	delayed teeth eruption and in unusual order	Tongue tie release at 2 months of age.	Dental caries	No	Delayed dental eruption - first tooth at 12mo	No	Normal	Laryngomalacia; Lip and tongue tie at birth - clipped	Narrow palate	No	Dysmorphic ears, small mouth, high palate, bifid uvula, nasal voice, nasal septum deviation
Cardiac problems	No	Small PFO noted at birth. Normal ECHO at 2yrs of age.	Ventricular septal defect (spontaneously closed); Mesocardia	No	No	No	No	Bicuspid aortic valve	No	No	Patent foramen ovale, interatrial defect
Respiratory problems	No	Recurrent upper respiratory tract infections	Recurrent aspiration pneumonias; Reactive airway disease; Sinuses essentially unremarkable on brain MRI	No	No	No	No	CT scan performed secondary to frequent sinus infections showed "underdeveloped maxillary sinus".	No	No	No
Gastrointestinal problems/ feeding difficulties	Hx feeding difficulty. Still struggles with hard foods due to delayed teeth eruption. Prefers soft foods and struggles a little to chew and swallow hard foods; uses a sippy cup and can drink from a straw	Diarrhoea	Constipation; Oro-motor feeding dysfunction; GERD; G-tube fed	No	Hx poor sucking and feeding difficulties as infant leading to FTT by 3mo. Formulas were tried with no success. Barium swallow showed GERD - tx Prevacid and Zantac with minimal improvement. Normal upper GI and small bowel series; endoscopy showed some mild inflammation, but was otherwise wnl. Hx chronic constipation.	intermittent diarrhea, of unclear etiology	No	FTT and poor suck/swallow coordination. GERD and blood in stool prompting several formula changes. He was diagnosed with milk protein allergy as infant, but skin test negative and now able to tolerate milk without symptoms / blood in stools.	Constipation	severe constipation	Constipation
Renal / genitourinary problems	No	No	Bilateral inguinal hernias	Incontinence, resolved at 8 yr with seizure control	No	Small penis and testicles (history of delayed puberty). Normal renal ultrasound	No	Bilateral cryptorchidism	incomplete foreskin	No	Increased corticomedullary differentiation
Hematologic problems	No	No	No	No	No	No	No	No	No	No	No
Endocrine problems	No	No	Neonatal hypoglycemia (resolved)	No	Hypothyroidism (IGF-1 41 ng/mL, TSH 15.2 uU/mL, free T4 1.43 ng/dL) tx w/ synthroid .05mg, Nl thyroid ultrasound	Delayed puberty	No	No	No	No	No
Musculoskeletal problems	No joint problems or muscle concerns. Hypotonia has improved with time	Mild kyphosis. Hypotonia has improved with time.	Right calcaneovalgus deformity at birth (resolved)	No	No	mild valgus deformity of knees. Decreased coverage of R femoral head on pelvic xray. Short stature at 3rd centile	No	No	Joint laxity	early hypotonia	Joint laxity
Immunological problems	No	No	Recurrent infections	No	Episodes of fevers	Bacterial meningitis at age 8y, no history of recurrent infections	No	No	few otitis, bronchitis	No	No
Skin	Normal	Eczema	Capillary hemangiomas; Nevus	Normal	Normal	sensitive skin to temperature change	Normal	May have immunological abnormalities (per parents report, we didn't have anything to review).	Normal	Normal	Normal
Malignancy	No	No	No	No	No	No	No	No	No	No	No
Other	Failure to thrive. Weight percentile <1%, length ~1%, weight for length ~32%, head circumference 2%. All growth parameters are increasing along his own curve indicating normal growth velocity.	Narrow/sloping shoulders		Nil		array CGH (60K) normal, frax normal	No	No	No	No	Dolicocephaly, macrocephaly (OFC = 54 cm at 3 y),
Family History											
Similarly affected family members	No. First child to both parents	No	No	No	No	no	no	No	no	no	No
Consanguinity	None	No	No	No	No	no	no	No	no	no	No
Full siblings	None	1	2	2	7	3				healthy sister	No
Other	Ashkenazi Jewish ancestry.	Nil	Maternal uncle with congenital heart disease	Nil	Mother had two spontaneous first trimester abortions; AJ ancestry	none contributory					-
Physical Examination	*at 22 months*						5y7m				
Height	76.20cm (Z=-2.85)	91 cm (10th centile)	125 cm (62nd centile) at 7y5m	138.2 at 11 yrs (22nd percentile)	<<1% (Normal at birth, by 3 months length was 39%, and by 12mo it was <3%)	154 .2 cm (3rd centile) at 15y (was previously at 25th centile)	114.5 cm (+1 SD)	92nd centile	147 cm (+1.5 SD)	166 cm (+1.5 SD)	116.5 cm (50th centile) at 6 y and 3 m
Weight	9.62kg (Z= -2.40)	12.3 kg (7th centile)	26 kg (74th centile) at 7y5m	32.2 at 11 yrs (26th precentile)	<<1% (Normal at birth, by 3 months weight fell below 3%)	52.8 kg (25-50th centile) at 15y	20 kg (+1 SD)	99th centile	33.3 Kg (+0.5 SD)	50.2kg (0 SD)	22 kg (59th centile) at 6 y and 3 m
Head circumference	45.60 cm (Z= -2.06)	50 cm (58th centile)	51.0 cm (34th centile) at 6y10m	52 cm at 5 yrs (85% percentile)	25% (consistent since birth)	55.8cm (75th centile) at 15y	53 cm (+1 SD)	90-98th centile	55.5 (+1.5 SD)	60cm (+3 SD)	54.5 cm (+2.5 SD) at 6 y and 3 m
Facial features	mild flattening of the occiput but otherwise normal head shape with anterior and posterior hairlines normal. Curly, dark brown hair. Level palpebral fissures with normal eye spaces. Pupils equally round and reactive to light with extraocular movements in tandem. Irises are brown. Ears normal formed and placed.There are no preauricular pits or tages. Prominent, somewhat high nasal bridge with normal nose and philtrum. Thin lips. Palate is intact and not high with single midline uvula. Teeth are primary teeth with normal enamel.	Epicanthic folds, depressed & broad nasal bridge, blue sclerae.	Low anterior hairline; Bilateral ptosis; Thin ear helix; Synophrys	Normal	Depressed nasal bridge, high arched palate, tented upper lip	Deep set eyes, mildly narrow pfs. flared eyebrows, long philtrum, prominent lips, large appearing frontal incisors	no	Ears that are mildly prominent and posteriorly rotated but otherwise normally formed and set, normal nasal bridge, good dentition, forehead is tall with a somewhat receded anterior hairline. Horizontal with mildly long palpebral fissures, periorbital fullness noted and gives impression of eyes being somewhat deep set, bilateral epicanthal folds.	small mouth	frontal bossing, downslant, small ears	Dysmorphic features: high forehead, dolichocephaly, wide and protrudin ears with uplifted earlobes, flat nasal philtrum, small mouth, malocclusion, ogival palate, bifid uvula, chin hypoplasia
Hands / feet	Mild fifth finger brachydactyly. Normal otherwise.	Normal	Bilateral single transverse palmar crease; Tapered fingers; Interphalangeal joint contracture of finger; Short phalanges of fingers; 2-3 toe syndactyly; Prominent calcaneus	Normal	Persistent fetal pads, single palmer crease	2-3 toe syndactyly	Normal	2nd toes bilaterally have a more dorsal insertion point and the 2nd toe overlaps toes 1 and 3, right > left, lymphedema of the dorsum of each hand that was not noted in the feet.	Normal	Normal	Pes planus, bilateral
Other findings	No	No	No	No	No	Supernumerary nipple	No	Mild distal pectus excavatum	No	No	Somatosensory evoked potentials and EMG: normal
			Was reported in cohort paper PMID 32960281								

Table S3: HPO terms associated with FBXW7 Neurodevelopmental syndrome

Prenatal history	Thickened nuchal skin fold HP:0000474
	Jaundice HP:0000952
	Breech presentation HP:0001623
	Neonatal hypoglycemia HP:0001998
	Hyperechogenic kidneys HP:0004719
	Neonatal respiratory distress HP:0002643

Neurological problems	Hypotonia HP:0001252
	Seizure HP:0001250
	Progressive spasticity HP:0002191
	Unsteady gait HP:0002317
	Broad-based gait HP:0002136
	Paroxysmal tonic upgaze HP:0033980
	Early onset absence seizures HP:0011152
	Achilles tendon contracture HP:0001771
	Abnormality of coordination HP:0011443
	Migraine HP:0002076
	Photophobia HP:0000613
	Ataxia HP:0001251
	Dyskinesia HP:0100660
	Stereotypy HP:0000733
	Drooling HP:0002307
	Atonic seizure HP:0010819

Brain Imaging	Enlarged cerebellum HP:0012081
	Arnold-Chiari type I malformation HP:0007099
	Thin corpus callosum HP:0033725
	Agenesis of corpus callosum HP:0001274
	Abnormal corpus callosum morphology HP:0001273
	Punctate periventricular T2 hyperintense foci HP:0030081
	Aplasia/Hypoplasia of the cerebellum HP:0007360
	Enlarged cisterna magna HP:0002280
	Abnormal brainstem morphology HP:0002363
	Brain atrophy HP:0012444
	Subcortical white matter calcifications HP:0007346
	Delayed myelination HP:0012448
	Extra-axial cerebrospinal fluid accumulation HP:0012510
	Polymicrogyria HP:0002126
	Ventriculomegaly HP:0002119
	Dilation of Virchow-Robin spaces HP:0012520

Developmental / cognitive / psychiatric problems	Global developmental delay HP:0001263
	Intellectual disability, borderline HP:0006889
	Anxiety HP:0000739
	Poor suck HP:0002033
	Motor delay HP:0001270
	Specific learning disability HP:0001328
	Delayed speech and language development HP:0000750
	Speech articulation difficulties HP:0009088
	Sleep disturbance HP:0002360
	Impulsivity HP:0100710
	Short attention span HP:0000736
	Autistic behavior HP:0000729
	Speech apraxia HP:0011098
	Developmental regression HP:0002376
	Hair-pulling HP:0012167
	Depression HP:0000716

Ophthalmologic problems	Astigmatism HP:0000483
	Hypermetropia HP:0000540
	Amblyopia HP:0000646
	Strabismus HP:0000486
	Nasolacrimal duct obstruction HP:0000579
	Esophoria HP:0025312
	Bilateral ptosis HP:0001488
	Cerebral visual impairment HP:0100704
	Myopia HP:0000545

Audiology / hearing	Mixed hearing impairment HP:0000410
	Conductive hearing impairment HP:0000405
	Sensorineural hearing impairment HP:0000407

Oral / dentition / other ENT problems	Otitis media with effusion HP:0031353
	Submucous cleft of soft and hard palate HP:0410031
	High palate HP:0000218
	Widely spaced teeth HP:0000687
	Cleft soft palate HP:0000185
	Dental malocclusion HP:0000689
	Midface retrusion HP:0011800
	Ankyloglossia HP:0010296
	Poor suck HP:0002033
	Impaired oropharyngeal swallow response HP:0031162
	Episodic upper airway obstruction HP:0012271
	Short uvula HP:0010812
	Anterior open-bite malocclusion HP:0009102
	Carious teeth HP:0000670
	Laryngeal cleft HP:0008751
	Delayed eruption of teeth HP:0000684
	Laryngomalacia HP:0001601
	Narrow palate HP:0000189
	Abnormal ear morphology HP:0031703
	Bifid uvula HP:0000193
	Nasal speech HP:0001611
	Deviated nasal septum HP:0004411

Cardiac problems	Bicuspid aortic valve HP:0001647
	Patent ductus arteriosus HP:0001643
	Atrial septal defect HP:0001631
	Ventricular septal defect HP:0001629
	Interrupted aortic arch HP:0011611
	Subvalvular aortic stenosis HP:0001682
	Abnormal left ventricular function HP:0005162
	Secundum atrial septal defect HP:0001684
	Persistent left superior vena cava HP:0005301
	Patent foramen ovale HP:0001655
	Mesocardia HP:0011599

Respiratory problems	Obstructive sleep apnea HP:0002870
	Snoring HP:0025267
	Asthma HP:0002099
	Recurrent pneumonia HP:0006532
	Recurrent sinusitis HP:0011108
	Abnormality of the maxillary sinus HP:0430023
	Recurrent upper respiratory tract infections HP:0002788
	Bronchitis HP:0012387

Gastrointestinal problems/ feeding difficulties	Feeding difficulties HP:0011968
	Nasogastric tube feeding in infancy HP:0011470
	Chronic constipation HP:0012450
	Polyphagia HP:0002591
	Gastroesophageal reflux HP:0002020
	Velopharyngeal insufficiency HP:0000220
	Constipation HP:0002019
	Failure to thrive HP:0001508
	Diarrhea HP:0002014

Renal / genitourinary problems	Bilateral cryptorchidism HP:0008689
	Multicystic kidney dysplasia HP:0000003
	Enlarged kidney HP:0000105
	Nocturia HP:0000017
	Inguinal hernia HP:0000023
	Urinary incontinence HP:0000020
	Micropenis HP:0000054
	Decreased testicular size HP:0008734
	Ventral shortening of foreskin HP:0012435
	Abnormal renal corticomedullary differentiation HP:0005932

Hematologic problems	Neutropenia HP:0001875
	Thrombocytopenia HP:0001873
	Normocytic anemia HP:0001897
	Iron deficiency anemia HP:0001891
	Anemia HP:0001903

Endocrine problems	Low levels of vitamin D HP:0100512
	Neonatal hypoglycemia HP:0001998
	Hypothyroidism HP:0000821

Musculoskeletal problems	Sprengel anomaly HP:0000912
	Webbed neck HP:0000465
	Joint laxity HP:0001388
	Short finger HP:0009381
	Broad thumb HP:0011304
	Increased muscle fatiguability HP:0003750
	Pectus excavatum HP:0000767
	Pectus carinatum HP:0000768
	Hemihypertrophy HP:0001528
	Scoliosis HP:0002650
	Hip dislocation HP:0002827
	Hypertonia HP:0001276
	Kyphosis HP:0002808
	Calcaneovalgus deformity HP:0001848
	Genu valgum HP:0002857

Immunological problems	Decreased circulating antibody level HP:0004313
	Recurrent fever HP:0001954

Skin problems	Acne HP:0001061
	Telangiectasia HP:0001009
	Blue nevus HP:0100814
	Hypertrichosis HP:0000998
	Melanocytic nevus HP:0000995
	Poliosis HP:0002290
	Hypopigmentation of the skin HP:0001010
	Distributed along Blaschko lines HP:0025293
	Cafe-au-lait spot HP:0000957
	Hyperpigmentation of the skin HP:0000953
	Nevus flammeus HP:0001052
	Capillary hemangioma HP:0005306

Growth	Short stature HP:0004322
	Tall stature HP:0000098
	Obesity HP:0001513
	Macrocephaly HP:0000256
	Microcephaly HP:0000252

Facial features	Broad forehead HP:0000337
	Abnormal nasal bridge morphology HP:0000422
	Periorbital fullness HP:0000629
	Malar flattening HP:0000272
	Deeply set eye HP:0000490
	Thin vermilion border HP:0000233
	Underdeveloped superior crus of antihelix HP:0011246
	Preauricular pit HP:0004467
	Epicanthus HP:0000286
	Thick eyebrow HP:0000574
	Synophrys HP:0000664
	Large earlobe HP:0009748
	Downturned corners of mouth HP:0002714
	Prominent forehead HP:0011220
	Hypertelorism HP:0000316
	Telecanthus HP:0000506
	Almond-shaped palpebral fissure HP:0007874
	Low-set, posteriorly rotated ears HP:0000368
	Prominent metopic ridge HP:0005487
	Dolichocephaly HP:0000268
	Flat occiput HP:0005469
	Wide nasal bridge HP:0000431
	Eversion of lateral third of lower eyelids HP:0007655
	Thickened helices HP:0000391
	Microtia HP:0008551
	Micrognathia HP:0000347
	Smooth philtrum HP:0000319
	Highly arched eyebrow HP:0002553
	Myopathic facies HP:0002058
	Hypotelorism HP:0000601
	Prominent eyelashes HP:0011231
	Long palpebral fissure HP:0000637
	Downslanted palpebral fissures HP:0000494
	Anteverted nares HP:0000463
	Overfolded helix HP:0000396
	Prominent inferior crus of antihelix HP:0011238
	Narrow mouth HP:0000160
	Short nose HP:0003196
	Prominent nasal tip HP:0005274
	Tented upper lip vermilion HP:0010804
	Deep philtrum HP:0002002
	Scaphocephaly HP:0030799
	Prominent occiput HP:0000269
	Anteverted ears HP:0040080
	Depressed nasal bridge HP:0005280
	Low anterior hairline HP:0000294
	Thick vermilion border HP:0012471
	Incisor macrodontia HP:0011081

Hands/feet	Tapered finger HP:0001182
	Single transverse palmar crease HP:0000954
	Short foot HP:0001773
	Pes planus HP:0001763
	Overlapping toe HP:0001845
	Clinodactyly HP:0030084
	Metatarsus adductus HP:0001840
	2-3 toe syndactyly HP:0004691
	Prominent fingertip pads HP:0001212
	Finger swelling HP:0025131
	Short 5th finger HP:0009237
	Interphalangeal joint contracture of finger HP:0001220
	Prominent calcaneus HP:0012428
	Abnormality of the 2nd toe HP:0010319

Other	Supernumerary nipple HP:0002558
	Narrow chest HP:0000774
	Umbilical hernia HP:0001537

Table S4: Impact of neurodevelopmental syndrome variants on protein stability and interaction with CYCLIN E1.

	mCSM-Stability (ΔΔG) - previous structure	mCSM-Stability (ΔΔG)	Change in protein stability	Distance to interface (Å)	mCSM-PPI 1&2 (ΔΔG)	Change in PPI binding affinity	Δ Charge	Δ Volume	Δ Residue nature
p.(Thr416Ile)	-0.134	-0.179	Decrease	15.1	-0.07	Decrease	0	50.6	Polar -> Hydrophobic
p.(Thr416Ala)		-0.788	Decrease	15.1	-0.134	Decrease	0	-27.5	Polar -> Hydrophobic
p.(His420Leu)		-0.823	Decrease	12.4	-0.469	Decrease	Partial	13.5	Partial charge -> Neutral
p.(Gly423Arg)	-1.031	-0.985	Decrease	7.8	-0.264	Decrease	1	113.3	Neutral -> Basic
p.(Arg441Gly)	-1.258	-1.367	Decrease	2.8	0.179	Increase	-1	-113.3	Basic -> Neutral
p.(Ser462Pro)		0.973	Increase	2.6	-2.449	Decrease	0	23.7	Polar -> Hydrophobic
p.(Arg465His)		-1.834	Decrease	5.1	0.286	Increase	Partial	-20.2	Basic -> Partial charge
p.(Arg479Gln)	-0.625	-1.346	Decrease	3.1	0.054	Increase	-1	-29.6	Basic -> Unchanged
p.(Asp480Gly)	0.327	1.401	Increase	4.5	-1.998	Decrease	1	-51	Acidic -> Neutral
p.(Arg505His)	-2.019	-2.032	Decrease	5.4	-0.038	Neutral	Partial	-20.2	Basic -> Partial charge
p.(Val544Gly)	-3.203	-3.16	Decrease	9.1	-1.114	Decrease	0	-79.9	Hydrophobic -> Hydrophobic
p.(His580Tyr)	-0.414	-0.422	Decrease	9.1	0.311	Increase	Partial	40.4	Partial charge -> Aromatic
p.(Ser582Ala)		0.033	Increase	3.54	-0.422	Decrease	0	-0.4	Polar -> Hydrophobic
p.(Ala599Val)	-0.451	-0.093	Neutral	4	0.265	Increase	0	51.4	Hydrophobic -> Hydrophobic
p.(Ala626Val)		-0.106	Decrease	4.4	0.291	Increase	0	51.4	Hydrophobic -> Hydrophobic
p.(Ser640Arg)	-0.639	-0.586	Decrease	11.1	-0.355	Decrease	1	84.4	Polar -> Basic
p.(Ile608Val)		-2.019	Decrease	22.3	-0.244	Decrease	0	-33.4	Hydrophobic -> Hydrophobic
p.(Arg674Pro)	-0.648	-0.614	Decrease	8.1	-0.321	Decrease	-1	-60.7	Basic -> Neutral
p.(Arg674Trp)	-0.283	-0.157	Decrease	8.1	0.013	Neutral	-1	54.4	Basic -> Aromatic
p.(Arg689Gln)	-0.079	-0.353	Decrease	3.4	-0.54	Decrease	-1	-29.6	Basic -> Neutral
p.(Arg689Trp)		-0.357	Decrease	3.4	-0.437	Decrease	-1	54.4	Basic -> Aromatic

mutation Cutoff Scanning Matrix (mCSM); Protein–protein interactions (PPI)

Table S5: Comparison of the impact of neurodevelopmental syndrome variants and gnomAD variants on protein stability and substrate binding

Variant	Amino acid reference	Amino acid position	amino acid change	mCSM-Stability (ΔΔG)	Distance to interface (Å)	mCSM-PPI 1&2 (ΔΔG)	Allele Count	Class	Chromosome	Position	rsID	Reference	Alternate	Source	Protein Consequence	Transcript Consequence
T416A	T	416	A	-0.788	15.1	-0.134	1	clin	4	153247315	-	G	A	This study	p.(Thr416Ile)	c.1247C>T
T416I	T	416	I	-0.179	15.1	-0.07	1	clin	4	153249532	-	T	C	This study	p.(Thr416Ala)	c.1246A>G
H420L	H	420	L	-0.823	12.4	-0.469	1	clin	4	153249519	-	T	A	This study	p.(His420Leu)	c.1259 A>T
G423R	G	423	R	-0.985	7.8	-0.264	2	clin	4	153249511	-	C	T	This study	p.(Gly423Arg)	c.1267G>A
R441G	R	441	G	-1.367	2.8	0.179	1	clin	4	153249457	-	G	C	This study	p.(Arg441Gly)	c.1321C>G
S462P	S	462	P	0.973	2.6	-2.449	1	clin	4	153249394	-	A	G	This study	p.(Ser462Pro)	c.1384T>C
R465H	R	465*	H	-1.834	5.1	0.286	1	clin	4	153249384	-	C	T	This study	p.(Arg465His)	c.1394G>A
R479Q	R	479*	Q	-1.346	3.1	0.054	1	clin	4	153247366	-	C	T	This study	p.(Arg479Gln)	c.1436G>A
D480G	D	480	G	1.401	4.5	-1.998	1	clin	4	153247363	-	T	C	This study	p.(Asp480Gly)	c.1439A>G
R505H	R	505	H	-2.032	5.4	-0.038	1	clin	4	153247288	-	C	T	This study	p.(Arg505His)	c.1514G>A
V544G	V	544	G	-3.16	9.1	-1.114	1	clin	4	153247171	-	A	C	This study	p.(Val544Gly)	c.1631T>G
H580Y	H	580	Y	-0.422	9.1	0.311	1	clin	4	153245453	-	G	A	This study	p.(His580Tyr)	c.1738C>T
A599V	A	599*	V	-0.093	4	0.265	1	clin	4	153245395	-	G	A	This study	p.(Ala599Val)	c.1796C>T
I608V	I	608	V	-2.019	22.3	-0.244	1	clin	4	153245369	-	T	C	This study	p.(Ile608Val)	c.1822A>G
S640R	S	640	R	-0.586	11.1	-0.355	1	clin	4	153244237	-	G	T	This study	p.(Ser640Arg)	c.1920C>A
R674P	R	674	P	-0.614	8.1	-0.321	1	clin	4	153244136	-	C	G	This study	p.(Arg674Pro)	c.2021G>C
R674W	R	674	W	-0.157	8.1	0.013	1	clin	4	153244137	-	G	A	This study	p.(Arg674Trp)	c.2020C>T
R689Q	R	689	Q	-0.353	3.4	-0.54	1	clin	4	153244091	-	C	T	This study	p.(Arg689Gln)	c.2066G>A
R689W	R	689	W	-0.357	3.4	-0.437	2	clin	4	153244092	-	G	A	This study	p.(Arg689Trp)	c.2065C>T
V265I	V	265	I	-1.029	57.368	0.119	1	gnomad	4	153259022	rs1393933844	C	T	gnomAD Genomes	p.Val265Ile	c.793G>A
H267R	H	267	R	-0.581	61.633	-0.111	1	gnomad	4	153259015	rs1172754641	T	C	gnomAD Exomes	p.His267Arg	c.800A>G
V271M	V	271	M	-0.254	64.686	-0.311	1	gnomad	4	153259004	rs764074483	C	T	gnomAD Exomes	p.Val271Met	c.811G>A
K286E	K	286	E	-0.462	60.444	-0.046	1	gnomad	4	153258959	rs1490325931	T	C	gnomAD Exomes	p.Lys286Glu	c.856A>G
L288F	L	288	F	-0.908	59.843	0.132	6	gnomad	4	153253869	-	C	A	gnomAD Exomes	p.Leu288Phe	c.864G>T
A289S	A	289	S	-1.765	57.647	0.121	6	gnomad	4	153253868	rs1444335835	C	A	gnomAD Exomes	p.Ala289Ser	c.865G>T
Y291C	Y	291	C	-0.467	55.112	-0.254	2	gnomad	4	153253861	rs948405432	T	C	gnomAD Exomes	p.Tyr291Cys	c.872A>G
Y291N	Y	291	N	-0.601	55.112	-0.017	2	gnomad	4	153253862	rs369187069	A	T	gnomAD Exomes	p.Tyr291Asn	c.871T>A
K299E	K	299	E	0.02	40.936	0.004	1	gnomad	4	153253838	rs750051282	T	C	gnomAD Exomes	p.Lys299Glu	c.895A>G
L302I	L	302	I	-0.922	44.101	-0.084	1	gnomad	4	153253829	rs150506693	G	T	gnomAD Exomes	p.Leu302Ile	c.904C>A
T307I	T	307	I	-0.413	54.949	-0.006	1	gnomad	4	153253813	rs764174613	G	A	gnomAD Exomes	p.Thr307Ile	c.920C>T
R309H	R	309	H	-0.992	59.667	0.003	1	gnomad	4	153253807	rs760675122	C	T	gnomAD Exomes	p.Arg309His	c.926G>A
L319I	L	319	I	-0.533	49.037	-0.066	1	gnomad	4	153253778	rs1369661240	G	T	gnomAD Genomes	p.Leu319Ile	c.955C>A
K326R	K	326	R	-0.425	39.317	0.12	1	gnomad	4	153253756	rs773325030	T	C	gnomAD Exomes	p.Lys326Arg	c.977A>G
K326T	K	326	T	-0.52	39.317	-0.056	1	gnomad	4	153253756	rs773325030	T	G	gnomAD Exomes	p.Lys326Thr	c.977A>C
E327D	E	327	D	-0.513	37.333	0.1	1	gnomad	4	153253752	rs148769501	T	G	gnomAD Exomes	p.Glu327Asp	c.981A>C
G329E	G	329	E	-1.067	34.737	0.145	1	gnomad	4	153252020	rs1358178925	C	T	gnomAD Genomes	p.Gly329Glu	c.986G>A
I330V	I	330	V	-1.265	36.875	-0.056	1	gnomad	4	153252018	rs767438108	T	C	gnomAD Exomes	p.Ile330Val	c.988A>G
I336M	I	336	M	-0.569	45.102	0.19	1	gnomad	4	153251998	rs1046708929	G	C	gnomAD Exomes	p.Ile336Met	c.1008C>G
K337Q	K	337	Q	-0.295	47.538	0.194	1	gnomad	4	153251997	rs750480880	T	G	gnomAD Exomes	p.Lys337Gln	c.1009A>C
R338K	R	338	K	-0.216	50.737	0.251	3	gnomad	4	153251993	rs1185005670	C	T	gnomAD Exomes	p.Arg338Lys	c.1013G>A
V341A	V	341	A	-0.617	55.273	-0.144	1	gnomad	4	153251984	rs1485389861	A	G	gnomAD Exomes	p.Val341Ala	c.1022T>C
I342T	I	342	T	-0.67	57.24	-0.602	2	gnomad	4	153251981	rs765495879	A	G	gnomAD Exomes	p.Ile342Thr	c.1025T>C
I342V	I	342	V	-0.424	57.24	0.344	1	gnomad	4	153251982	rs1247097813	T	C	gnomAD Exomes	p.Ile342Val	c.1024A>G
I347V	I	347	V	-0.956	53.902	-0.016	1	gnomad	4	153251967	rs762013076	T	C	gnomAD Exomes	p.Ile347Val	c.1039A>G
H359R	H	359	R	-0.889	35.47	0.035	1	gnomad	4	153251930	rs1014611334	T	C	gnomAD Genomes	p.His359Arg	c.1076A>G
T363N	T	363	N	-1.29	31.186	-0.004	3	gnomad	4	153251918	rs1381320045	G	T	gnomAD Exomes	p.Thr363Asn	c.1088C>A
N364S	N	364	S	-1.14	29.412	-0.243	2	gnomad	4	153251915	rs775885576	T	C	gnomAD Exomes	p.Asn364Ser	c.1091A>G
R367Q	R	367	Q	-0.102	29.26	-0.019	7	gnomad	4	153251906	rs745418631	C	T	gnomAD Exomes,gnomAD Genomes	p.Arg367Gln	c.1100G>A
K371R	K	371	R	-0.371	27.686	0.115	1	gnomad	4	153251894	rs761747465	T	C	gnomAD Exomes	p.Lys371Arg	c.1112A>G
P373R	P	373	R	-0.297	23.003	-0.033	1	gnomad	4	153251888	rs748952220	G	C	gnomAD Exomes	p.Pro373Arg	c.1118C>G
K374E	K	374	E	0.473	21.263	-0.168	1	gnomad	4	153251886	rs937391131	T	C	gnomAD Exomes	p.Lys374Glu	c.1120A>G
L387V	L	387	V	-1.645	13.766	0.063	1	gnomad	4	153250901	rs1338105130	A	C	gnomAD Exomes	p.Leu387Val	c.1159T>G
S407L	S	407	L	-0.153	23.243	-0.1	1	gnomad	4	153250840	-	G	A	gnomAD Genomes	p.Ser407Leu	c.1220C>T
V418L	V	418	L	-0.209	15.903	-0.155	2	gnomad	4	153249526	rs755422880	C	A	gnomAD Exomes	p.Val418Leu	c.1252G>T
V418M	V	418	M	-0.517	15.903	-0.098	2	gnomad	4	153249526	rs755422880	C	T	gnomAD Exomes	p.Val418Met	c.1252G>A
N432I	N	432	I	0.078	26.504	-0.075	2	gnomad	4	153249483	rs772668762	T	A	gnomAD Exomes	p.Asn432Ile	c.1295A>T
I433F	I	433	F	-1.662	23.411	0.361	3	gnomad	4	153249481	rs761173677	T	A	gnomAD Exomes	p.Ile433Phe	c.1297A>T
I433V	I	433	V	-1.665	23.411	-0.172	2	gnomad	4	153249481	rs761173677	T	C	gnomAD Exomes	p.Ile433Val	c.1297A>G
I435V	I	435	V	-1.87	16.772	-0.377	1	gnomad	4	153249475	rs1190126709	T	C	gnomAD Exomes	p.Ile435Val	c.1303A>G
V445L	V	445	L	-0.729	18.426	-0.093	1	gnomad	4	153249445	rs776371212	C	A	gnomAD Exomes	p.Val445Leu	c.1333G>T
T456N	T	456	N	-0.895	14.647	-0.131	1	gnomad	4	153249411	rs775244232	G	T	gnomAD Exomes	p.Thr456Asn	c.1367C>A
L457F	L	457	F	-1.16	12.355	0.603	1	gnomad	4	153249407	rs1433184454	T	A	gnomAD Exomes	p.Leu457Phe	c.1371A>T
G459V	G	459	V	-0.347	9.584	-0.311	1	gnomad	4	153249402	rs772056210	C	A	gnomAD Exomes	p.Gly459Val	c.1376G>T
R465C	R	465*	C	-1.48	5.148	0.035	1	gnomad	4	153249385	rs867384286	G	A	gnomAD Exomes	p.Arg465Cys	c.1393C>T
E471G	E	471	G	-0.856	25.356	-0.243	12	gnomad	4	153249366	rs756238684	T	C	gnomAD Exomes	p.Glu471Gly	c.1412A>G
R479G	R	479*	G	-0.614	3.072	-1.265	1	gnomad	4	153247367	rs747241612	G	C	gnomAD Exomes	p.Arg479Gly	c.1435C>G
V485I	V	485	I	-1.163	17.029	-0.053	2	gnomad	4	153247349	rs1325363774	C	T	gnomAD Exomes	p.Val485Ile	c.1453G>A
I488T	I	488	T	-2.861	20.45	-0.025	1	gnomad	4	153247339	rs1222797439	A	G	gnomAD Exomes	p.Ile488Thr	c.1463T>C
H495R	H	495	R	-1.47	17.376	0.073	3	gnomad	4	153247318	rs750717620	T	C	gnomAD Exomes	p.His495Arg	c.1484A>G
Y509C	Y	509	C	-2.06	19.683	-0.627	2	gnomad	4	153247276	rs1334352027	T	C	gnomAD Exomes	p.Tyr509Cys	c.1526A>G
V515I	V	515	I	-0.697	16.152	-0.323	1	gnomad	4	153247259	rs757683191	C	T	gnomAD Exomes	p.Val515Ile	c.1543G>A
T532I	T	532	I	-0.371	20.341	-0.005	1	gnomad	4	153247207	rs1179476070	G	A	gnomAD Exomes	p.Thr532Ile	c.1595C>T
T541S	T	541	S	-0.708	6.634	0.083	1	gnomad	4	153247181	rs1184403966	T	A	gnomAD Exomes	p.Thr541Ser	c.1621A>T
N542S	N	542	S	-1.271	3.775	-0.02	1	gnomad	4	153247177	rs1462861861	T	C	gnomAD Exomes	p.Asn542Ser	c.1625A>G
R564C	R	564	C	-1.983	15.026	-0.448	1	gnomad	4	153245501	rs1024060344	G	A	gnomAD Genomes	p.Arg564Cys	c.1690C>T
T576M	T	576	M	0.072	16.356	-0.047	2	gnomad	4	153245464	rs1429385222	G	A	gnomAD Exomes	p.Thr576Met	c.1727C>T
M587I	M	587	I	-0.303	12.55	-0.345	1	gnomad	4	153245430	rs1269436440	C	T	gnomAD Exomes	p.Met587Ile	c.1761G>A
E588D	E	588	D	-1.234	15.447	0.029	2	gnomad	4	153245427	rs751435265	T	A	gnomAD Exomes	p.Glu588Asp	c.1764A>T
K590E	K	590	E	0.269	22.181	-0.234	1	gnomad	4	153245423	-	T	C	gnomAD Exomes	p.Lys590Glu	c.1768A>G
K590R	K	590	R	-0.309	22.181	-0.109	1	gnomad	4	153245422	rs1290448722	T	C	gnomAD Exomes	p.Lys590Arg	c.1769A>G
A599G	A	599*	G	-0.412	3.998	-0.372	1	gnomad	4	153245395	rs766088325	G	C	gnomAD Exomes	p.Ala599Gly	c.1796C>G
P620S	P	620	S	-0.557	16.899	-0.062	1	gnomad	4	153244299	rs1375643251	G	A	gnomAD Exomes	p.Pro620Ser	c.1858C>T
N633S	N	633	S	-0.757	23.914	-0.073	3	gnomad	4	153244259	rs758163453	T	C	gnomAD Exomes	p.Asn633Ser	c.1898A>G
K634R	K	634	R	0.026	27.347	-0.05	1	gnomad	4	153244256	rs1199177582	T	C	gnomAD Genomes	p.Lys634Arg	c.1901A>G
K652Q	K	652	Q	0.136	26.65	0.13	1	gnomad	4	153244203	rs1182453513	T	G	gnomAD Exomes	p.Lys652Gln	c.1954A>C
T653K	T	653	K	-0.363	24.831	-0.116	1	gnomad	4	153244199	rs775781675	G	T	gnomAD Exomes	p.Thr653Lys	c.1958C>A
T653M	T	653	M	0.115	24.831	0.066	1	gnomad	4	153244199	rs775781675	G	A	gnomAD Genomes	p.Thr653Met	c.1958C>T
F656Y	F	656	Y	-0.584	18.778	-0.201	1	gnomad	4	153244190	rs1176237755	A	T	gnomAD Exomes	p.Phe656Tyr	c.1967T>A
R658Q	R	658	Q	-0.906	20.288	0.191	2	gnomad	4	153244184	rs759610249	C	T	gnomAD Exomes	p.Arg658Gln	c.1973G>A
T662A	T	662	A	-0.612	17.859	-0.022	1	gnomad	4	153244173	rs974902950	T	C	gnomAD Exomes	p.Thr662Ala	c.1984A>G
S665I	S	665	I	-0.629	11.47	-0.132	1	gnomad	4	153244163	rs957874517	C	A	gnomAD Exomes	p.Ser665Ile	c.1994G>T
I675V	I	675	V	-2.065	14.286	0.097	1	gnomad	4	153244134	rs1446303596	T	C	gnomAD Exomes	p.Ile675Val	c.2023A>G
A677T	A	677	T	-0.939	20.339	0.086	2	gnomad	4	153244128	rs781679859	C	T	gnomAD Exomes	p.Ala677Thr	c.2029G>A
N679D	N	679	D	0.186	27.125	0.429	1	gnomad	4	153244122	rs746489993	T	C	gnomAD Exomes	p.Asn679Asp	c.2035A>G
V686I	V	686	I	-0.703	11.334	-0.086	1	gnomad	4	153244101	rs1307998016	C	T	gnomAD Genomes	p.Val686Ile	c.2056G>A
N690S	N	690	S	-0.255	4.292	-0.391	1	gnomad	4	153244088	rs1237327125	T	C	gnomAD Genomes	p.Asn690Ser	c.2069A>G
M706T	M	706	T	-0.185	41.053	-0.248	1	gnomad	4	153244040	rs764051432	A	G	gnomAD Exomes	p.Met706Thr	c.2117T>C

*residue affected in both clincal cohort and gnomAD. Mutation Cutoff Scanning Matrix (mCSM); Protein–protein interactions (PPI).